I. Quantum-Mechanical Chemical Exchange

II. Stochastic Averaging in Magnetic Resonance

Thesis by

Daniel Hall Jones

In Partial Fulfillment of the Requirements

for the Degree of

Doctor of Philosophy

California Institute of Technology

Pasadena, California

1993

(submitted May 24, 1993)

c 1993
Daniel Hall Jones
All Rights Reserved

Acknowledgments

First and foremost, I would like to acknowledge the guidance and support of Dan Weitekamp. Dan's enthusiasm for this work provided great motivation for me. The Weitekamp group deserves special mention as a great group of people who made working on a floor with no windows or bathrooms more enjoyable than I thought possible. Special thanks go to Steve Buratto, K.D. Kurur, and Pedro Pizarro.

I would also like to thank John Bercaw and Jay Labinger for discussions and collaboration which led to the investigations presented in this thesis. I would like to thank members of the Bercaw group, especially Bryan Coughlin, for help in preparing samples and letting a physical chemist use their vac lines and dry boxes.

I can't envision what the last six years would have been like without the following people: Mike Rock, Gary and Dawn Guthart, Steve and Laura Buratto, Pedro Pizarro and Monica Kohler, Marc Hillmyer, Todd and Missy Richmond, and Wayne Larson. Wayne deserves special recognition for being my roommate for five years, a feat that won't soon be matched. I would also like to thank Laura Thomas for being there for me through the final throes of my graduate career. Thanks to my other roommates, Stu and Floyd, for always keeping their sense of humor.

I would like to thank two people who motivated me to go to graduate school: Jeff Reimer, my undergraduate research advisor, and Grant Haddix. They taught me what doing scientific research is and isn't about.

My family deserves special thanks for providing many needed breaks from life at Caltech. From trips to Catalina to substituting for my brother in Lamaze class, these diversions kept me in touch with life outside the lab. Finally, I cannot thank my parents enough for their encouragement and support.

Abstract

I. Quantum-Mechanical Chemical Exchange

A quantum-mechanical treatment of both spin and space degrees of freedom is derived which accounts for both tunnelling splittings and lineshape behavior in the observed NMR of exchanging proton pairs. In this self-consistent treatment, the chemical exchange rate is expressed in terms of a correlation function of the operator which couples space and spin. A master equation formulation of the correlation function is presented which can be solved for any model of discrete rovibrational states. In contrast to previous descriptions of intramolecular chemical exchange, which either use transition state theory and the notion of molecular tunnelling or ad hoc ideas of incoherent tunnelling, the present treatment places chemical exchange among the class of transport and relaxation rates described by the quantum-statistical fluctuation-dissipation theorem. Results from simple models of the tunnelling system are analyzed in order to relate the observed NMR lineshape of certain transition metal hydrides to the underlying Born-Oppenheimer potential for the quantized nuclear motion.

II. Stochastic Averaging in Magnetic Resonance

As a result of the typical smallness of spin Hamiltonian parameters relative to the rates of relaxation of spatial degrees of freedom, many magnetic resonance spectra are understood to be stochastic averages over thermally accessible molecular configurations or spatial (e.g., rovibrational) eigenstates. The temperature dependence of the average spin parameters is widely used to provide information on the potential energy functions which determine molecular conformation. It is universal practice in computing these

averages that the energies (or free energies) multiplying β (= 1/kT) in the Boltzmann probability factors are the spatial contributions only. It is argued that any such averaging procedure is inconsistent with statistical mechanics and an alternative procedure is presented for calculating the stochastically-averaged spin Hamiltonian. The experimental conditions and possible test systems for validating the traditional or alternative forms of the stochastic average are discussed.

Contents

List of Figures

Part I

Quantum-Mechanical Chemical Exchange

Chapter 1

Introduction

1.1 Historical Review

After the initial observation of nuclear magnetic resonance absorption in bulk materials,[1-2] the emphasis of research in the field of NMR changed drastically. Early investigators, determined to measure gyromagnetic moments for various nuclei, soon discovered that the observed resonance frequency depended on the molecular environment of the subject nucleus. Instead of being a tool for investigating the structure of the nucleus, NMR spectroscopy proved to be a powerful characterization technique for chemistry. The two most significant parameters for the characterization of samples in the liquid phase became known as the "chemical shift" and the "spin coupling."

The first account of the chemical shift[3] began, "Most unexpectedly, it has been found that for ^{19}F the value of the applied magnetic field H_0 for nuclear magnetic resonance at a fixed frequency depends on the chemical compound containing the fluorine nucleus." Other investigators,[4] observing these effects simultaneously, wrote: "Until it is clearly understood, the accuracy of magnetic moments determined under certain chemical conditions remains somewhat in doubt." The subsequent observation[5] of resonances for each of the three chemically different protons in CH_3CH_2OH marked the beginning of the use of NMR as a characterization technique. Certain values of chemical shifts are associated with particular functional groups or bonding environments. Although much subsequent work has attempted to place the chemical shift on firm theoretical ground, most applications of NMR are unhindered by an empirical treatment of chemical shifts.

Early observations of the "nuclear spin coupling" were made using spin-echo[6] and steady-state[7] (field-sweep) magnetic resonance techniques. A form of the spin coupling interaction had been discovered previously in the NMR of protons in solids. The explanation of the effect in solids, however, did not allow for the observation of the effect in the liquid phase, since the interaction observed in the solid state would average out with motional tumbling of the liquid-state molecules. The isotropic spin coupling must arise from an interaction that is not averaged to zero with the motion of the whole molecule. Perhaps as critical to NMR's use as a characterization technique, spin couplings indicate the number and type of nuclei coupled to the subject nucleus. Like the chemical shift, the interpretation of spin couplings in NMR also depends on empirical measurements, particularly with regard to the magnitude of the observed couplings.

1.2 Origins of the Chemical Shift and Spin-Spin Coupling

The usual descriptions of both the chemical shift and spin coupling relate these effects to the electron density around and between nuclei in the subject systems. Chemical shifts result from diamagnetic and paramagnetic electron shielding terms. For proton environments, where the electrons have low-energy, s-type ground states and relatively high-energy, paramagnetic excited states, the contribution from the paramagnetic term is very small. The resulting chemical shift range of protons in different functional groups is relatively smaller than the chemical shift range of heavier nuclei that may have lower lying paramagnetic electron levels of p-type symmetry. Temperature-dependent behavior of the chemical shift requires a perturbation of the shielding electrons. The energies necessary for such perturbations are typically too great to allow for significant changes over a small temperature range. For a "stationary" nucleus, one that undergoes neither intermolecular nor conformational transport, it is usually a good assumption that the chemical shift is a temperature-independent parameter.

The spin-spin coupling is described as a nucleus-electron-nucleus interaction and is mediated by the electron density between the two coupled nuclei. In the usual "indirect" scalar coupling described by Ramsey,[8] the magnitude of spin couplings is proportional to the product of the gyromagnetic ratios of the coupled nuclei. This can make the use of certain isotopes, particularly the isotopes of hydrogen, useful for the study of spin couplings. The magnitudes of scalar couplings scale roughly with the electron density between the coupled nuclei. As with the usual mechanism of the chemical shift, any temperature dependence of scalar couplings would result from changing the mediating electron distribution. Such a process usually requires a great deal of energy, making the assumption of temperature independence a valid one for the majority of NMR studies.

Because both the chemical shift and spin coupling prove to be fairly temperature-independent, the interpretation of liquid-state NMR is primarily in terms of electronic structure. The effects of the nuclear motion within the ground electronic state are often of secondary importance. This is not always the case, however, and this thesis examines chemical systems in which both the spin and spatial degrees of freedom impact the observed NMR spectra.

1.3 Outline

Chapter 2 investigates the spin-space interaction that result in the recently observed anomalous NMR of certain metal hydrides. The novel effects observed in these systems were previously unknown in NMR and warranted a quantum-mechanical treatment of the chemical exchange effects observed in these systems. This is the subject of Chapter 3, which includes a derivation of the chemical exchange rate in the presence of tunnelling which differs radically from previous treatments.

The quantum-mechanical viewpoint needed for the metal hydrides discussed in Part I led to the much broader investigations presented in Part II. Part II addresses the well-known and much-studied problem of stochastic averaging in NMR. Chapter 4

examines the conceptual foundation of traditional methods for calculating averaged spin parameters in NMR. The weakness of the accepted derivations prompted the development of an alternative hypothesis, the JKW (Jones, Kurur, Weitekamp) hypothesis, for how to calculate a stochastically averaged NMR frequency. Chapter 5 presents the physical properties required of systems which can discriminate between the two formulations presented in Chapter 4 and a discussion of why this issue remains unsettled. Experimental data of possible test systems is also presented in Chapter 5. Appendices 1 and 2 provide detailed derivations of the results presented in Chapter 3.

References

1. E.M. Purcell, H.C. Torrey, and R.V. Pound, *Phys. Rev.* **69**, 37 (1946).
2. F. Bloch, W.W Hansen, and M. Packard, *Phys. Rev.* **69**, 127 (1946).
3. W.C. Dickinson, *Phys. Rev.* **77**, 736 (1950).
4. W.G. Proctor and F.C. Yu, *Phys. Rev.* **77**, 717 (1950).
5. J.T. Arnold, S.S. Dharmatti, and M.E. Packard, *J. Chem. Phys.* **19**, 507 (1951).
6. E.L. Hahn and D.E. Maxwell, *Phys. Rev.* **88**, 1070 (1952).
7. H.S. Gutowsky, D.W. McCall, and C.P. Slichter, *Phys. Rev.* **84**, 589 (1951).
8. N.F. Ramsey, *Phys. Rev.* **91**, 303 (1955).

Chapter 2

Quantum-Mechanical Tunnelling in Transition Metal Hydrides

2.1 Introduction

"Quantum-mechanical tunnelling" refers to the ability of an atomic particle to penetrate barriers of heights greater than the kinetic energy of the particle, an event that is classically forbidden. In particular, the present work is concerned with pairwise tunnelling exchange of two protons bound in a molecule. The resulting wavefunctions of a particle undergoing tunnelling between two sites are a superposition of the two localized wavefunctions of the particle at each site in the absence of tunnelling. This superposition of spatial states can be symmetric or antisymmetric linear combinations of the single-site wavefunctions. In certain systems containing particles with spin, the symmetrization postulate of quantum mechanics requires that the space-spin product wavefunctions have definite symmetries which depend on the spin nature of the particles in the system. The number of systems in which these symmetry requirements impact the magnetic resonance spectroscopy of the subject system is not great. However, during the last decade, nuclear magnetic resonance spectra of a number of transition metal hydrides have been shown to demonstrate the effects of the symmetry requirements placed on quantum particles by the symmetrization postulate of quantum mechanics. These metal hydrides provide the first known system where these effects have been observed in liquid-state NMR.[1,2] This chapter reviews the experimental observations that led to subsequent theoretical work on these systems. Sections reviewing the symmetrization postulate and quantum-mechanical

tunnelling provide a basis for a treatment which successfully accounts for the observed behavior of these systems.

2.2 Experimental History of the Transition Metal Hydrides

Anomalously large and temperature-dependent scalar couplings have been observed since 1982 between chemically inequivalent proton sites on several classes of L_nMH_3 complexes.[3-14] A common feature of these molecules is that at least one ligand is a cyclopentadiene. Although the solution-state geometries are not known, they are commonly drawn as "four-legged piano stools" with the cyclopentadiene ring capping the metal and the three hydrogens and another terminal ligand as legs. This picture has been confirmed by a single crystal neutron structure.[10]

While scalar couplings between terminal hydrides on a metal are often in the 5 - 10 Hz range, proton-proton scalar couplings up to 10^4 Hz have been observed for some of the tunnelling hydrides. For $[(C_5H_5)IrH_3(AsPh_3)]$,[9] the coupling increased from 376 Hz to 570 Hz when the temperature increased from 176 K to 189 K. Both these properties are extraordinary in light of the usual description of scalar couplings reviewed in Chapter 1. Table 2.1 shows the magnitude and temperature dependence of the scalar couplings in some metal hydrides.

Table 2.1. The magnitude and temperature dependence of the scalar couplings in some transition metal hydrides.

Compound	T (K)	J (Hz)	Reference
$[(C_5H_5)IrH_3(AsPh_3)]$	176-189	376-570	9
$[(C_6H_6)OsH_3(PPh_3)]$	148-173	200-374	11
$[(C_5H_5)_2WH_3]$	153-203	450-1000	12
$[(C_5Me_5)RuH_3(P\text{-}i\text{-}Pr_3)]$	168-203	57-131	13
$[(C_5Me_5)RuH_3(PCy_3)(CuCl)]_2$	188-230	20-70	14

Without an alternative description of scalar couplings available, initial attempts to explain these unusual NMR spectra relied on the traditional indirect mechanism[15] and unusual bonding character between the protons.[7-9,13,14] In the early 1980s, the isolation of transition metal complexes with dihydrogen ligands[16-17] raised the possibility of other unusual bonding pictures of hydrogens at metal centers. The dihydrogen complexes display behavior in both their NMR and infra-red (IR) spectra which is characteristic of significant bonding between the protons. The isolation of these complexes led researchers to propose the existence of "trihydrogen" ligands for certain transition metal trihydrides.[9] Such bonding pictures soon appeared in explanations of the anomalous NMR spectra of certain metal hydrides. These explanations relied on the action of a trihydrogen ligand or a dihydrogen-hydride equilibrium to account for the observed anomalous behavior. Such proposals are difficult to quantify and cannot account for the magnitude or temperature-dependence of the couplings, or for the observed constancy of the chemical shift with temperature. Such explanations also fail to account for the disappearance of the anomalies upon isotope substitution of even one of the coupled sites.[6,9] For example, J_{HD} in deuterated $RuH_3Cp^*(PMe_3)$ was less than the linewidth of 5 Hz, while the corresponding perproto compound showed J_{HH} up to 206 Hz.[6] Any explanation needs to explain why $J_{HD} \cong (\gamma_D/\gamma_H)J_{HH} = 32$ Hz, as expected from indirect scalar coupling, is not observed.

Another mechanism of scalar coupling, tunnelling exchange, was known to be operative in some low-temperature solids.[18,19] The recognition[1,2] that it was operative in the liquid-state NMR of transition metal hydrides resolved the anomaly. Because the first compounds to display these anomalies were all trihydrides with AB_2 proton spectra, it was not clear initially whether cyclic tunnelling exchange of the three protons, as occurs in methyl groups,[18,19] was a contributing mechanism. This mechanism would contribute equally to the three scalar couplings, but J^e_{BB} would not appear in the spectrum due to the magnetic equivalence. This possibility can be ruled out[1] on the basis of either of two observations. Cyclic exchange contributions to the coupling would be eliminated in the

ABX species formed by isotopic substitution at one of the B sites, but $[(C_5H_5)IrLH_3]^+$ with a single deuteron at a B site shows J_{AB} between the remaining protons to only increase slightly. A chiral ligand in $[(C_5H_5)IrLH_3]^+$ gave an ABC spectrum with J_{BC}, the coupling between the formerly equivalent sites, to be 3.4 Hz and independent of temperature while J_{AB} and J_{AC} are large, similar in value and temperature dependent.[2,10] This also indicates that cyclic exchange between the (nearly) isochronous sites is negligible.

The experimental data is limited at high temperature by the collapse of the multiplets. This collapse could occur simply from the growth of in $J^e_{AB}(T)$, since a point is reached where $J_{AB} \gg \Delta\nu_{zAB}$ and an AB becomes an A_2 spectrum, and an AB_2 becomes a triplet of peaks with intensity ratios of 1:10:1.[20] Experimentally, however, it is found[2-9,12-14] that the collapse happens at values of J_{AB} small enough that multiplet structure would still be expected in the absence of "chemical exchange" effects. Application to these systems was made[4,12,21-22] of the usual two-site lineshape theories for intermediate exchange,[23-24] and analysis based on the notion of a stochastic hopping over a barrier between sites with spin Hamiltonians differing in chemical shift. This model includes no role for tunnelling as occurs in the quantum-mechanical description of a double well and is thus conceptually suspect. In particular, if the hopping rate extracted in this way is analyzed with the usual Arrhenius form, the activation energies found substantially underestimate the barrier height calculated from the double-well model which fits the tunnel splitting observed. This is because transient occupation of states with energy below the barrier in the double well model, but with $J(n) \gg \Delta\nu_{zAB}(n)$, will quench the chemical shift difference before classically allowed crossing is activated. The problem of quantitatively accounting, in a self-consistent manner, for both the observed tunnel splittings and tunnelling contributions to chemical exchange effects will be solved in Chapter 3.

2.3 The Symmetrization Postulate of Quantum Mechanics

The symmetrization postulate of quantum mechanics determines the states that systems of indistinguishable particles can occupy.[25] The first statement of the symmetrization postulate was made by Wolfgang Pauli in what is now known as the "Pauli exclusion principle." The Pauli principle states that no two electrons can occupy the same state. However, experiments at the time had shown that two electrons could occupy states of equal energy, requiring that, in order not to be in the same state, electrons possess some other intrinsic property, which Pauli called spin. Later work revealed that electrons, as spin-1/2 particles, can occupy two spin states of +1/2 or -1/2.

The Pauli exclusion principle determines the symmetry properties of the particle systems. Considering the possible states of each electron to be +1/2 (α state) or -1/2 (β state) and that for a single spatial orbital the electrons must be in opposite spin state, the possible product states of the system are $|\alpha(1)\beta(2)\rangle$ and $|\beta(1)\alpha(2)\rangle$. Since the two electrons are indistinguishable, the antisymmetric linear combination of the above product can be constructed from the determinant:

$$|m_S(1)m_S(2)\rangle = \begin{vmatrix}\alpha(1) & \alpha(2)\\ \beta(2) & \beta(2)\end{vmatrix} = |\alpha(1)\beta(2)-\beta(1)\alpha(2)\rangle \qquad (2.1)$$

The operator that permutes particle labels acts upon this antisymmetric wavefunction to yield the same wave function but with a sign change.

$$\hat{P}|\alpha(1)\beta(2)-\beta(1)\alpha(2)\rangle = |\alpha(2)\beta(1)-\beta(2)\alpha(1)\rangle = -|\alpha(1)\beta(2)-\beta(1)\alpha(2)\rangle \qquad (2.2)$$

The above expression for the two-particle wavefunction would equal zero if the α and β states were the same, that is if the property of spin did not exist or enter into the construction of the wavefunction. The Pauli principle states that only antisymmetric wavefunctions can describe the two-electron system. The statistics describing the allowed states of the above system is known as Fermi statistics and particles for which total wavefunctions must be antisymmetric have 1/2-integer spin and are known as fermions.

Likewise, particles with integer spin are known as bosons and must have symmetric wavefunctions, as described by Bose statistics. A general statement of the symmetrization postulate of quantum mechanics would be:

Systems of fermions must exist in states which are antisymmetric with respect to particle label interchange. Systems of bosons must exist in states which are symmetric with respect to particle label interchange.

The symmetrization postulate supplied the explanation to a mystery which had been known for many years before the advent of quantum mechanics. Hydrogen gas was known to be separable into two distinct species. The species could be distinguished by their heat capacities, but the origin of these differences was not known. The H_2 system, consisting of two spin-1/2 protons, is required through the symmetrization postulate to have a total wavefunction antisymmetric in exchange of the proton labels. Rotational states with an even number of rotational quanta possess a symmetric spatial symmetry and must combine with the antisymmetric spin wavefunction for the two protons, the singlet state. The odd rotational states exist with the symmetric triplet states. The spin factors in the wavefunctions are:

$$\text{Singlet} \equiv \frac{1}{\sqrt{2}}|\alpha\beta - \beta\alpha\rangle \tag{2.3}$$

$$\text{Triplet} \equiv \begin{cases} |\alpha\alpha\rangle \\ \frac{1}{\sqrt{2}}|\alpha\beta + \beta\alpha\rangle \\ |\beta\beta\rangle \end{cases}. \tag{2.4}$$

The states of hydrogen that are represented by the singlet spin state are known as parahydrogen (p-H_2); the states represented by the spin triplet are orthohydrogen (o-H_2). The conversion of one species to another is very slow except in the presence of bond breaking or paramagnetic catalysts which break the symmetry of the molecule.

The number of cases in which the symmetrization postulate directly effects the interpretation of NMR spectra is limited. The failure of the traditional descriptions of the chemical shift and spin coupling to account for the observed NMR of certain metal hydrides led to consideration of the effects of the symmetrization postulate on the protons in these systems. Consideration of the interaction between the symmetrization postulate and these unusual NMR effects was in no small part motivated by previous work carried out in the Weitekamp group at Caltech. The discovery that addition of parahydrogen enriched H_2 creates non-equilibrium distributions of product spin states detectable by NMR is a dramatic example of the symmetrization postulate affecting NMR spectroscopy.[26-27] Although the signal enhancement afforded by this PASADENA (Parahydrogen And Synthesis Allow Dramatically Enhanced Nuclear Alignment) effect decays fairly rapidly, unlike the unusual NMR behavior of the metal hydrides which results from static spin parameters, the similarities in the two systems were striking enough to consider connections between the operative mechanisms of each. Considering the consequences of the symmetrization postulate on the space-spin coupling in hydrogen and the subsequent demonstration of the PASADENA effect, the question becomes, "What models of the spin and space degrees of freedom in the metal hydride molecules could account for the observed NMR behavior?"

2.4 Quantum-Mechanical Tunnelling

Questions about the role of the symmetrization postulate in bringing about the unusual NMR behavior led to the possibility that quantum-mechanical tunnelling was an important mechanism in the hydrides. Potential energy surfaces which allow the exchange of identical particles through quantum-mechanical tunnelling would require that the symmetrization postulate be obeyed.[28]

The first experimental observation of quantum-mechanical tunnelling was field-assisted emission of electrons by metals. Quantum-mechanical tunnelling also proves to

be operative in the emission of α-particles by radioactive nuclei. These examples involve the tunnelling of bound particles with a defined energy through a barrier into free space. The application of tunnelling to chemical kinetics presents a more complex situation. Evidence for tunnelling in chemical reactions is shown by non-Arrhenius temperature dependence of reaction rates. Tunnelling in chemical reactions involves a Boltzmann distribution over the vibrational and rotational manifolds of the products and reactants. The transfer of protons between bound states in a molecular system is well-known, having been studied through the use of the isotopes of hydrogen.[28]

For two protons bound to a metal center, site exchange yields a final configuration that is indistinguishable from the initial one. Systems with such symmetries can be modeled using a symmetric double-well potential, a model that was first considered to explain the doubling of lines in the vibrational spectrum of ammonia. The tunnelling of the ammonia molecule leading to its inversion is responsible for these splittings. Quantum-mechanical tunnelling could serve as the mechanism by which two protons at a metal center could undergo site exchange with energies much less than the potential barrier restricting such motion. Unlike the situation in ammonia, in exchange tunnelling the coordinate is a relative coordinate of the protons. It is in such situations that tunnelling will have consequences for scalar coupling.

2.5 The Metal Hydrides

Now that the general features and effects of the symmetrization postulate and quantum-mechanical tunnelling have been discussed, the unusual behavior of the metal hydrides can be accounted for. When tunnelling permutes the coordinates of two or more identical particles, there will be observable consequences of the requirement that the wavefunctions for the system obey the symmetrization postulate. The metal hydrides are a particular case where, through the requirements of the symmetrization postulate, the resulting coupling occurs between the spin and spatial coordinates. One example that has

been discussed is the coupling of the spin and space degrees of freedom in H_2, where the singlet and triplet nuclear spin states are separated by a rotational quantum. Another familiar example is the exchange energy that separates the singlet electronic ground state of H_2 and the first excited triplet. The phenomenon of exchange tunnelling had been previously recognized in NMR only in the case of low-temperature solids,[18,19,29-32] but now it will be shown to be responsible for the unusual liquid-state NMR behavior of certain metal hydrides.

Consider the case of two protons at nearby sites in a molecule. A quantum-mechanical model for the two particle system that allows for the possibility of the protons exchanging places is the double well shown in Figure 2.1. The potential for the proton motion has identical values at coordinates related by exchange of the proton labels. This one-dimensional model will be solved for quantitative fits to the data. While the one-dimensional potential model is certainly a simplification of the true multi-dimensional nuclear potential of the molecule, the general features are the same in any number of dimensions that might be used to accurately describe the molecular potential. No assumptions about the dimensionality are needed in the derivation here and in Chapter 3, but only in numerical uses of the derived formulas. The symmetry of this model does not assume that the two proton sites are chemically equivalent, but only that the energy of the molecule is the same when the two protons exchange places. This is purely a spatial problem so far and the character of its solutions are well known.[33] The eigenvalues cluster in pairs, becoming doubly degenerate in the limit of an infinite barrier. The wave function of the lower state in each pair is gerade (symmetric) with respect to exchange of the spatial coordinates of the particles and the upper is ungerade (antisymmetric). The probability density in the barrier region and the intrapair splitting, known as the tunnel splitting, both increase with energy, but are finite even for eigenstates below the barrier height. When the tunnelling coordinate exchanges two identical particles the process is called exchange tunnelling or quantum-mechanical exchange. More graphically, a state

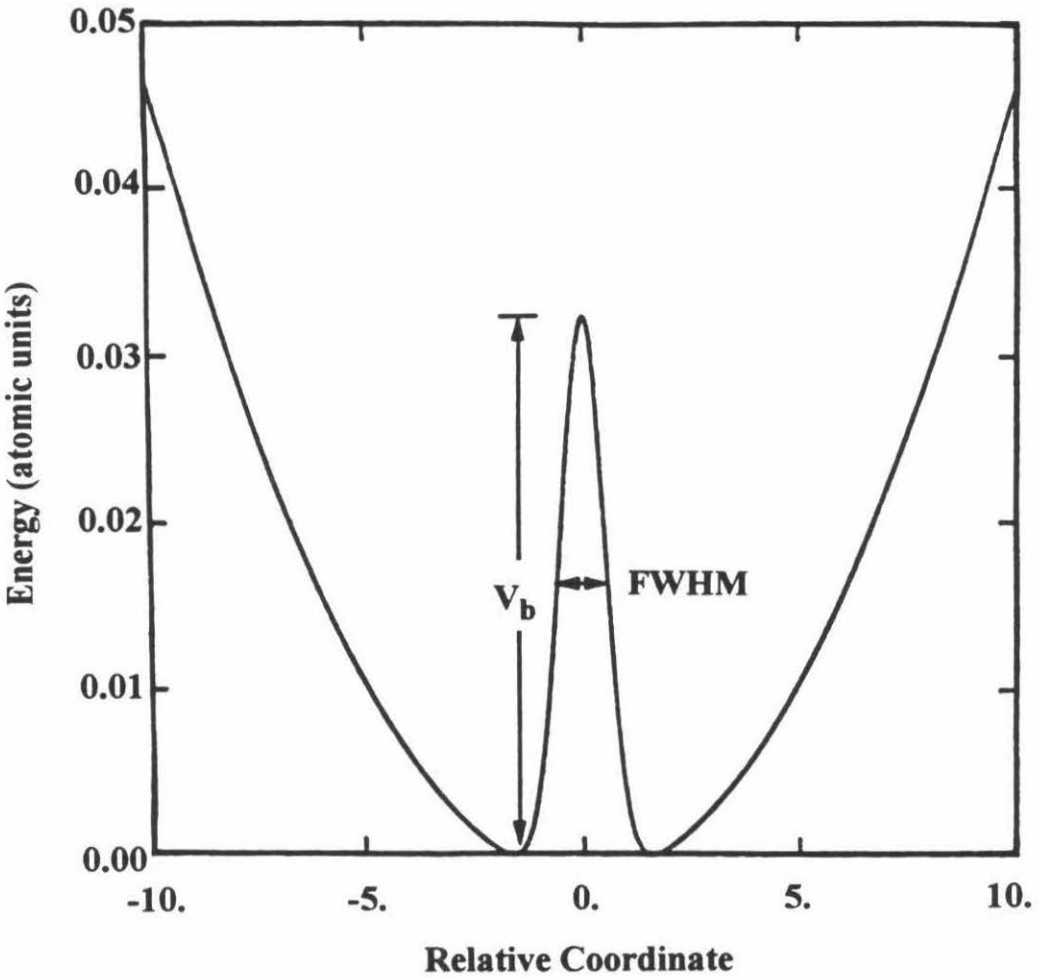

Figure 2.1. The symmetric double-well potential characterized by the barrier height, V_b, and FWHM (full width at half maximum).

which is a coherent superposition of eigenstates of opposite parity in the tunnelling coordinate will have an oscillatory expectation value for the tunnelling coordinate. As will be shown, the symmetrization postulate will couple the spins to these levels in such a way that in magnetically inequivalent systems Larmor frequency pulses will actually create coherences with this character.

A qualitative expectation of the relevant potential energy parameters would include a barrier height about an order of magnitude greater than kT at 200 K, tunnel splittings of pairs of eigenstates below the barrier having a Boltzmann average of 10^1-10^4 Hz and the

lower interpair splittings are typical of vibrational quanta, say 10^{12}-10^{14} Hz (i.e., within an order of magnitude one way or the other of kT/h).

Just as with H_2, the possible spin states associated with each spatial state are restricted by the symmetrization postulate; the gerade states are nuclear spin singlets like parahydrogen and the ungerade states are spin triplets like orthohydrogen. If the successive pairs of states are indexed by n and the gerade and ungerade member of each pair by plus and minus signs, respectively, then the situation is summarized by a Hamiltonian for each n of the form (in Hz)

$$H_J^e(n) = J_{AB}^e(n) I_A \cdot I_B, \tag{2.5}$$

where $hJ_{AB}^e(n) = E_{n+} - E_{n-}$ is the tunnel splitting, the difference in energy between the ungerade and gerade states of the n^{th} pair that emerges from solving the Schrödinger equation. While Eq. 2.5 employs the definition of a scalar coupling that is traditional in high-resolution NMR, much of the literature on exchange coupling uses a J that is -1/2 times $J_{AB}^e(n)$. The exchange couplings $J_{AB}^e(n)$ are not magnetic in origin; they are independent of the magnetic moment of the nuclei. For the model discussed, they are positive quantities, though in general this need be true only for the ground state. This issue will be addressed in later discussions of alternative tunnelling potentials. Any contribution from the usual[15] indirect (magnetic) scalar coupling through the electrons will add algebraically to this effect.

So far the Zeeman interactions have been neglected. Because of chemical shielding, the Zeeman interactions depend on the particle positions and could be included in our Schrödinger equation. The existence of a chemical shift difference between the exchanging sites is one essential difference in the physics of exchange in the metal hydrides as opposed to solid-state systems where exchange coupling has been discussed. It is magnetic inequivalence (a chemical shift difference or unequal scalar coupling to a third spin) that allows the exchange couplings to be measured as spectral splittings in the liquid

state. To model this with a spatial Schrödinger equation an ungerade function of the appropriate magnitude would need to be added to the potential, thereby making the double well slightly asymmetric in a spin-dependent manner. Thought of as a perturbation of the eigenstates $|g^M(n)\rangle$ and $|u^M(n)\rangle$ of the symmetric double-well problem, the chemical shift difference will be off-diagonal with finite elements only between gerade and ungerade M = 0 states, $|g^0(n)\rangle$ and $|u^0(n')\rangle$, with different spin parts. The significant matrix elements are those between such states with the same n. Thus the problem reduces to a family of problems of the familiar AB type, but with a chemical shift difference that may depend on n. Specifically, the spin Hamiltonian is

$$H_{cs}(n) = \Delta\nu_{zAB}(n)(I_{zA} - I_{zB}), \tag{2.6}$$

where $\Delta\nu_{zAB}(n) = \gamma H_0\langle g^0(n)|f(r)|u^0(n)\rangle$, with some ungerade f(r) modeling the spatial dependence of the shielding. Here r indicates the spatial coordinates.

Note that here the labels A and B are necessarily viewed as site, rather than particle, labels, but the forms of Eqs. 2.5 and 2.6 are otherwise ordinary. The transition from particle to site labels is presented in more detail in Chapter 3. The spin mechanics has now been reduced to the commonplace, with the interesting physics in the spin Hamiltonian parameters. These depend on discrete quantum state n, which is physically different from, but formally analogous to, the way they are often thought of as depending on discrete classical configurations of a molecule.

This analogy can be taken further. In the same way that interconversion of molecular configurations (chemical exchange) leads to motionally averaged NMR parameters, thermally activated interconversion among manifolds, labeled here by n, will lead to a quantum-mechanical treatment of chemical exchange, an example of which will be discussed in Chapter 3. This concept should not be confused with quantum-mechanical exchange, which figures in that example, but would be meaningful even in its absence. Phonon-mediated change in n does not require interconversion of states differing in any spin quantum number. Thus, it will often be much faster than any NMR timescale. If it is

much faster than the inverse of the spectral width, line positions will be described by the ensemble average parameters. The average exchange coupling actually observed is expected from traditional formulations of average NMR parameters to be

$$J^{e}_{AB}(T) = \frac{\sum_{n} J^{e}_{AB}(n)\exp\left(-E(n)/kT\right)}{\sum_{n}\exp\left(-E(n)/kT\right)}, \qquad (2.7)$$

where $E(n) = (E_{n+} + E_{n-})/2$ is the average energy of the states in manifold n. A similar expression could be written for the average chemical shift. The status of such expressions and a possible alternative are discussed in Chapter 4. Here it is taken as correct, since the present trihydride data does not allow a critical test of this aspect.

Note that it is the correlation between spin and spatial degrees of freedom enforced by the symmetrization postulate that allows these small spatial energy differences to survive averaging in the liquid environment. Phonons that in the absence of spin restrictions would connect gerade and ungerade spatial states are presumably abundant, but are ineffective in the experimental range of J(T), unless they can also flip spins. Thus the well-known inertness of spin states, which makes high-resolution NMR possible, is here shared with a spatial degree of freedom. This reasoning suggests that the analogous spatial splittings that one would find in a system where *heteronuclei* exchange through tunnelling will not show up as NMR couplings at temperatures where vibrational relaxation is rapid on the NMR timescale, in agreement with existing observations.

The process described by this quantum-statistical average is mathematically analogous to the fast-exchange limit of chemical exchange. The quantum treatment of intermediate or slow exchange will be pursued in Chapter 3 and will be developed for the full treatment of line shape and relaxation effects.

At this point, the qualitative expectations for the temperature-dependent NMR of an inequivalent, quantum-mechanically exchanging pair of protons can be described. At a

sufficiently low (but liquid-state) temperature the system is confined to states well below the barrier. These have the property that $\Delta\nu_{zAB}(n)$ is nearly constant with n, so long as the probability density is predominantly localized near the centers of the two wells, where f(r) is slowly varying. The tunnel splittings $J^{e}_{AB}(n)$, however, increase rapidly with n. The result is that, as the temperature is raised, probability shifts to states of higher n, and $J^{e}_{AB}(T)$ increases without much change in $\Delta\nu_{zAB}$.

2.6 Simulations with a Separable Tunnelling Coordinate

In this section a model for tunnelling is solved numerically and shown to give excellent fits for several compounds to the experimental data for J(T) with chemically plausible potentials. To keep things as simple as possible, it is assumed that the motion of the proton pair is a separable (six-dimensional) problem with the interactions of the two protons with one another and with the rest of the molecule included in some potential to be modeled. Again for expediency, assume that one dimension of the relative proton coordinate is separable from the other five coordinates. One such model would be a rigid rotor constrained to plane; exchange would correspond to a rotation by π in the rotor coordinate. Another model is one in which the relative motion of the two protons along paths parallel to the line connecting their equilibrium positions is a separable coordinate $x = x_1 - x_2$. The proton motion is not constrained to a line, but the other degrees of freedom are assumed to be separable and the corresponding factors in the wave functions of thermally accessible states are assumed to be gerade, as they would be in their ground states. This model does not exclude the protons passing through one another as x changes sign, but also includes more plausible paths where finite values for the relative coordinates y and z prevent unphysical proximity. The assumed separability in effect replaces the different trajectories by some average coordinate. This hypothetical construct will be called the tunnelling coordinate. It will allow an exploration of the idea of exchange of

two protons in a way that is both solvable and, perhaps unfortunately, adequate to fit the available data. Various *a priori* objections can be made to such a simplified model, but are difficult to quantify until a more elaborate model is exactly solved. While this is a desirable goal, the model is presented as a step in this direction.

The potential used for the tunnelling coordinate is sketched in Figure 2.1 and has the form

$$V(x) = \frac{1}{2}kx^2 + b\exp(-x^2/2\sigma^2). \tag{2.8}$$

This is a harmonic well converted into a double well by a Gaussian barrier. Note that the curve is not locally symmetric about each of the minima; the potential is steeper for motion of the protons toward one another than for motion apart. The Schrödinger equation, $H\Psi = E\Psi$, is solved with

$$H = -(\hbar^2/2\mu)(d^2/dx^2) + V(x). \tag{2.9}$$

This introduces the effective mass μ for the tunnelling coordinate, which is assumed to be the reduced mass $m_1m_2/(m_1 + m_2) = m_p/2$ for the two protons each of mass m_p. Each of the two minima corresponds to the equilibrium geometry, so they are located at $\pm r_{eq}$, where r_{eq} is the distance between site A and site B.

It is unnecessary for the purpose of extracting $J^e_{AB}(n)$ to include the Zeeman terms in the calculation, and by excluding them the calculation is simplified; separate diagonalizations within the gerade and ungerade manifolds are possible thereby reducing the dimension of the matrices. Some experimental justification for this is available; the exchange couplings are observed to be independent of magnetic field.[2] The harmonic oscillator states for the potential $(1/2)kx^2$, with the same k as in Eq. 2.8 were used as the initial basis.[34] For the molecules fit in detail, 50 or more states of each parity were sufficient to insure that $J^e_{AB}(T)$ given by Eq. 2.7 was independent of basis set size over the range of experimentally reported temperatures.

The experimental $J_{AB}(T)$ data are related to the values calculated according to Eq. 2.7 by

$$J_{AB}(T) = J^{i}_{AB} + J^{e}_{AB}(T), \tag{2.10}$$

where the indirect term J^{i}_{AB} is taken as temperature independent. The best estimate for the magnitude $\left|J^{i}_{AB}\right|$ is given by taking the tritium-proton couplings of 29 and 24 Hz measured for $[IrH_2TCp(AsPh_3)]^+$ with the tritium in the A or B positions, respectively.[2] The reason why these values differ is unknown, but is presumably a subtle mass effect on the electronic wave function. Since there is no exchange coupling expected in this case of heteronuclei, the observed couplings are entirely due to the indirect mechanism. The corresponding proton-proton value can be estimated by multiplying the average proton-triton values by a ratio of the magnetic moments $\gamma_H/\gamma_T = 0.94$. The tritium results do not give any evidence of the sign of the coupling. The absolute sign of the proton-proton coupling for the transition metal dihydride $RhH_2Cl(PPh_3)_2$ has been established as negative using the PASADENA spectrum.[27] Thus, J^{i}_{AB} = -25 Hz was assumed for all the trihydrides considered here.

The data on r_{eq} is limited and so a value of 1.7 Å, determined by both neutron diffraction on $[IrH_3Cp(PMe_3)]BF_4$,[10] and solid-state NMR data on $[IrH_3Cp(PPh_3)]BF_4$,[2] was used for all the molecules. The other parameters were varied using a simplex algorithm[35] that searched for the best fit in the two-dimensional parameter space of the barrier width and the barrier height V_b indicated in Figure 2.1. The fitting parameter minimized was the sum of the squares of the deviations between experimental and theoretical $J_{AB}(T)$. The resulting fits for the representative data sets are shown in Figures 2.2 and 2.3. The rms deviation ranges from 3.3 to 7.7 Hz per data point for the different molecules. The fits are nearly as good as the data, if one assumes that the scatter in the data away from a smooth curve is a measure of experimental uncertainty in line position and temperature. The simulation procedure has not yet been applied successfully to

compounds with higher J(T), because the basis set size needed is prohibitively large with the current approach.

The results of the fitting procedure described are barrier widths and heights as tabulated in Table 2.2. These should be interpreted with caution for several reasons. The use of a separable one-dimensional tunnelling coordinate is an unevaluated simplification, though frequently used in other contexts.[36] Even assuming its approximate validity, the distance, effective mass, and functional form assumed are uncertain parameters. With these caveats, it is worthwhile to comment on the parameters found. The barrier heights are higher by factors of 1.5-2.5 than have been suggested[4,21,22] on the basis of the standard formulation of chemical exchange, but this must be viewed as a success of the present model. As already mentioned, transition state theory will lead to underestimates of the barrier height, since it neglects the possibility that states with large $J^{e}_{AB}(n)$ below the barrier can serve the same role as the hypothetical transition-state complex. The energy of this complex or, more rigorously, of a delocalized state at the nominal barrier height appears as the activation energy in the exponential factor of such theories. In this regard it is worth noting that for the various molecules, 5-6 pairs of spatial states contribute at least 1% to the calculated J^{e}_{AB} at the highest experimental temperature. These pairs have values of J(n) increasing monotonically from 10^1 to 10^7 Hz. The highest such pairs have energies E(n) from 23 to 45% of the barrier height. With $J(n) \gg \Delta\nu_{zAB}$, the eigenvalues and eigenstates are insensitive to the chemical shift difference and thus such states are indistinguishable by NMR from those above the barrier.

Note that above the barrier one still has the alternation of singlet and triplet states, but their separation would be described in the present model as a vibrational quantum or in a more complex potential perhaps as a quantum of internal rotation; the distinction

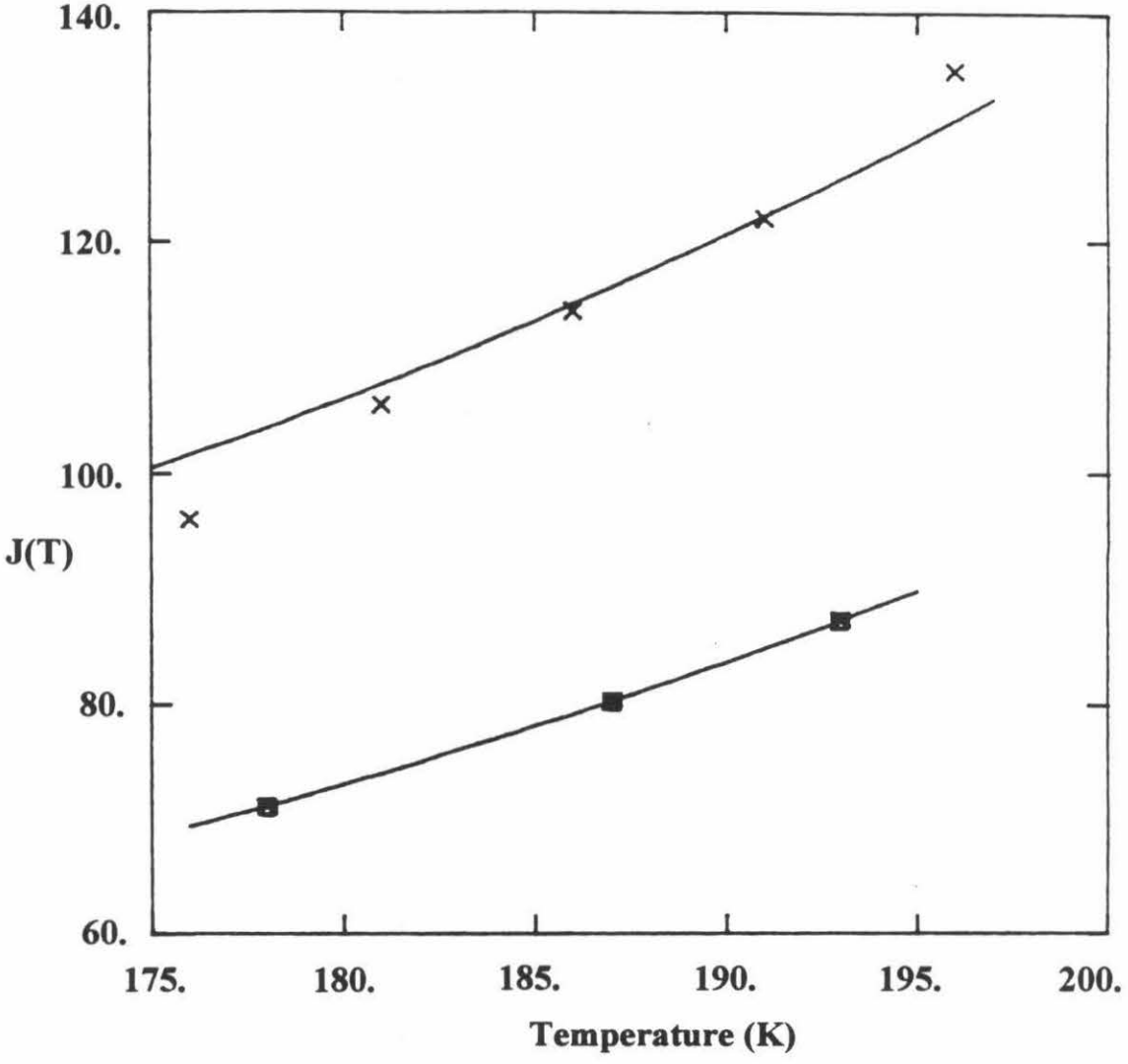

Figure 2.2. The theoretical fits (lines) to the experimental values of the temperature-dependent scalar couplings in $[(C_5H_5)IrH_3(PMe_3)]^+$ (x) and $[(C_5Me_5)RuH_3(PCy_3)]$ (⊠). The parameters yielding the fits are given in Table 2.2.

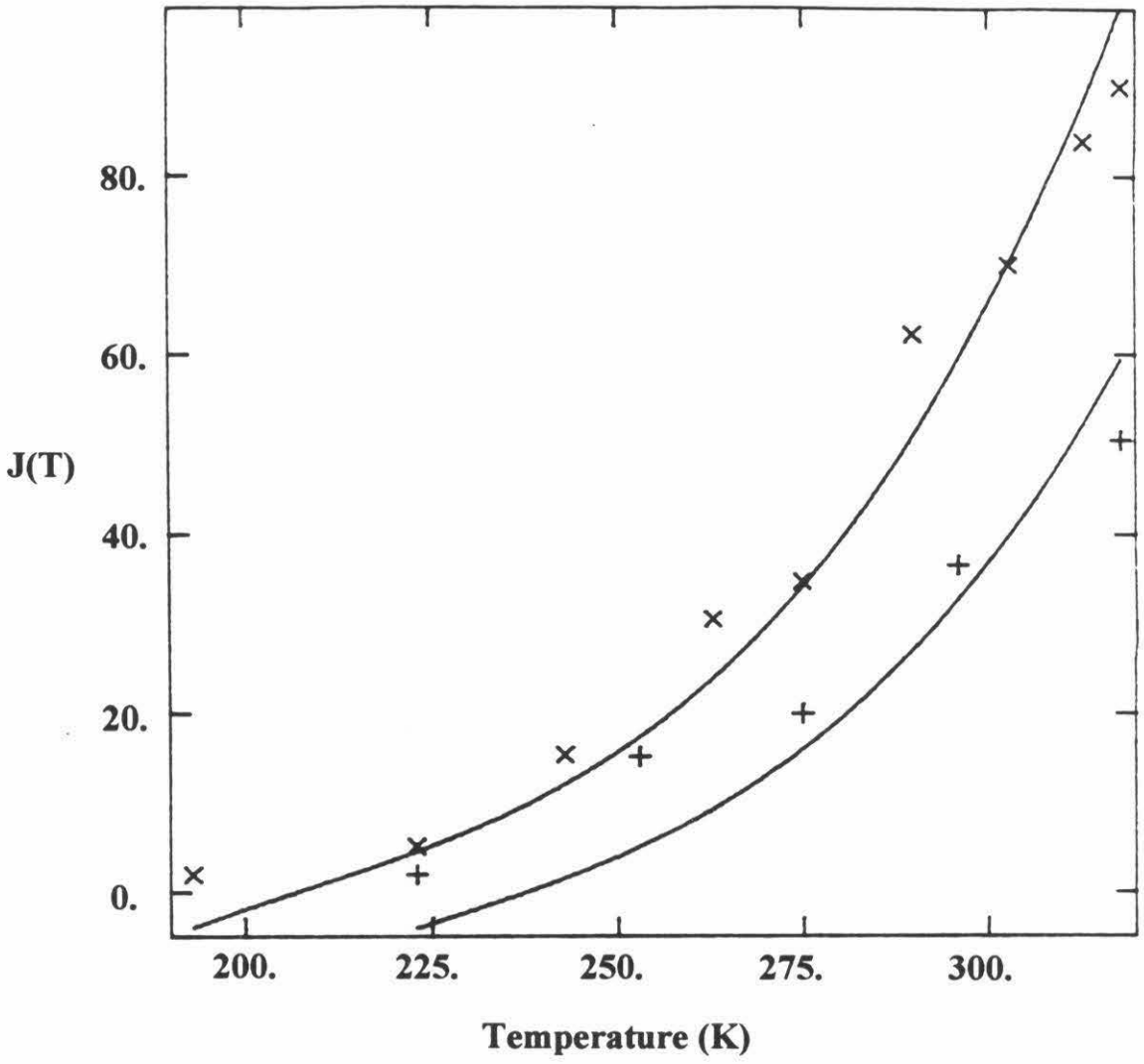

Figure 2.3. The theoretical fits (lines) to the experimental values of the temperature-dependent scalar couplings in $NbH_3[C_5H_3(SiMe_3)_2]_2$ (x) and $NbH_3(C_5H_4SiMe_3)_2$ (+). The parameters yielding the fits are given in Table 2.2.

between the two sometimes being moot. In any case these states do not enter into the observables of interest here and so the accuracy of their representation in the present model is irrelevant.

Table 2.2. The barrier height and barrier width parameters that yielded the best fit for each of the compounds.

Compound	Barrier Height (kJ $mol^{-1)}$	FWHM (Å)
$[(C_5H_5)IrH_3(PMe_3)]+$	79.4	1.51
$[(C_5Me_5)RuH_3(PCy_3)]$	85.2	1.39
$NbH_3[C_5H_3(SiMe_3)_2]_2$	98.8	1.34
$NbH_3(C_5H_4SiMe_3)_2$	101.5	1.33

The barrier widths of 1.33-1.51 Å in the relative coordinate might more intuitively be viewed as angular widths of 24°-27° in molecular coordinates, if one imagines the tunnelling coordinate as an arc at the metal-proton distance of 1.6 Å measured by neutron diffraction[37] of $[H_2Ir(SiEt_3)_2(C_5Me_5)]$. The energies associated with a change of unity in the principal quantum n are found to be 450-500 cm^{-1}. These are below the range of 700-900 cm^{-1} that have been observed for terminal hydride bends and wags in other metal hydrides.[17] Vibrational spectra or inelastic neutron scattering for these low-frequency modes are not presently available for the molecules that show exchange coupling, although such data, together with structural and J(T) results, will be critical to the construction of a compelling multidimensional model.

During optimization, the least-squares fits showed marked dependence on small changes in either V_b or the FWHM (full width at half maximum) of the barrier. There is no doubt that the problem is underdetermined by the presently available data. While the full range of r_{eq} over which the data could be fit is not known, it is evident that the

parameters can compensate for one another. This raises the question of uniqueness of solutions; the present fits should not be taken as independent evidence of r_{eq}. The method of fitting with fixed distance was found to be reliable in the sense that starting the simplex procedure at different initial points led to either the same minimum or a local minimum with a much less satisfactory fit to the $J^{e}_{AB}(T)$.

Other calculations were performed to address the issue of isotope effects. A doubling of the effective mass without a change in the potential for $NbH_3[C_5H_3(SiMe_3)_2]_2$, as would occur in the perdeuterated analog, decreases $J^{e}_{AB}(318\ K)$ from 120 to 0.1 Hz, an undetectably small value.

2.7 Other Descriptions of the Exchange Couplings

It would be desirable to confirm with a less idealized model that the results obtained with a separable one-dimensional tunnelling coordinate are qualitatively correct. A multidimensional numerical approach, for example, using a basis set and matrix methods, has not been attempted. Landesman, in the context of ^3He, has made an analytical calculation for the low-temperature limit only of the exchange coupling of two identical particles interacting with each other and with two harmonic wells fixed in the lattice.[38] The accuracy of this calculation as a solution to the given model is unknown; the approximations made are analogous to the Heitler-London treatment of the electronic wavefunction of H_2. The two-particle wavefunctions are not calculated, but are assumed to be the gerade and ungerade linear combinations of the ground states of the one-particle isotropic oscillators multiplied by a window function that sets the probability to zero within a certain interparticle distance. The parameters are this cutoff distance, the harmonic frequency, and the distance between the minima. These parameters simultaneously determine the overlap of the one-particle states and the barrier shape, which thus has a discontinuity at the midpoint between the minima and the rather arbitrary

property that the barrier height increases quadratically with internuclear distance. One objection[39] is that this highly constrained form of the trial wave function is not likely to simultaneously give the correct wavefunction both near the potential minima and under the barrier.

The Landesman model with hard-sphere repulsion has been applied to the NMR of the anomalous hydrides[21-22] by the Yale groups of Zilm and Heinekey. Additional difficulties are encountered here. The model has none of the anisotropy or topology of two protons bound to a common metal center and the accuracy with which it is solved is indeterminable. In order to extend the theory to finite temperature, it is simply assumed that the relationship between one-particle rms displacement and exchange coupling found by Landesman for this ground-state model applies also at any temperature. No mathematical justification is given. With the cutoff parameter fixed at 1 Å, the distance between minima and the harmonic frequency are varied. Good fits to J(T) are found[21] for various molecules including those of Figures 2.2 and 2.3.

Both the extended Landesman model and the one-dimensional tunnelling coordinate model presented here succeed in fitting the available data with parameters that are not obviously unreasonable. The trend is that the exactly solved model presented here uses potential barrier heights and vibrational splittings similar to those found with the alternative model. Considering the differences between the models and the simplicity of both of them relative to a real molecule, comparisons between them are of limited significance, only highlighting the need for more realistic, but accurately solvable, multidimensional models and lineshape calculations that take into account the multilevel structure of the spatial problem.

2.8 Conclusions

Quantum-mechanical exchange between proton sites in dissolved molecules is striking for having been so long overlooked after the appearance of the experimental data,

but even more so for having been observed in such a small number of molecules. There is a common conception that tunnelling is a phenomenon of low-temperature solids or of isolated gas-phase molecules. Large kinetic isotope effects on reaction rates involving hydrogen transfer frequently persist in the condensed state to room temperature or above,[28,40] but NMR splittings due to tunnelling are apparently limited, so far, to the metal hydride systems discussed. This is probably best viewed as accidental. The prerequisites for observability by NMR splittings are that the exchanging sites are magnetically inequivalent and that the exchange coupling is not too small to go unnoticed or attributed to indirect coupling or too large to truncate the magnetic inequivalence and lead to the fast-exchange limit. Evidently nearly all molecules fall outside this narrow window, though variable temperature studies and higher magnetic fields will likely bring some known species within it.

There is considerable progress to be made in understanding exchange couplings in liquids. Though quantitative fits are possible with simple theories, the data is still inadequate to test these or any theory quantitatively. The working hypothesis in the theoretical work so far is that the proton motion can be described in terms of a static temperature-independent molecular potential. This is an attractive approach and has served well in both vibrational and magnetic resonance spectroscopy, where the effects of the physical state and molecular surroundings usually play a small enough role that frequencies characteristic of particular functional groups can be tabulated and used for identification. One might hope then that exchange couplings will come to be reliable indicators of features of the nuclear potential that are not sensitively probed by average nuclear position or vibrational frequencies. However, alternative outcomes can be imagined in which the dynamic interactions with the solvent play an important role in determining the average exchange coupling by modulating the free-molecule potential. If this turns out to be a dominant effect, then the interpretation of the temperature dependence of the exchange coupling may prove to be subtler than outlined here.

References

1. D.H. Jones, J.A. Labinger, and D.P. Weitekamp, *J. Amer. Chem. Soc.* **111**, 3087 (1989).
2. K.W. Zilm, D.M. Heinekey, J.M. Millar, N.G. Payne, and P. Demou, *J. Amer. Chem. Soc.* **111**, 3089 (1989).
3. J.A. Labinger, in "Comprehensive Organometallic Chemistry," (G. Wilkinson, F.G.A. Stone, and E.W. Abel, eds.), vol. 3, p. 707, Pergamon, Oxford (1982).
4. T.M. Gilbert and R.G. Bergman, *J. Amer. Chem. Soc.* **107**, 3502 (1985).
5. M.D. Curtis, L.G. Bell, and W.M. Butler, *Organometallics* **4**, 701 (1985).
6. R.A. Paciello, Ph.D. Dissertation, California Institute of Technology, Pasadena (1987).
7. T. Arliguie, B. Chaudret, J. Devillers, and R. Poilblanc, *C.R. Sceances Acad. Sci., Ser. 2* **305**, 1523 (1987).
8. A. Antinolo, B. Chaudret, G. Commenges, M. Fajardo, F. Jalon, R.H. Morris, A. Otero, and C.T. Schweltzer, *J. Chem. Soc., Chem. Commun.*, 1210 (1988).
9. D.M. Heinekey, N.G. Payne, and G.K. Schulte, *J. Amer. Chem. Soc.* **110**, 2303 (1988).
10. D.M. Heinekey, J.M. Millar, T.F Koetzle, N.G. Payne, and K.W. Zilm, *J. Amer. Chem. Soc.* **112**, 909 (1990).
11. D.M. Heinekey, *J. Amer. Chem. Soc.* **113**, 6074 (1991).
12. D.M. Heinekey and T.G.P. Harper, *Organometallics* **10**, 2891 (1991).
13. T. Arliguie, C. Border, B. Chaudret, J. Devillers, and R. Poilblanc, *Organometallics* **8**, 1308 (1989).
14. T. Arliguie, B. Chaudret, F.A. Jalon, A. Otero, J.A. Lopez, and F.J. Lahoz, *Organometallics* **10**, 1888 (1991).
15. N.F. Ramsey, *Phys. Rev.* **91**, 303 (1955).
16. G.J. Kubas, R.R. Ryan, B.I. Swanson, P.J. Vergamini, and H.J. Wasserman, *J. Amer. Chem. Soc.* **106**, 451 (1984).

17. G.J. Kubas, *ACC. Chem. Res.* **21**, 120 (1988).

18. F. Apaydin and S. Clough, *J. Phys. C* **1**, 932 (1968).

19. C.S. Johnson and C. Mottley, *Chem. Phys. Lett.* **22**, 430 (1973).

20. P.L. Corio, "Structure of High Resolution NMR Spectra," Academic Press, New York (1966).

21. K.W. Zilm, D.M. Heinekey, J.M. Millar, N.G. Payne, S.P. Neshyba, J.C. Duchamp, and J. Szczyrba, *J. Amer. Chem. Soc.* **112**, 920 (1990).

22. K.W. Zilm and J.M. Millar, *Adv. Magn. Reson.* **15**, 163 (1990).

23. L.M. Jackman and F.A. Cotton, eds., "Dynamic Nuclear Magnetic Resonance Spectroscopy," Academic Press, New York (1975).

24. G. Binsch and H. Kessler, *Angew. Chem., Int. Ed. Engl.* **19**, 411 (1980).

25. P.A.M. Dirac, "Principles of Quantum Mechanics," 4th ed., Chapter IX, Oxford Univ. Press (Clarendon), London and New York (1958).

26. C.R. Bowers and D.P. Weitekamp, *Phys. Rev. Lett.* **57**, 2645 (1986).

27. C.R. Bowers and D.P. Weitekamp, *J. Amer. Chem. Soc.* **109**, 5541 (1987).

28. R.P. Bell, "The Tunnel Effect in Chemistry," Chapman & Hall, London (1980).

29. D.J. Thouless, *Proc. Phys. Soc. London* **86**, 893 (1965).

30. M. Roger, J.H. Hetherington, and J.M. Delrieu, *Rev. Mod. Phys.* **55**, 1 (1983).

31. M.C. Cross and D.S. Fisher, *Rev. Mod. Phys.* **57**, 881 (1985).

32. J.M. Delrieu and N.S. Sullivan, *Phys. Rev. B: Condens. Matter* **23**, 3197 (1981).

33. C. Cohen-Tannoudji, B. Diu, and F. Laloe, "Quantum Mechanics," p. 455, Wiley, New York (1977).

34. D.O Harris, G.G. Engerholm, and W.D. Gwinn, *J. Chem. Phys.* **43**, 1515 (1965).

35. W.H. Press, B.P. Flannery, S.A Teukalsky, and W.T. Vetterling, "Numerical Recipes," Cambridge Univ. Press, London and New York (1986).

36. D.G. Truhlar and B.C. Garrett, *J. Chem. Phys.* **84**, 365 (1987).

37. J.S. Ricci, T.F. Koetzle, M.-J. Fernandez, P.M. Maitlis, and J.C. Green, *J. Organomet. Chem.* **299**, 383 (1986).

38. A. Landesman, *Ann. Phys. (Leibzig)* **1**, 53 (1973-74).

39. A. Abragam and M. Goldman, "Nuclear Magnetism: Order and Disorder," p. 108ff., Oxford Univ. Press (Clarendon), London and New York, 1982.

40. Y. Cha, C.J. Murray, and J. Klinman, *Science* **243**, 1325 (1989).

Chapter 3

Tunnelling Effects on NMR Lineshapes

3.1 Introduction

The usual description of intramolecular chemical exchange invokes the classical notion of molecular configurations and uses transition state theory to describe the rate of interconversion between such configurations.[1] As mentioned in Chapter 2 such a formulation cannot self-consistently treat systems such as certain transition metal hydrides in solution, which show in their NMR lineshape both resolved tunnel splittings and the broadening and collapse typical of chemical exchange. This paradox can be resolved only by describing both the spatial and spin degrees of freedom quantum-mechanically. In this chapter, the chemical exchange is described as arising from the coupling of delocalized bound eigenstates to a thermal bath. This description accounts for both the tunnel splittings and chemical exchange effects, relating them to the quantum-mechanical motion of the exchanging particles in contact with the lattice. In this way the usual assumptions of transition state theory are avoided and states above and below the barrier are treated on an equal footing. The chapter begins with a description of exchange effects on NMR spectra, followed by an outline of the density matrix formalism to be used in the treatment of thermally fluctuating couplings. Simple spatial models that provide adequate descriptions of the splittings and exchange effects in the metal hydrides are then discussed.

3.2 Chemical Exchange Effects in NMR

Nuclear magnetic resonance spectroscopy has proven to be a powerful tool for measuring rates of chemical exchange. Broadly defined, chemical exchange is any process

which transports spins among sites or configurations in a chemical system. NMR spectra can provide measurements of rates in the $1\text{-}10^6$ s^{-1} range. An understanding of the effects of chemical exchange on NMR spectra can be gained through the examination of the simplest two-spin, two-site system.[2] Two equally populated sites A and B, with Larmor frequencies ν_A and ν_B, respectively, can be characterized by the lifetimes that the nuclei remain at each site.

$$\tau_A = \tau_B = 2\tau \tag{3.1}$$

The exchange rate, R, is given by:

$$R = \frac{1}{2\tau}. \tag{3.2}$$

If the linewidths in the absence of chemical exchange, resulting from field inhomogeneities and the spin-spin relaxation times, are negligible, then

$$\frac{1}{T_{2A}} \approx \frac{1}{T_{2B}} \approx 0. \tag{3.3}$$

The corresponding resonance lineshape from the Bloch equations modified to include chemical exchange is

$$g(\nu) = K \frac{\tau(\nu_A - \nu_B)^2}{\left[\frac{1}{2}(\nu_A + \nu_B) - \nu\right]^2 + 4\pi^2\tau^2(\nu_A - \nu)^2(\nu_B - \nu)^2}, \tag{3.4}$$

where K is a normalizing constant. In slow exchange, where $0 < R < (\nu_A - \nu_B)$, the two peaks are separated by less than $(\nu_A - \nu_B)$.

$$\frac{\text{Peak Separation}}{(\nu_A - \nu_B)} = \left[1 - \frac{1}{2\pi^2\tau^2(\nu_A - \nu_B)^2}\right]^{1/2} \tag{3.5}$$

The average lifetime, τ, is easily determined knowing the ν_A and ν_B values under conditions of no exchange, and the peak separation in the intermediate exchange regime. The coalescence point is given by:

$$\tau = \frac{1}{\sqrt{2}\pi(\nu_A - \nu_B)}. \qquad (3.6)$$

The fast exchange regime, $\tau \gg (\nu_A - \nu_B)$, is characterized by a single resonance at $(1/2)(\nu_A - \nu_B)$, the average of the low-temperature slow-exchange frequencies.

The collapse of spin multiplets can occur for a nucleus A if it is coupled to a spin B undergoing chemical exchange. For the present case of mutual exchange of A and B, now coupled by J_{AB}, half of the B exchanges will cause the A resonance to change from $[\nu_A + (J_{AB}/2)]$ to $[\nu_A - (J_{AB}/2)]$; likewise, half of the B exchanges will cause the A resonance to change from $[\nu_A - (J_{AB}/2)]$ to $[\nu_A + (J_{AB}/2)]$. In slow exchange where $(\nu_A - \nu_B) \gg \tau, J_{AB}$, Eqns. 3.4 and 3.5 provide the expression for the A resonance with J_{AB} replacing $(\nu_A - \nu_B)$. This exchange process leads to collapse of spin multiplets at the Larmor frequency in the same way that site exchange leads to coalescence of peaks at the average of the Larmor frequencies.

In the case of non first-order spectra, the description of chemical exchange provided by the modified Bloch equations, while qualitatively illuminating, cannot quantitatively account for observed lineshapes. In such strongly coupled systems, transitions cannot be modelled in terms of single nucleus transitions, rather the whole system must be considered together. For this reason, density matrix descriptions of the spin system have been applied to non first-order NMR spectra. Important aspects of the density matrix formalism will be presented later in this chapter as part of the treatment of tunnelling effects.

3.3 Quantum-Mechanical Tunnelling and Chemical Exchange

Quantum-mechanical tunnelling of bound systems has numerous manifestations in molecular spectroscopy,[1] which are described as tunnel splittings in the frequency domain or as tunnel oscillations when states separated by such splittings are in coherent

superposition. Recently considerable attention has focused on the modification of tunnelling by coupling to other degrees of freedom. Important issues that have been illuminated include the way in which stochastic coupling to a thermal bath can lead to a modification of the tunnel splitting, damping of the coherent oscillation, or even indefinite suppression of tunnelling.[3-5] In certain cases where tunnelling is invoked to explain the temperature dependence of nuclear magnetic resonance lineshapes,[6-13] it has proven necessary to include the effect of thermally excited tunnelling states on the observed average behavior. In most cases, the hypothesis has been made that the observed tunnelling is a thermal average of that which would occur in each system eigenstate. A theoretical framework for this sort of quantum-mechanical motional averaging for a single particle in a double well has been given.[4] Such a description, extended to the two-particle case with spin, was presented in Chapter 2 to describe the observed tunnel splittings in certain metal hydrides.

Here, the understanding of tunnelling in motionally averaged systems is extended by considering the spectroscopic effects of the *fluctuations* of the tunnel splitting as the observed system is driven by its stochastic coupling to a lattice which is at equilibrium. The specific example will be a pair of identical spin-1/2 nuclei coupled by delocalization so that the energy eigenvalues for the spatial Hamiltonian of the two-particle potential energy surface cluster in pairs with the corresponding spatial eigenstates being symmetric or antisymmetric in exchange of the particle labels 1 and 2. Overall antisymmetry, as required by the symmetrization postulate of quantum mechanics,[14] is achieved by assignment of the singlet nuclear spin state $|0_-\rangle \equiv (2)^{-1/2}|\alpha\beta-\beta\alpha\rangle$ only to spatially symmetric levels, $|+_n\rangle$, and of the triplet states ($|1\rangle \equiv |\alpha\alpha\rangle$, $|0_+\rangle \equiv (2)^{-1/2}|\alpha\beta+\beta\alpha\rangle$, $|-1\rangle \equiv |\beta\beta\rangle$) only to spatially antisymmetric levels, $|-_n\rangle$. The situation may be summarized by a system Hamiltonian (in radians/s)

$$
\begin{aligned}
H_S = \sum_n & \left[(\omega_n - J_n/2)|+_n\rangle\langle+_n|(|0_-\rangle\langle 0_-|)\right] \\
& + \left[(\omega_n + J_n/2)|-_n\rangle\langle-_n|(|1\rangle\langle 1| + |0_+\rangle\langle 0_+| + |-1\rangle\langle -1|)\right] \\
& + \left[\omega_{0n}(|-_n\rangle\langle-_n|)(|1\rangle\langle 1| - |-1\rangle\langle -1|)\right] \\
& + \left[(\Delta\nu_{Zn}/2)(|-_n\rangle\langle+_n|)|0_+\rangle\langle 0_-| + (|+_n\rangle\langle-_n|)|0_-\rangle\langle 0_+|\right].
\end{aligned}
\tag{3.7}
$$

The subscript n indexes groups of states containing one of each of the four nuclear spin states. The first two terms account for the energy levels in zero magnetic field, where the singlet nuclear spin state $|0_-\rangle$ is associated with the n^{th} spatially symmetric spatial state $|+_n\rangle$ and lies J_n below the nuclear spin triplet ($|1\rangle$, $|0_+\rangle$, $|-1\rangle$) associated with the spatially antisymmetric eigenstate $|-_n\rangle$. The third term is the average Zeeman interaction of the spin pair, and the fourth is the chemical shift difference.

In general the spatial states could refer to any degrees of freedom not specified by the spin operators. The spin system has for simplicity been limited to two like spins interacting only through a scalar coupling. The states of unlike spins could be included in the spatial index n. The average effect of a bath is to "renormalize" the parameters defining the system.[4] It is assumed that this effect is already included in the definition of Eq. 3.7.

The goal is to describe the NMR spectrum of this system subject to the fluctuations that result from coupling to the bath. In the most general case, this coupling could have matrix elements connecting any of the states used in Eq. 3.7 and a master equation incorporating them could be derived given models of the various coupling mechanisms. Together with the Liouvillian associated with Eq. 3.7, this would give an equation of motion for any observable of the system. The Liouville space of this time evolution has a dimension $(4N)^2$, where N is the number of values of n. While a model of this sort may in some cases be needed, a great simplification will often be possible because

of two timescale separations. First, under most conditions there is a large separation in rates between the *spin-independent* processes that change n (e.g., rovibrational relaxation $\geq 10^8$ s^{-1}) and the usual spin-lattice processes (≤ 10 s^{-1}). Secondly, we will assume that for those states that have significant thermal weight, $J_n \ll \omega_n$. In order to incorporate these simplifications and to make contact with the way in which spin Hamiltonians are universally used in the literature of chemical exchange, the system Hamiltonian can be written as:

$$\begin{aligned} H_S = \sum_n |n\rangle\langle n|[(\omega_n + J_n/4) + J_n I_{zA}\cdot I_{zB} \\ +\omega_{0n}(I_{zA}+I_{zB}) + (\Delta\nu_n/2)(I_{zA}-I_{zB}). \end{aligned} \tag{3.8}$$

A *fictitious* factorization of space and spin degrees of freedom has been introduced through the projection operator

$$|n\rangle\langle n| \equiv \left[|+_n\rangle\langle+_n|\left(|0_-\rangle\langle 0_-|\right) + |-_n\rangle\langle -_n|\left(|1\rangle\langle 1| + |0_+\rangle\langle 0_+| + |-1\rangle\langle -1|\right)\right]$$

and the spin angular momentum operators $\bar{I}_A$ and $\bar{I}_B$ for the sites A and B in which the spins 1 and 2 would be located in the classical limit of localized nuclei. The forms of Eqs. 3.7 and 3.8 are exactly equivalent in the sense of having identical matrix representations, but are in different bases. The basis set in the case of Eq. 3.7 is the physically correct product of spatial and spin eigenstates allowed by the symmetrization postulate. The same matrix is obtained from Eq. 3.8 if the *fictitious* basis $\{|n,\Psi\rangle = |n\rangle|\Psi\rangle\}$ is used. Here the $|n\rangle$ are defined by the matrix elements $\langle n|(|n\rangle\langle n|)|n'\rangle = \delta_{n,n'}$ and the $|\Psi\rangle$ are identical to the singlet and triplet spin states of the two nuclei, but these are now viewed as being associated with specific molecular sites A and B, rather than with specific particles 1 and 2.

If the projection operators $|n\rangle\langle n|$ were viewed as molecular "configurations" (assignments of nuclei to molecular sites with a resulting spin Hamiltonian) then Eq. 3.8, augmented by a master equation describing the rates between configurations, would describe the usual treatments of chemical exchange.[15,16] Here the problem is

mathematically similar, but entirely different in interpretation. The operators $|n\rangle\langle n|$ and the corresponding Hamiltonian parameters have precise quantum-mechanical significance being defined in terms of the properly antisymmetrized *delocalized* states of Eq. 3.7.

Noting that terms of the Hamiltonian Eq. 3.8 for different n commute and that for a given n the first three terms commute and the chemical shift differences are small compared to kT, the equilibrium density operator is to a good approximation

$$\begin{aligned}\rho_{eq} \cong Q^{-1}\prod_n \exp(-\beta E_n|n\rangle\langle n|)\exp(-\beta\hbar\sum_n|n\rangle\langle n|J_n\bar{I}_A\cdot\bar{I}_B)\\ \times\exp(-\beta\hbar\sum_n|n\rangle\langle n|\omega_{0n}(I_{zA}+I_{zB})),\end{aligned} \tag{3.9}$$

where $\beta = 1/kT$ and Q is the partition function.

It remains to specify the master equation describing the time dependence of $|n\rangle\langle n|$ due to the coupling of the system to the lattice. A simplifying assumption is made based on the very large rate difference between bath-induced transitions which involve spin flips and those that do not. The former will be neglected at the level of the master equation and the latter will be taken as independent of both spin and of the differences in spatial state which are associated with spin through the symmetrization postulate. This last assumption is identical to that made in other contexts where the spin energies are magnetic in origin. It is certainly an approximation and its possible consequences for thermally averaged line positions are described in Chapter 4. In the context of rates, the thermal averaging over many states on the NMR timescale will result in the effect of rovibrational relaxation being characterized by a single spectral density, so little is lost by ignoring this nuance. Much is gained in simplicity, however, since now there is a single rate parameter $k_{n,n'}$ for each pair of spatial projection operators. Since nothing specific is known about the rovibrational relaxation, it is desirable to summarize it by a single parameter. To this end the downward rates will be assumed to be related to one another by $k_{n,n'} = nk_{1,0}\delta_{n,n'+1}$, where the Kronecker delta specifies stepwise relaxation along the ladder of states and the factor of n

accounts for the expected increase in rate with energy, as is seen for a harmonic oscillator linearly coupled to a bath.[17-18] The reverse rates are given by detailed balance. These issues are discussed further in Section 3.5, where the solution of the master equation describing the averaging over spatial eigenstates is presented.

3.4 Spin Dynamics of Tunnelling and Chemical Exchange

Relaxation effects arising from large, temperature-dependent couplings in the AB spin system are calculated using the Wangsness-Bloch-Redfield matrix formalism of NMR.[19-20] The Redfield formalism has been used in studying the coupling of electronic states of dimers in crystal lattices by Wertheimer and Silbey.[5]

The oscillations of the exchange coupling around its average value create oscillating, off-diagonal couplings between density matrix elements of the static spin-lattice Hamiltonian. The effects of an oscillating scalar coupling of arbitrary size relative to the chemical shift difference were calculated by adding a relaxation term resulting from such a coupling to the unperturbed Hamiltonian of the spin system.

Surprisingly, this calculation is apparently absent from the magnetic resonance literature. The textbook cases treated[21] are for no chemical shift and for a difference in Larmor frequencies much greater than the scalar coupling. These cases do not contain the physics of the general case. In the former case, the fluctuating coupling has no effect on the spectrum, while in the latter it is incapable of causing collapse of the distinct resonance lines into one. One possible reason for the present case having been overlooked is the nearly universal use of an interaction representation in which all thermally averaged spin interactions are transformed away.[20] In such a representation, the off-diagonal part of the scalar coupling gives rise to time-dependent relaxation superoperator matrix elements which are usually discarded without adequate justification. In the present approach, the interaction representation used removes only the average Larmor frequency of the two sites. The average chemical shift difference and scalar coupling are included in a

Liouvillian which together with the relaxation superoperator specifies the time dependence in this frame. As will be shown, the relaxation superoperator due to the fluctuating scalar coupling is then time-independent and the differential equations are straightforward.

The spin system Hamiltonian can be written:

$$H_T = H_0 + H_R(t), \tag{3.10}$$

where H_0 is the average spin Hamiltonian and $H_R(t)$ is the time-dependent relaxation term caused by the fluctuating coupling. The H_0 and $H_R(t)$ are written as

$$H_0 = \omega_A I_{ZA} + \omega_B I_{ZB} + \bar{J}(\bar{I}_A \cdot \bar{I}_B) \tag{3.11}$$

$$H_R(t) = \delta J(t)(\bar{I}_A \cdot \bar{I}_B). \tag{3.12}$$

The relaxation Hamiltonian arises from instantaneous fluctuations of the scalar coupling around its equilibrium, average value; this is represented by the term $\delta J(t) = J(t) - \bar{J}$. The equation of motion under the action of the Hamiltonians, Eqs. 3.11 and 3.12, is given by:

$$\frac{d\rho(t)}{dt} = [\rho, H_0] - \int_0^\infty [H_R(t), [H_R(t-\tau), \rho(t) - \rho^0]]d\tau. \tag{3.13}$$

The above equation of motion (Eq. 3.13) is usually expressed as a matrix in order to facilitate numerical evaluations. Two methods for representing this in matrix form exist: evaluating matrix elements of relevant operators in a basis of *basis functions*,[19-20] or representing operators as vectors in a basis of basis operators.[21] The current treatment uses the later method known as the superoperator formalism, discussed in detail by Hoffman.[22] The operator basis for this treatment will consist of the level-shift operators formed by the singlet/triplet spin state basis. The problem factors according to the number of Larmor frequency quanta connecting the levels in superposition. Two sets of level-shift operators that correspond to dipole allowed or single-quantum transitions ($\Delta m = \pm 1$) exist. Choosing the $\Delta m = +1$ will yield the same results as choosing the $\Delta m = -1$, so that a sufficient basis of level shift operators is

$|0_+\rangle\langle -1|$, $|0_-\rangle\langle -1|$, $|1\rangle\langle 0_+|$, $|1\rangle\langle 0_-|$.

As a check, the same treatment has also be carried out in the simple product basis of the AB spin pair and yields the same results.

In the superoperator formalism, the master equation of motion for the density matrix is given by:

$$\frac{d\rho_{ij}}{dt} = (\Gamma_{jk} - i\Lambda_{jk})\rho_{ij} \tag{3.14}$$

where Γ_{jk}, the relaxation superoperator, and Λ_{jk}, the Liouvillian of the unperturbed Hamiltonian, are given by:

$$\begin{aligned}\Gamma_{jk} &= \int_0^\infty \mathrm{Tr}\{[Q_j, H_R(t)][Q_k^+, H_R(t-\tau)]\} \\ &= k_J \mathrm{Tr}\{[Q_j, I_A \cdot I_B][Q_k^+, I_A \cdot I_B]\}\end{aligned} \tag{3.15}$$

and

$$\Lambda_{jk} = \mathrm{Tr}\{[Q_j, Q_k](H_0)\}. \tag{3.16}$$

In these expressions for the superoperators, Q_j is the level-shift operator basis, and k_J is the zero-frequency spectral density of the autocorrelation function of the fluctuating part of the scalar coupling. The calculation of k_J for a given model of rovibrational relaxation and tunnelling will be discussed in a subsequent section on the spatial aspects of the problem. Evaluating the spin commutators and traces in the elements of (Γ - iΛ) matrix yields a 4x4 matrix which consists of two 2x2 matrices.

$$(\Gamma - i\Lambda)_1 = \begin{matrix}|0_+\rangle\langle -1| \\ |0_-\rangle\langle -1|\end{matrix}\begin{bmatrix} -i(\nu_A + \nu_B)/2 & -i(\nu_A - \nu_B)/2 \\ -i(\nu_A - \nu_B)/2 & -k_J/2 - iJ - i(\nu_A + \nu_B)/2 \end{bmatrix}$$

$$(\Gamma - i\Lambda)_2 = \begin{matrix}|+1\rangle\langle 0_+| \\ |+1\rangle\langle 0_-|\end{matrix}\begin{bmatrix} -i(\nu_A + \nu_B)/2 & i(\nu_A - \nu_B)/2 \\ i(\nu_A - \nu_B)/2 & -k_J/2 + iJ - i(\nu_A + \nu_B)/2 \end{bmatrix} \tag{3.17}$$

Comparing this result with the well-known phenomenological equations for two-site chemical exchange, it is found that k_J is the chemical exchange rate. In contrast to the usual treatment, the present approach derives this rate from a specific mechanism (fluctuating tunnel splitting) and provides a microscopic recipe for its evaluation in the next section.

For some specified initial conditions of the spin system, expressions for the time-dependent density matrix can now be found. Assuming that the evolution of the density matrix starts with the initial conditions present after a $(\pi/2)_Y$ pulse, the expression for the complex signal proportional to the two components of transverse magnetization is given by:

$$S(t) = \mathrm{Tr}\{\sigma(t) I_+\}. \tag{3.18}$$

After solving for the eigenvalues and eigenvectors of the $(\Gamma - i\Lambda)$ matrix, the signal can be expressed as

$$\begin{aligned} S(t) = {} & (1/4)\{[(c/2+Q)/Q]\exp[(-(c+2ia)/2+Q)t]\} \\ & -(1/4)\{[(c/2-Q)/Q]\exp[(-(c+2ia)/2-Q)t]\} \\ & +(1/4)\{[(c^*/2+Q^*)/Q^*]\exp[(-(c^*+2ia)/2+Q^*)t]\} \\ & -(1/4)\{[(c^*/2+Q^*)/Q^*]\exp[(-(c^*+2ia)/2-Q^*)t]\}. \end{aligned} \tag{3.19}$$

In the above expression, $a \equiv (\nu_A + \nu_B)/2$, $d \equiv (\nu_A - \nu_B)/2$, $c \equiv k_J/2 + iJ$, and $Q \equiv [(c/2)^2 - d^2]^{1/2}$. Note that c^* is the complex conjugate of c, and Q^* is analogous to Q with c^* substituted for c. The full derivation of Eq. 3.19 is carried out in Appendix 1.

3.5 Spatial Dynamics of Tunnelling and Chemical Exchange

Abragam[21] presents two descriptions of spin-lattice coupling for the treatment of relaxation effects in NMR, one classical and the other quasi-classical. The formulation of the correlation function relating fluctuations in lattice parameters to relaxation of the spin

system depends critically on how the lattice is treated. The earliest treatment of relaxation effects in NMR was put forth by Bloembergen, Purcell, and Pound (BPP).[23] The BPP theory assumes classical behavior of the lattice parameters affecting the spin system, assigning random functions to describe the time dependence of these degrees of freedom. The quasi-classical description of the lattice results from the assumption that there exist a large number of lattice degrees of freedom, forming a continuum of lattice states. Both these models include simplifications which are not valid in the case of the metal hydrides. The model of a well-defined ladder of spatial states which are responsible for the modulation of the exchange coupling allow the correlation function to be treated in a completely quantum-mechanical way. The expression for the autocorrelation function of the scalar coupling may be written:

$$\langle J(0)J(t)\rangle = \sum_{i,j} J_i p_i J_j c_i^j(t). \tag{3.20}$$

The $c_i^j(t)$ are the conditional probabilities that a particle is in state j at time t when it started in state i at time zero. The probability p_i is the fractional equilibrium population of state i. The master equation describing the time-dependent populations of the spatial states as a function of time is given by:

$$\frac{dp_i}{dt} = -\sum_i k_{ij} p_i + \sum_j k_{ji} p_j \tag{3.21}$$

where the k_{ij} are the transition rates between pairs of eigenstates. The solution of Eq. 3.21 (coupled first-order differential equations with constant coefficients) by finding eigenmodes, leads to the expression for the for the $c_i^j(t)$:[24]

$$c_i^j(t) = \sum_k \hat{U}_{jk}^{-1} \hat{U}_{ki} \exp(-\lambda_k t), \tag{3.22}$$

where $\hat{U}$ is the transformation which diagonalizes the matrix of rates in Eq. 3.21.

The calculation of the chemical exchange rate resulting from fluctuations in the tunnel splitting can now be calculated. Recalling that the exchange rate k_J is the area under the autocorrelation function of $\delta J(t)$, it has the form:

$$k_J = \int_0^\infty (\langle J(0)J(t)\rangle - \bar{J}^2)dt. \tag{3.23}$$

The average value of the exchange coupling, $\bar{J}$, is the Boltzmann-weighted average over the pairs of spatial states. The usual expression is

$$\bar{J} = \frac{\sum_i J_i \exp(-\beta E_i)}{Q}, \tag{3.24}$$

where $\exp(-\beta E_i)/Q = p_i$, the equilibrium population of the i^{th} spatial manifold and $Q = \sum_i \exp(-\beta E_i)$. The validity of Eq. 3.24 will be discussed in Chapters 4 and 5. The autocorrelation function for the scalar coupling is modulated by the changing populations of the spatial pairs over which J is summed.

$$\langle J(0)J(t)\rangle = Q^{-1}\sum_{i=1}^{n} J_i \exp(-E_i / kT) \times \sum_{i=1}^{n} J_i c_i^j(t) \tag{3.25}$$

$J_i \equiv$ the tunnelling splitting of the i^{th} state, $E_i \equiv$ the energy of the i^{th} pair of spatial states, and $c_i^j(t) \equiv$ the population of the j^{th} pair of spatial states at a time t given that at t=0 the population was all in the i^{th} pair.

3.6 Results and Summary

The dynamic NMR spectra of the tunnelling trihydrides result from the temperature dependence of the scalar coupling and the factor k_J. These two quantities are dependent upon the nature and kinetics of the ladder of spatial states which determine the randomly fluctuating exchange coupling. At this time, there is only one set of

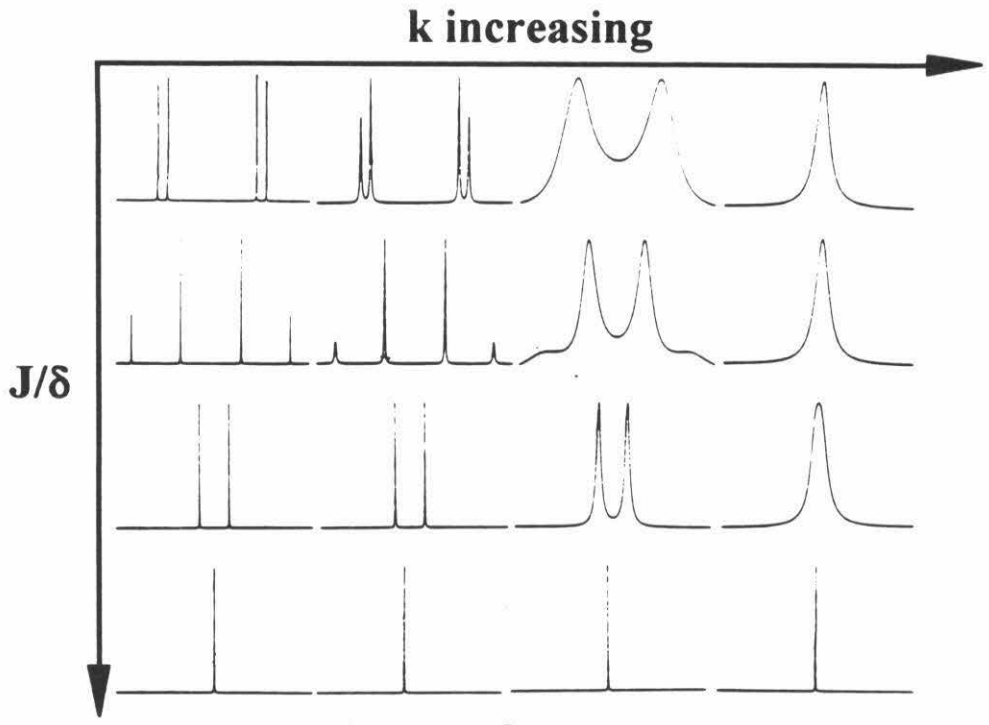

Figure 3.1. Effects of increasing J/δ and k_J on an AB spin system. Temperature-dependent spectra show the effects of increasing J/δ and k_J.

experimental lineshapes as a function of temperature available for a tunnelling trihydride system, the molecule $Cp^*RuH_3[P(CHMe_2)_3]$.[25] The low-temperature appearance of the spectra is typical of a weakly coupled AB_2 spin system, where $J/(\nu_A - \nu_B) \ll 1$. With a small increase in temperature, the system becomes a strongly coupled AB_2 system ($J/(\nu_A - \nu_B) \geq 1$), displaying characteristic overlap of and exchange broadening of the spectral lines. Figure 3.1 show the separate and combined effects of a changing $J/(\nu_A - \nu_B)$ ratio and an increasing exchange rate on an AB system. In order to extract the experimental value for pairwise exchange from the published AB_2 spectra, it was assumed that identical rates for the two possible A⇔B exchange processes and the values of k_J and $\bar{J}$ were systematically varied to find a best fit spectrum. These calculations used the standard phenomenological program DNMR5.

The forms of the potential energy surface that determine the magnitude of the fluctuations and the value of k_J were discussed in Chapter 2. A symmetric double well yields fits to the data of Arliguie *et al* for $Cp^*RuH_3[P(CHMe_2)_3]$.[25] The barrier height found for the double well that yields fits to the temperature dependent tunnel splittings is 6.8 kJ mol^{-1}. A plot of ln*k* vs. 1/T for the classically determined exchange rate yields an Arrhenius activation energy for exchange of 50 kJ mol^{-1}.

In the quantum-mechanical treatment, the tunnel splitting in each level of a harmonic ladder was calculated using a form which approximately parametrizes the exact values found in a previous treatment.[24] This expression is given by:

$$J(n) = p^n(J_0). \tag{3.26}$$

The asymptotic value of the tunnel splitting at or above the barrier was chosen as the semiclassical WKB value

$$J(n) = \frac{\omega_0}{\pi}\exp\left(-\frac{1}{\hbar}\int_{-a}^{a}\sqrt{2m(V(x)-E)}dx\right), \tag{3.27}$$

where -a and a are the classical turning points. The large rate difference between *spatial* transitions that involve a spin transition and those that do not allows the former to be neglected in this treatment. This simplification, mentioned earlier in reducing the dimension of the Liouville space for which the fluctuating terms were calculated, allows the use of a single rate parameter for each spatial level.

Representative temperature dependent spectra are provided by Arliguie *et al*.[25] Over the temperature range 193-243 K, the average coupling increases from a value of 105 Hz to 300 Hz (extrapolated value). The chemical exchange rate that one extracts for these spectra increases over the same temperature range from 0.1 Hz to 1500 Hz. Both scalar coupling and chemical exchange rates are plotted versus temperature in Figure 3.3. Fits resulting from the present treatment are also shown in Figure 3.3.

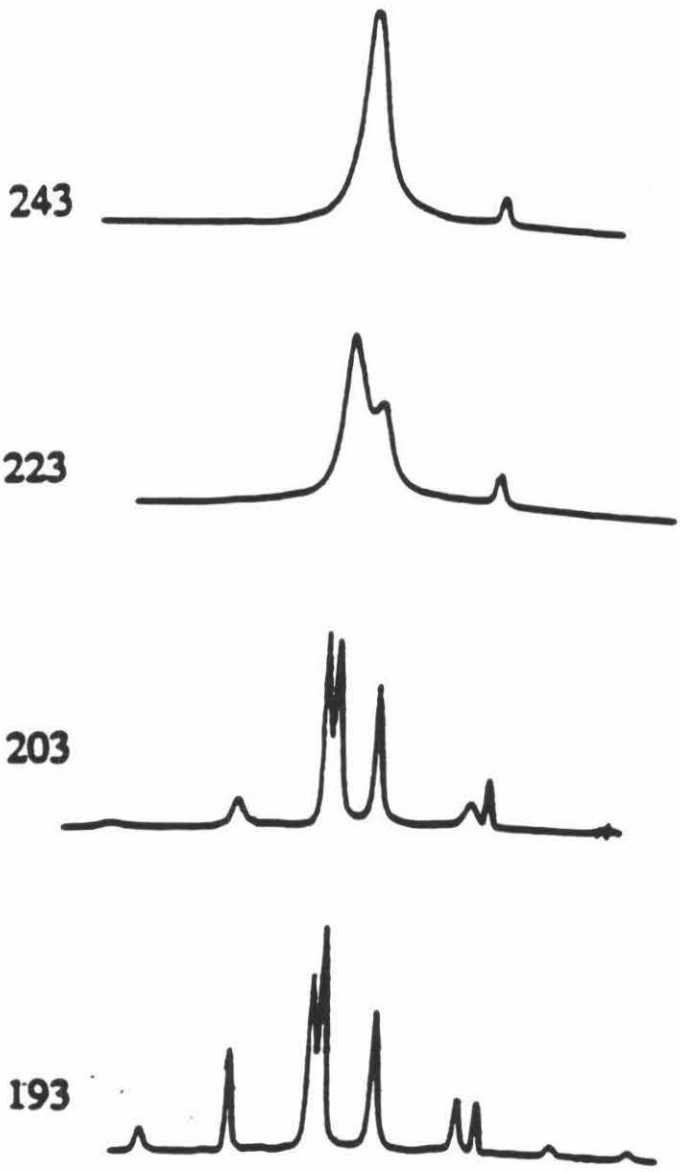

Figure 3.2. The dynamic NMR spectra observed for the AB_2 spin system of $Cp^*RuH_3[P(CHMe_2)_3]$.[25]

From Figure 3.3, it is readily seen that the temperature increase for the exchange rate is much sharper than that for the average scalar coupling. Any theory which yielded the same temperature dependence for both of these quantities would be unable to fit available data. Such relationships have been postulated (but not derived) in other contexts where tunnelling effects are seen in NMR lineshapes.[7,8]

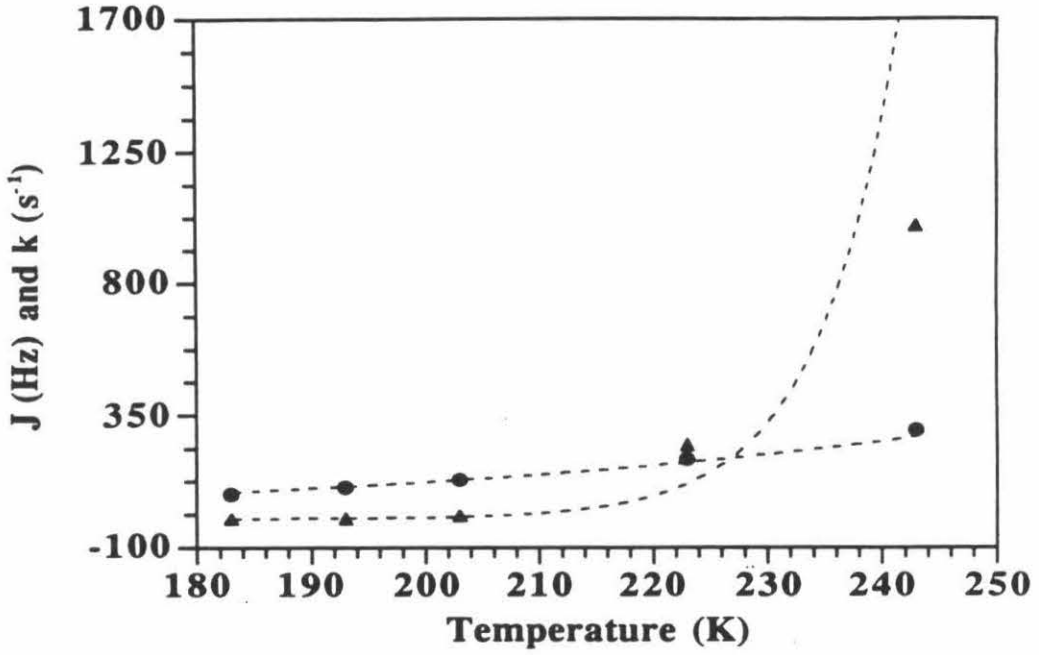

Figure 3.3. The scalar coupling and exchange rate vs. temperature for $Cp^*RuH_3[P(CHMe_2)_3]$. Fits to experimental values for scalar couplings (•) and exchange rates (▲) as a function of temperature are given by the dashed lines.

The parameters that yield the fits in Figure 3.3 differ from the parameters that one obtains from treating the exchange process classically using transition state theory. The fitting procedure consisted of varying the ground state tunnel splitting and harmonic frequency in a grid search to match the temperature-dependent scalar couplings observed. For sets that yielded good fits, the exchange rate was calculated by varying the vibrational relaxation rate k_{10}. Best fits to the exchange rate were obtained with a relaxation rate of k_{10} = 100 ps. The barrier height corresponding to the best-fit parameters is 57 kJ mol^{-1}. A total of nine states below the barrier contribute to the observed behavior. For the average tunnel splitting, 95% of the observed total resulted from the lowest-lying 7 states. However, for the exchange rate, the three highest energy states contributed nearly 85% of the observed rate.

Additional computational effort in modeling the space-spin dynamics of tunnelling metal hydrides will only be warranted at such time as more experimental data is available.

Low wavenumber infra-red absorption spectra will determine the vibrational quanta which affect both the average tunnel splitting and its fluctuations from equilibrium. While the solution of one-dimensional potential energy surfaces or parametrized harmonic ladders obviously approximates the real potential surface governing the quantum-mechanical tunnelling in these systems, the solutions to higher dimensional potentials cannot be validated by currently available experimental data. Results from infra-red and additional dynamic NMR experiments will establish the connection between various spatial parameters, such as the barrier heights and vibrational quanta, and the resulting NMR spectra.

The treatment of fluctuating couplings presented in this chapter was motivated by the dynamic behavior of proton magnetic resonance spectra of certain metal hydrides. This treatment provides a unified framework to account for the observed tunnel splittings and chemical exchange processes observed in these compounds. Other treatments which neglect the quantum-mechanical behavior of these metal hydrides in calculating chemical exchange effects fail in presenting a self-consistent physical model for the intramolecular particle exchange.

The similarity of the correlation function derived in the present treatment to expressions in other examples of fluctuation-dissipation theories[26-27] is quite apparent. This similarity underscores the fundamental differences between the present treatment and previous treatments of chemical exchange. The chemical exchange rate k_J is related to the large fluctuations of the autocorrelation function of the scalar coupling around its average value $\overline{J}$. It may also be viewed as the dephasing rate of the coherent tunnelling motion whose frequency is $\overline{J}$. For the spatial model used, the calculated exchange rate has a magnitude and temperature dependence strikingly different from the average scalar coupling, yielding a satisfactory fit to the data as shown in Figure 3.3. The results presented place quantum-mechanical chemical exchange in the wider class of problems involving the fluctuation-dissipation theorem.

References

1. R.P. Bell, "The Tunnel Effect in Chemistry," Chapman and Hall, London, 1980.
2. E.D. Becker, "High Resolution NMR, Theory and Chemical Applications," Academic Press, New York, 1980.
3. R. Silbey and R.A Harris, *J. Chem. Phys.* **93**, 7062 (1989).
4. P.E. Parris and R. Silbey, *J. Chem. Phys.* **83**, 5619 (1985).
5. R. Wertheimer and R. Silbey, *Chem. Phys. Lett.* **75**, 243 (1980).
6. a) D.J. Thouless, *Proc. Phys. Soc. London* **86**, 893 (1965); b) M. Roger, J.H. Hetherington, and J.M. Delrieu, *Rev. Mod. Phys.* **55**, 1 (1983); c) M.C. Cross and D.S. Fisher, *Rev. Mod. Phys.* **57**, 881 (1985); d) J.M. Delrieu and N.S. Sullivan, *Phys. Rev. B.* **23**, 3197 (1973).
7. a) E.O. Stejskal and H.S. Gutowsky, *J. Chem. Phys.* **28**, 388 (1958); b) F. Apaydin and S. Clough, *J. Phys. C.* **1**, 932 (1968); c) C.S. Johnson and C. Mottley, *Chem. Phys. Lett.* **22**, 430 (1973).
8. H.H. Limbach and J. Hennig, *J. Chem. Phys.* **71**, 3120 (1979).
9. D.H. Jones, J.A. Labinger, and D.P. Weitekamp, *J. Amer. Chem. Soc.* **111**, 3087 (1989).
10. C.R. Bowers, D.H. Jones, N.D. Kurur, J.A. Labinger, M.G. Pravica, and D.P. Weitekamp, *Adv. Magn. Reson.* **14**, 269 (1990).
11. K.W. Zilm, D.M. Heinekey, J.M. Millar, N.G. Payne, and P. Demou, *J. Amer. Chem. Soc.* **111**, 3089 (1989).
12. D.M. Heinekey, J.M. Millar, T.F. Koetzle, N.G. Payne, and K.W. Zilm, *J. Amer. Chem. Soc.* **112**, 909 (1990).
13. K.W. Zilm, D.M. Heinekey, J.M. Millar, N.G. Payne, S.P. Neshyba, J.C. Duchamp, and J. Szczyrba, *J. Amer. Chem. Soc.* **112**, 920 (1990).
14. P.A.M. Dirac, "Principles of Quantum Mechanics," (4^{th} ed.), chap. IX, Oxford, Clarendon Press, 1958.

15. "Dynamic Nuclear Magnetic Resonance Spectroscopy," (L.M. Jackman and F.A. Cotton, eds.), Academic Press, New York, 1975.

16. G. Binsch and H. Kessler, *Angew. Chem., Int. Ed. Engl.* **19**, 411 (1980).

17. R.J. Rubin and K.E. Shuler, *J. Chem. Phys.* **25**, 59 (1956).

18. E.W. Montroll and K.E. Shuler, *J. Chem. Phys.* **26**, 454 (1957).

19. R.K. Wangsness and F. Bloch, *Phys. Rev.* **89**, 728 (1953).

20. A.G. Redfield, *Adv. Magn. Reson.* **1**, 1 (1965).

21. A. Abragam, "The Principles of Nuclear Magnetism," chap. 8, Oxford University Press, London and New York, 1961.

22. R.A. Hoffman, *Adv. Magn. Reson.*, **4**, 87 (1970).

23. N. Bloembergen, E.M. Purcell, and R.V. Pound, *Phys. Rev.* **73**, 679 (1948).

24. N.D. Kurur, Ph.D. Dissertation, California Institute of Technology, 1992.

25. T. Arliguie, C. Border, B. Chaudret, J. Devillers, and R. Poilblanc, *Organometallics* **8**, 1308 (1989).

26. D. Chandler, "Introduction to Modern Statistical Mechanics," Oxford University Press, Oxford and New York, 1987.

27. R. Kubo, *J. Phys. Soc. Japan* **12**, 570 (1970).

Part II

Stochastic Averaging in Magnetic Resonance

Chapter 4

Stochastic Averaging in Magnetic Resonance

4.1 Introduction

Through the measurement of state-dependent spectra, magnetic resonance can provide information on molecular potentials controlling equilibria and chemical exchange. In the metal hydrides, the coherent tunnel splitting (Chapter 2) and the chemical exchange (Chapter 3) result directly from the tunnelling exchange of spatial degrees. "Stochastic averaging" refers more generally to the motional or thermal averaging of spin parameters on the timescale of the NMR experiment. This averaging of spin parameters can be the result of averaging over any degrees of freedom in a molecule, such as vibrational or rotational levels, or conformers of a molecule. The quantity $\overline{J}$ of Eq. 3.25 is an example of the accepted concept of a stochastically averaged spin Hamiltonian parameter. The quantum-mechanical consideration of nuclear motion in the transition metal hydrides led to a reexamination of the much broader question of the validity of such averages, which seems to have gone unquestioned through nearly forty years of use in magnetic resonance.

The traditional form of the average spin parameter is based on an implicit factorization of spin and spatial degrees of freedom. Such averages neglect spin-dependent energies in the potential for nuclear motion and are therefore not results of equilibrium statistical mechanics. In this chapter a new form of the average spin parameter is proposed which is shown to differ both conceptually and quantitatively from the traditional form. Section 4.2 reviews the history and use of the traditional form. Section 4.3 presents the new expression for the average spin parameter. Other expressions for

temperature-dependent spin parameters and a discussion of the qualitative differences between the various formulations are discussed in Sections 4.4 and 4.5.

4.2 The Traditional Stochastic Average

For over forty years it has been accepted[1-36] that spin states are transported between spatial states with spin-independent rates. This unexamined assumption was stated clearly in the seminal work of Bloembergen, Purcell and Pound:[1] "The atom or molecule is simply a vehicle by which the nucleus is conveyed from point to point. We thus neglect the reaction of magnetic moments of the nuclei upon the motion." This notion is the basis for all existing formalisms for calculating the magnetic resonance lineshapes of spin systems undergoing spatial rate processes, most importantly, chemical exchange.

Some of the earliest investigations in NMR involved the observation of temperature-dependent spin parameters. Early studies of the chemical shift effect found that observed shifts in methanol and ethanol were temperature-dependent.[37,38] The temperature dependence was correctly attributed to the associative equilibrium of the hydroxyl protons in the molecule. Other temperature-dependent spin parameters were recognized as averages over the conformers of the molecule. Many early subject molecules for studying these effects were those with distinguishable conformers resulting from rotation around a carbon-carbon single bond.

Quantum-statistical examples of the traditional average of a spin parameter as a population-weighted sum over n spatial eigenstates can be traced to early NMR studies of tunnelling in low-temperature methyl groups, where the bound rotational eigenstates of the three-fold well act as separate conformers with different spin parameters. While the validity of the traditional form was questioned in some of the earlier treatments of the tunnelling methyl system,[39-41] no rigorous derivation has been carried out.

The well-known and universally accepted expression for a spin Hamiltonian parameter (chemical shift, scalar coupling, dipolar coupling, etc.) in the fast-exchange limit is:

$$\overline{X} = \frac{\sum_n X_n \exp(-\beta E_n)}{\sum_n \exp(-\beta E_n)} = \sum_n p_n X_n, \tag{4.1}$$

where X_n is the value of this parameter in the spin Hamiltonian of the n^{th} spatial manifold and p_n is viewed as the probability of the system being in that manifold, irrespective of spin state. The sum may be over molecular eigenstates, as in the tunnelling methyl groups or metal hydrides, or over large groups of eigenstates, as when n indexes molecular conformers. Thus, this expression converges with earlier prescriptions where averages were taken over classical configurations of the nuclear positions.[2-4] The traditional prescription, which neglects spin energies, is to express the molecular partition function q as a sum of parts q_n associated with each indexed manifold. The probability for each manifold is $p_n = q_n/q$, and the ratio of two such probabilities is

$$p_n / p_{n'} = \exp\left[-\Delta A_{nn'} / RT\right] = \exp\left[(-\Delta U_{nn'} + T\Delta S_{nn'}) / RT\right], \tag{4.2}$$

where $\Delta A_{nn'} = -RT\ln(q_n / q_{n'})$ is the difference in the molar Helmholtz free energies of the manifolds. These energy differences can be divided into differences in energy $\Delta U_{nn'}$ and entropy $\Delta S_{nn'}$. The connection to molecular energies is $\Delta U_{nn'} = N_A(E_n - E_{n'})$, where E_n is the common spatial contribution to free energy of the n^{th} manifold of spin states and N_A is Avogadro's number.

Several aspects of the traditional average render it conceptually suspect. The weighted average of any spatial state is independent of the spin state as the spin energies are ignored in the Boltzmann weightings. Thus, Eq. 4.1 is not a result of equilibrium statistical mechanics. The neglect of spin energies could be justified if transitions between spatial states are rigorously concerted for all spin states, a dynamic of the factorization of

the Liouville space into spin and space factors. Then Eq. 4.1 can be viewed as the average parameter associated with the zero-frequency eigenmode of such a set of rate equations for the spatial Liouville space alone. This factorization results in the spin trajectories depending on the spatial degrees of freedom, but the spatial trajectories being rigorously independent of spin. This cannot, however, be strictly correct, since dynamic equations which neglect the effect of spin-dependent energies cannot embody the return to equilibrium since spin energies unambiguously contribute to the total energy at equilibrium. Thus, the traditional form of the average spin parameter is not derivable from equilibrium statistical mechanics and is only clearly derivable from a dynamic picture with an assumption which is at best approximate and the effects of which are unexamined.

4.3 An Alternative Stochastic Average

This section presents a treatment of spin parameters averaged over n spatial states or configurations, yielding expressions for the stochastic average of a spin parameter which are derivable from equilibrium statistical mechanics. The conceptual departure from previous treatments of stochastic averages in NMR is that the current formulation treats the desired quantity as a difference between well-defined average energies of spin system eigenstates. The spin eigenbasis $|\gamma\rangle$ is often independent of spatial state and if this is assumed it is the basis needed to describe the stochastically averaged spectrum. The actual molecular energy eigenvalues may be written as:

$$E_n^{\gamma} = E_n + E_{\gamma}(n), \tag{4.3}$$

where γ indexes a spin eigenstate within the n^{th} manifold. Since spin Hamiltonians are traceless by construction, the spin-dependent contributions $E_{\gamma}(n)$ sum to zero in each manifold. The spatially-averaged energy of a particular spin eigenstate $|\gamma\rangle$ is

$$E_\gamma = \frac{\sum_n E_n^\gamma \exp(-A_n^\gamma / RT)}{\sum_n \exp(-A_n^\gamma / RT)} = \sum_n p_n^\gamma E_n^\gamma . \qquad (4.4)$$

Note that Eq. 4.4 uses the complete manifold free energy, $A_n^\gamma = N_A E_n^\gamma - TS_n$, including spin terms, according to the prescription of equilibrium statistical mechanics. Each such summation is restricted to a particular spin state and the distribution among spatial states for each spin state is assumed to be the equilibrium distribution defined by the lattice temperature. Thus p_n^γ is the conditional probability of being in the n^{th} spatial manifold, given that the spin state is $|\gamma\rangle$. As in the usual formulation, no specification of the distribution of population among spin states is needed.

The JKW hypothesis[42] is that the spectral line positions for sufficiently fast exchange between spatial manifolds are the Bohr frequencies corresponding to differences between the average energies given in Eq. 4.4:

$$\nu_{\gamma\gamma'} = (E_\gamma - E_{\gamma'}) / h . \qquad (4.5)$$

The corresponding motionally-averaged spin Hamiltonian parameters are those which generate this spectrum. This extremely simple hypothesis had apparently never been considered as an alternative notion of stochastic averaging, although it has the conceptual advantage of being based purely on equilibrium statistical mechanics and requiring no approximations in its evaluation for a given model.

A simple illustration of the new formulation can be carried out for a spin Hamiltonian with only two distinct eigenvalues, $\pm X_n/2$ (in Hz), for each n. The proposed alternative to Eq. 4.1 is (with $\gamma = \pm$)

$$\langle X \rangle = h^{-1} \sum_n (p_n^+ E_n^+ - p_n^- E_n^-) \qquad (4.6)$$

$$= (2h)^{-1} \sum_n \left[(p_n^+ - p_n^-)(E_n^+ + E_n^-) + (p_n^+ + p_n^-)(E_n^+ - E_n^-) \right] \tag{4.7}$$

$$= \sum_n \left[(p_n^+ - p_n^-) E_n / h + \frac{1}{2}(p_n^+ + p_n^-)(X_n) \right]. \tag{4.8}$$

Since $p_n \cong (p_n^+ + p_n^-)/2$ for typical parameters, the difference between the formulations of Eq. 4.1 and Eq. 4.8 is essentially the sum over n of the first term in brackets of Eq. 4.8. The difference vanishes at infinite or zero temperature and at all temperatures if either the E_n or the X_n are all degenerate. In all cases where $\langle X \rangle$ might provide information on the molecular potentials, this difference is finite. It may be viewed as arising from the dependence of average molecular configuration on the spin Hamiltonian, in contrast to the usual analysis which includes only the dependence of the spin Hamiltonian on molecular configuration.

The derivation of the expression for an averaged scalar coupling using the new formulation illustrates the differences between the two forms of the stochastic average. The derivations are carried out from two different starting points: the simple-product, weakly coupled case, and the strongly coupled, or zero-field, case.

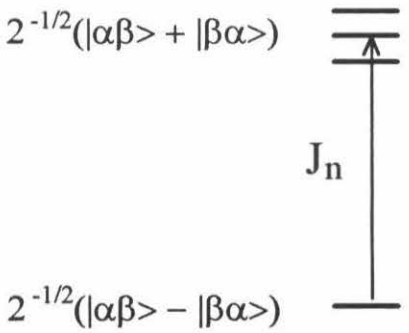

Figure 4.1. Eigenstates and transition energy for the strongly coupled, low-field AB spin pair

Figure 4.1 shows the energy level diagram for the strongly coupled, or low-field, AB spin pair. Neglecting chemical shift terms and, for illustration, considering a harmonic spatial energy and a scalar coupling J, the spin states are separated by the quantity J, having total energies given by:

$$E_n^{\pm} = E_0 + n\omega \pm (J_n/2). \tag{4.9}$$

The average of the spin parameter J is written as a difference between the average energies of states with a +J/2 spin energy term and those with a -J/2 spin energy term.

$$\langle J \rangle = \sum_n [p_n^+ (E_n + J_n/2) - p_n^- (E_n - J_n/2) \tag{4.10}$$

$$= \sum_n [p_n^+ (E_0 + n\omega + J_n/2) - p_n^- (E_0 + n\omega - J_n/2)] \tag{4.11}$$

$$= \sum_n [(p_n^+ - p_n^-)E_0 + (p_n^+ - p_n^-)n\omega + (p_n^+ + p_n^-)J_n/2)] \tag{4.12}$$

$$= \sum_n [(p_n^+ - p_n^-)n\omega + (p_n^+ + p_n^-)J_n/2)]. \tag{4.13}$$

The first term in Eq. 4.12 is dropped from the final result because any term that is a constant multiplied by the sum over n of the differences in populations of the "plus" and "minus" states will necessarily equal zero. In this case:

$$\sum_n [(p_n^+ - p_n^-)E_0] = E_0 \sum_n [(p_n^+ - p_n^-)] = 0. \tag{4.14}$$

This is a result of the fact that the "plus" and "minus" spin states are summed over separately in obtaining the average energies. These ladders of states over the n spatial levels have separate partition functions, thereby removing any dependence of the averaged parameter on any zero-point energy as in any equilibrium calculation. Eq. 4.14 also shows that a constant term added to Eq. 4.9 to make the spin Hamiltonian traceless would not affect the results. The harmonic spatial energy $n\omega$ can be replaced by any set of values E_n.

An alternative approach to formulating the expression for the new form of the averaged spin parameter uses the weakly coupled, high-field AB spin system. The diagram for this picture is given in Figure 4.2.

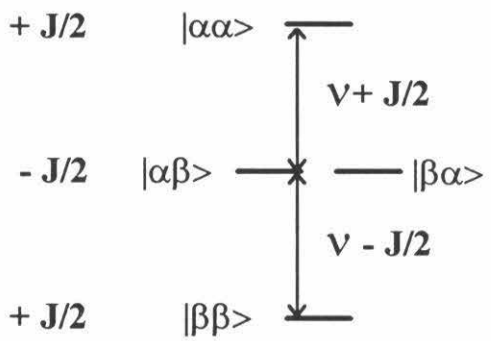

Figure 4.2. Eigenstates, transition energies, and scalar coupling terms for the weakly coupled, high-field AB spin pair.

The Zeeman terms in the summation can be simplified using the average of the A and B Zeeman frequencies, $\nu = (\nu_A + \nu_B)/2$. By defining the population of the $|\alpha\alpha\rangle$ state as $p_{\alpha\alpha}$ and the other populations in an analogous manner, the expression for the average scalar coupling becomes:

$$\langle J \rangle = \sum_n [p_{\alpha\alpha}(E_n + \nu + J_n/4) - p_{\beta\alpha}(E_n - J_n/4)] - [p_{\alpha\beta}(E_n - J_n/4) - p_{\beta\beta}(E_n - \nu + J_n/4)] \tag{4.15}$$

$$= \sum_n [(p_{\alpha\alpha} - p_{\beta\alpha} - p_{\alpha\beta} + p_{\beta\beta})E_0 + (p_{\alpha\alpha} - p_{\beta\alpha} - p_{\alpha\beta} + p_{\beta\beta})n\omega + (p_{\alpha\alpha} + p_{\beta\alpha} + p_{\alpha\beta} + p_{\beta\beta})(J_n/4) + (p_{\alpha\alpha} - p_{\beta\beta})\nu] \tag{4.16}$$

$$= \sum_n [(p_{\alpha\alpha} - p_{\beta\alpha} - p_{\alpha\beta} + p_{\beta\beta})n\omega + (p_{\alpha\alpha} + p_{\beta\alpha} + p_{\alpha\beta} + p_{\beta\beta})(J_n/4)]. \tag{4.17}$$

Eqs. 4.13 and 4.17, derived from two different starting points, do not depend on the spin system and energy terms used. The resulting expressions were used in numerical

simulations of high temperature averaged spin parameters. Both formulations yielded the same high temperature averages to well beyond experimental accuracies for a scalar coupling averaged over a ladder of states. The results were also shown to be field-independent. The conceptual and quantitative differences between the new formulation and the traditional formulation of the average spin parameters led to the investigation of systems which might definitively validate one or the other formulation. These efforts will be discussed in Chapter 5.

4.4 Other Expressions of Temperature-Dependent Spin Parameters

While other formulations for calculating the temperature-dependent behavior of spin parameters exist, these should not be confused with the formulations of stochastically averaged spin parameters outlined above. These alternative expressions for temperature-dependent quantities do not involve averages of slow-exchange spin parameters, but are derived from approximate forms of spin interactions. Aspects of these expressions are presented to emphasize the differences between these procedures and Eqs. 4.1 and 4.8.

In order to calculate the temperature dependence of the scalar coupling in acetaldehyde, Powles and Strange[43] introduced a temperature-dependent form of the well-known Karplus equation. Karplus[44,45] had originally modeled proton-proton scalar couplings in ethanic and ethylenic molecules with the equation (general form):

$$J_{HH'} = A + B(\cos\phi) + C(\cos 2\phi), \tag{4.18}$$

where ϕ is the dihedral angle between the coupled protons. The Karplus equation is an approximate form of valence bond theoretical treatments of the spin-coupling. Powles and Strange introduced temperature dependence by calculating the probability $p(\phi)d\phi$ of the occurrence of the position ϕ in $d\phi$. The average scalar coupling can then be written:

$$\bar{J} = \int_{-\pi}^{\pi} J(\phi)p(\phi)d\phi. \tag{4.19}$$

With rotational energies determining the probability distribution in ϕ, the $p(\phi)$ is a temperature-dependent quantity. The $J(\phi)$ is expressed as a series of $\cos n\phi$ terms as dictated by the form of the Karplus equation, Eq. 4.18.

Subsequent investigations[29,46] extended the approach of Powles and Strange to 1,2-disubstituted and 1,1,2-trisubstituted ethanes. The outputs of these approaches are the coefficients of the expansion in $J(\phi)$ and potential energy surface parameters which yield good fits to the data. These approaches have been used for calculating the temperature-dependence of parameters in the slow-exchange regime where spin parameters might show the effects of the molecule "sloshing" in a particular conformer like a rotational pendulum. These effects were the subject of the substituted ethanes studies.[29,46]

The fast-exchange spectra of acetaldehyde and related species do not raise the question of how to average correctly over molecular conformers because of the symmetry of the molecules. Because of the C_3 symmetry, the rotamers of acetaldehyde are equal in energy and the resulting temperature dependence is due only to the changing angular distribution within any well. In such cases, $J(T)$ may still yield information on the molecular potential, but since $J(\phi)$ at fixed ϕ or J_n in a torsional eigenstate n are not available experimentally in an unambiguous way, such torsional averaging must rely on theoretical modeling. An extensive comparison between theory (using *ab initio* $J(\phi)$ and torsional states) and experimental $J(T)$ for C_3 substituted ethanes using the traditional stochastic average demonstrated very poor agreement[47] with the sign or magnitude of the temperature dependences.

All Karplus equation expressions extract parameters that are not independently verifiable by experimental evidence. The coefficients obtained for the expansion of $J(\phi)$ do not correlate to values of the scalar coupling measured at certain values of ϕ.

The effects modeled by these temperature-dependent Karplus equations would still be present in asymmetric molecules but are small in comparison to changes in spin

parameters due to averaging over conformers. The spin-spin coupling in acetaldehyde changes only 0.15 Hz over a 171 K temperature range. Small temperature dependences such as this could be measured in the slow-exchange regime and included in the other forms of the stochastic average.

4.5 Discussion

The theoretical justification for Eq. 4.1 is weaker than has generally been appreciated. Such an average follows from dynamic models based on the assumption that spins in superposition are transported between different spatial states in perfect concert. Any such model exists in the truncated Liouville space that excludes superpositions of states that differ in both their spin and spatial factors. Whether such a truncated space suffices to describe magnetic resonance lineshapes is an open question. What is clear is that such a space cannot describe the approach to equilibrium of the total system, since this requires spin-dependent rates between spatial manifolds. Thus a full dynamic solution is needed in this complete Liouville space. One result of such a full solution will be the equilibrium average energies of Eq. 4.4. Less clear is under what dynamic assumptions either these energies or those that follow from the traditional Eq. 4.1 will describe the fast-exchange spectrum.

The use of a simple weighted average in the traditional treatment of averaged spin parameters suffices only for calculating averages of quantities which are eigenvalues of the states themselves. The conceptual difference between the old and new formulation can be summarized in the following statement: the new form is a difference of static averages, as opposed to the traditional form which is an average of static differences. Here, the term "static" refers to those quantities which are associated with a molecular eigenstate or, classically, with a molecular configuration.

The accepted idea of how to calculate a stochastically averaged spectrum is universal in the literature of magnetic resonance, underlying the interpretation of average

chemical shifts, dipolar couplings, tunnel splittings, quadrupole couplings, and hyperfine interactions. In most situations, the number of unknowns is such that it is not possible to verify the form of the stochastic average, but valuable information could be obtained if the correct form were known. If the traditional ideas are generally incorrect, many thousands of experiments would need to be reinterpreted to in fact obtain the quantitative information on molecular structure that they were designed to yield. Ultimately, the choice of theory will be decided by a preponderance of data. The present work indicates clearly that the issue must be reopened and is a first step in the reexamination of the experimental basis of Eq. 4.1.

Precisely the same issue of how to calculate a stochastic average also arises in the (*ab initio*) theoretical calculation of a measurable spin Hamiltonian from expectation values of the underlying molecular eigenstates, which are almost never sufficiently long-lived to measure individually by magnetic resonance. Application of the correct statistical prescription will often be needed to test experimentally whether the quantum-mechanical part of the calculation is adequate.

References

1. N. Bloembergen, E.M. Purcell, and R.V. Pound, *Phys. Rev.* **73**, 679 (1948).
2. E.R. Andrew and R. Bersohn, *J. Chem. Phys.* **18**, 159 (1950).
3. E.L. Hahn and D.E. Maxwell, *Phys. Rev.* **88**, 1070 (1952).
4. H.S. Gutowsky, D.W. McCall, and C.P. Slichter, *J. Chem. Phys.* **21**, 279 (1953).
5. D.M. Graham and J.S. Waugh, *J. Chem. Phys.* **27**, 968 (1957).
6. J.N. Shoolery and B.L. Crawford, Jr., *J. Mol. Spectrosc.* **1**, 270 (1957).
7. J.A. Pople, W.G. Schneider, and H.J. Bernstein, *Can. J. Chem.* **35**, 1060 (1957).
8. J.A. Pople, *Mol. Phys.* **1**, 3 (1958).
9. H.M. McConnell, *J. Chem. Phys.* **28**, 430 (1958).
10. J.I. Kaplan, *J. Chem. Phys.* **28**, 278 (1958); **29**, 462 (1958).
11. S. Alexander, *J. Chem. Phys.* **37**, 967 (1962); **37**, 974 (1962).
12. C.S. Johnson, *J. Chem. Phys.* **41**, 3277 (1964).
13. C.S. Johnson, *Adv. Magn. Reson.* **1**, 33 (1965).
14. J.C. Schug, P.E. McMahon, and H.S. Gutowsky, *J. Chem. Phys.* **33**, 843 (1960).
15. R.J. Abraham and H.J. Bernstein, *Can. J. Chem.* **39**, 39 (1961).
16. T.D. Alger, H.S. Gutowsky, and R.L. Vold, *J. Chem. Phys.* **47**, 2818 (1967).
17. H.S. Gutowsky, G.G. Belford, and P.E. McMahon, *J. Chem. Phys.* **36**, 3353 (1962).
18. R.A. Newmark and C.H. Sederholm, *J. Chem. Phys.* **43**, 602 (1965).
19. R.A. Newmark and C.H. Sederholm, *J. Chem. Phys.* **39**, 3131 (1963).
20. S. Ng, J. Tang, and C.H. Sederholm, *J. Chem. Phys.* **42**, 79 (1965).
21. R.R. Dean and J. Lee, *Trans. Faraday Soc.* **65**, 1 (1969).
22. W.S. Brey, Jr., and K.C. Ramey, *J. Chem. Phys.* **39**, 844 (1963).
23. G. Govil and H.J. Bernstein, *J. Chem. Phys.* **47**, 2818 (1967).
24. G. Govil and H.J. Bernstein, *J. Chem. Phys.* **48**, 285 (1968).
25. R.M. Lynden-Bell, *Prog. NMR Spec.* **2**, 163 (1967).
26. G. Binsch, *Top. Stereochem.* **3**, 97 (1968).

27. G. Binsch, *J. Amer. Chem. Soc.* **91**, 1304 (1969).

28. F. Heatley and G. Allen, *Mol. Phys.* **16**, 77 (1969).

29. W.-C. Lin, *J. Chem. Phys.* **52**, 2805 (1970).

30. A. Vega and D. Fiat, *J. Magn. Reson.* **19**, 21 (1975).

31. L.M. Jackman and F.A Cotton, eds., "Dynamic Nuclear Magnetic Resonance Spectroscopy," Academic Press, New York, 1975.

32. S. Szymanski, M. Witanowski, and A. Gryff-Keller, *Ann Rept. NMR Spec.* **8**, 227 (1978).

33. G. Binsch and H. Kessler, *Angew. Chem., Int. Ed. Engl.* **19**, 411 (1980).

34. K.G.R. Pachler and P.L. Wessels, *J. Molec. Struc.* **68**, 145 (1980).

35. J. Kaplan and G. Fraenkel, "NMR of Chemically Exchanging Systems," Academic Press, New York, 1981.

36. J. Jeener, *Adv. Magn. Reson.* **10**, 1 (1982).

37. U. Liddel and N.F. Ramsey, *J. Chem. Phys.* **19**, 1608 (1951).

38. J.T. Arnold and M.E. Packard, *J. Chem. Phys.* **19**, 1608 (1951).

39. T.P. Das, *J. Chem. Phys.*, **25**, 896 (1956) and **27**, 763 (1957).

40. E.O. Stejskal and H.S. Gutowsky, *J. Chem. Phys.* **28**, 388 (1958).

41. C.S. Johnson and C. Mottley, *Chem. Phys. Lett.* **22**, 430 (1973).

42. D.H. Jones, N.D. Kurur, and D.P. Weitekamp, *Bull. Mag. Res.* **14**, 214 (1992).

43. J.G. Powles and J.H. Strange, *Mol. Phys.* **5**, 329 (1962).

44. M. Karplus, *J. Chem. Phys.* **30**, 11 (1959).

45. M. Karplus, *J. Amer. Chem. Soc.* **85**, 2870 (1963).

46. J.-S. Chen, R.B. Shirts, and W.-C. Lin, *J. Phys. Chem.* **90**, 4970 (1986).

47. J.W. Emsley and J.M. Tabony, *Mol. Phys.* **28**, 423 (1974).

Chapter 5

Experimental Evidence in the Verification of Stochastic Averaging Procedures

5.1 Introduction

Because of the absence of any alternative formulation of a stochastically averaged spin parameter, the experimental evidence supporting the traditional form seems to have been less scrutinized than it might have been otherwise. With the introduction of a concise and quantitatively different alternative, the experimental basis for such procedures must be reexamined. Several classes of test systems will be examined with particular attention to whether they hold promise for resolving the question of validity between the two formulations. These systems will possess one or more parameters which cannot easily be measured with present techniques, but discussing such systems will emphasize the requirements of a satisfactory test system. All the systems to be discussed are well-known for their dynamic NMR behavior.

Although many hundreds of NMR studies have measured and modeled the temperature-dependent averaging of NMR spectra, finding a completely determined and unambiguous data set turns out to be surprisingly difficult. Many systems displaying temperature-dependent spin parameters do not have experimentally observable slow-exchange spectra. The averaging procedure is carried out in the absence of any knowledge of the individual manifold or conformer spin parameters, X_n. Such studies also lack precise information on the population distribution among the conformers of the system. While satisfactory fits to the fast-exchange data are often obtained, many sets of

parameter values can yield these fits and are not distinguished by the experiment. Systems for which slow-exchange data is not available are often modeled with approximate forms of temperature-dependent parameters, such as the temperature-dependent Karplus equations reviewed in Chapter 4.

Even in systems where the slow-exchange parameters are available, the traditional form of the stochastic average often makes predictions dramatically different from the observed fast-exchange values. Some experimental considerations which are cited as possible causes for these failures are temperature-dependent behavior of the X_n and solvent-solute interactions. These effects will be addressed in sections on the various test systems.

5.2 Experimental Features of Test Systems

In both formulations it is ideally possible to predict the fast-exchange observations from slow-exchange observations without adjustable parameters. If a test system supplied a complete data set, the ability to validate one or the other form would depend only on experimental uncertainty. In practice, there seems to be no case where NMR spectra of individual molecular eigenstates have been obtained separately and also as a thermal average. Thus, it seems necessary to look at cases where n indexes conformers (manifolds of eigenstates).

The experimental concept is simple and well-known. At low temperature, the spin Hamiltonian for each conformer can be determined, since, in the limit of negligible chemical exchange between them, separate spectra are seen for each. The relative areas of these spectra at each slow-exchange temperature provide the relative populations and thus the free-energy difference between conformers. A linear fit to the temperature dependence of this free-energy difference allows it to be separated into two terms, which can be viewed as an energy difference and an entropy difference, if one additionally

assumes that the temperature dependence of these is negligible over the experimental range.

Since a conformer is a set of molecular eigenstates, additional dependence on thermodynamic state (e.g., temperature dependence) is possible due to averaging within this set. Theoretically, one has precisely the same problem in deciding how to take this average as for the averaging over conformers. However, if one can measure such temperature dependence within the slow-exchange regime and extrapolate to fast exchange, then the stochastic theory need not enter at this level.

Thus, the following is the set of criteria which need to be met for a compelling, fully experimental test of any theory relating slow-exchange and fast-exchange spectra.

1. The system must have state-dependent rates such that measurements in both the slow- and fast-exchange regimes are possible. For fluids this typically requires barriers between conformers on the order of 10 kcal mol^{-1}.
2. The state dependence of the conformer spin Hamiltonians and the free-energy differences must be measured in the slow-exchange region to allow extrapolation through the fast-exchange region. This is often the major source of uncertainty because of the small temperature range corresponding to slow exchange. The difference in thermodynamic state between these regimes ideally is small or even zero, so as to minimize the propagation errors due to phenomenological extrapolation. Using different NMR transitions or field conditions to measure the same spin parameter can help in this regard; since the criterion for motional collapse varies with the transition being observed, there is no minimum difference in thermodynamic state between slow and fast exchange.
3. Some or all of the fast-exchange data should fall outside the error bars on the predictions of one of the theories, thereby disproving it. The traditional and alternative theories presented in Chapter 4 have identical predictions for mutual

exchange and whenever the occupied conformers are degenerate in spatial energy or in spin Hamiltonians, as mentioned in Chapter 4 in the averaging of spin parameters in acetaldehyde. For two-site problems, the theories will typically differ measurably when the conformer free energies differ by $> 10^2$ cal mol^{-1}. When this difference exceeds $\sim 10^3$ cal mol^{-1}, sensitivity will usually preclude observing the slow-exchange spectrum of the minor conformer.

The above conditions are not extremely restrictive; a substantial fraction of the molecules whose conformer equilibria have been studied by solution-state NMR fall into this range of free-energy differences. Since the traditional theory has been in increasing use for four decades, it might be expected that it would have substantial and diverse experimental support. While it is difficult to have confidence in the completeness of a search through such a large literature, no published data set has been found in the course of these investigations that meets the criteria above. Thus, neither theory has presently been evaluated by this seemingly reasonable standard.

The only theory ever considered previously is the traditional form. Numerous authors have noted failures in its application, but these failures have usually been plausibly attributed to inadequacies in the data, most commonly uncertainties in conformer assignment or unmeasured temperature dependence of a conformer spin parameter.

5.3 Tunnelling Trihydrides

Because the tunnelling trihydrides provided the motivation for examining stochastic averaging procedures, they are the first class of compounds to be examined here. As mentioned in Chapter 2, the total scalar coupling observed in the tunnelling trihydrides is a sum of the scalar coupling due to tunnelling and the usual magnetic interaction. Except at low temperatures, the total coupling J_{AB} is dominated by the behavior of the tunnelling splitting. The asymptotic behavior of the total scalar coupling at

low temperatures is critical to understanding the validity of the different formulations for the high-temperature average. The different formulations depend on the spatial model chosen to model the particle exchange. Various models have been examined and make different predictions for the magnitude and even the sign of the high-temperature average for a given set of input parameters.[1-4] However, all the theories are able to fit the available data with chemically plausible parameters. Thus, this is not a fruitful field for deciding between stochastic averaging theories. However, it would be possible to exclude certain models if the sign of J_{AB} were known, and thus a proposal for doing so is outlined here.

The following reviews information from the literature which would be critical to determining the sign of the average tunnel splitting J_{AB}. Gilbert and Bergman[5] and Paciello[6] measure the signs and magnitudes of the phosphorous-hydride couplings in their investigations of tunnelling hydrides. Several studies of square-planar and octahedral complexes provide additional information on the scalar couplings in phosphine-substituted metal hydrides.

Two values of the phosphorous-hydride coupling in $Ir(C_5Me_5)(PMe_3)H_3$ are observed at low temperature. The AB_2 spectrum of the hydrides undergoes a coalescence with increasing temperature, yielding a single hydride resonance split by the average value of the phosphorous-hydride scalar coupling. Gilbert and Bergman report the low-temperature values for the phosphorous-hydride scalar couplings as: $^2J_{PA}$ = -12.6 Hz and $^2J_{PB}$ = 21.5 Hz. The signs are determined to be opposite because of the fact that at high temperature an average value of 10 Hz is measured. The A proton is identified as being *cis* to the phosphorous while the two B protons are identified as *trans*, with the fast-exchange value being given by $[J_{PH}(cis) + 2J_{PH}(trans)]/3$. For $Ru(C_5Me_5)(PMe_3)H_3$, Paciello reports approximate magnitudes of 5 and 20 Hz for the *cis* and *trans* couplings, respectively. An average J_{PH} = 11 Hz was measured at room temperature, again indicating that the signs of the two phosphorous-hydride couplings are opposite.

Although the positions of the protons are not verified by a crystal structure, the stereochemical assignment of signs made by Gilbert and Bergman agree with other measurements of *cis* and *trans* phosphorous-proton couplings in the literature.

Through the use of ^{31}P and ^{195}Pt double irradiation techniques, McFarlane[7] measured a negative sign for $^2J_{PH}(cis)$ coupling in *trans*-$[(Et_3P)_2PtHCl]$. The experiment showed the sign of $^2J_{PH}(cis)$ to be opposite to that of $^3J_{HH}$ in the phosphine ligand, which had been found by Lauterbur and Kurland[8] to be positive in an early study of geminal and vicinal couplings in substituted ethylenes. In studies of the *fac-* and *mer-* isomers of $IrH_3(PEt_2Ph)_3$ and $IrH_3(PPh_3)_3$, $^2J_{PH}(cis)$ and $^2J_{PH}(trans)$ were found to be of opposite sign,[9] thereby establishing that the $^2J_{PH}(trans)$ is positive. Similar studies of platinum(II) hydrides also establish that the signs of these two couplings are opposite and that $|^2J_{PH}(trans)| > |^2J_{PH}(cis)|$.[10] An important feature of these complexes is their non first-order NMR spectra from which relative signs of certain couplings can be deduced without the use of double resonance techniques. This feature is shared by the tunnelling trihydride $Ru(C_5Me_5)(PMe_3)H_3$ and could be used to establish the sign of the scalar coupling J_{AB}.

Early analyses of AB_2X spin systems[11,12] examined those spectral characteristics which allow the determination of the relative signs of the couplings. The fact that the X spectrum is asymmetric with respect to the sign of the J_{AB} has been used to study the AB_2X system of *m*-dinitrobenzene. An extension of the AB_2X analysis to the AB_2M_nX spin system[11] allowed the measurement of couplings in several platinum(II) hydrides.[13]

The trihydride $Ru(C_5Me_5)(PMe_3)H_3$ can also be modeled as an AB_2M_nX system where n = 9. In this notation, the A and B are hydride protons, the M is a methyl proton, and the X denotes the phosphorous nucleus. A number of simulations have been carried out in order to determine which experiments will yield the relative signs of the couplings. Over a wide temperature range, the trihydride fulfills the requirement that A and B be strongly coupled. In the absence of any J_{MX} coupling, the X spectrum is quite asymmetric. By simulating the full AB_2M_9X spectrum, it can be determined whether the

asymmetry in the phosphorous spectrum will be experimentally resolvable in the presence of coupling to the nine methyl protons. The full AB_2M_9X spectrum is a superposition of ten AB_2X spectra. The relative offsets of the ten spectra are determined by the value of J_{MX} and the relative intensities of the ten spectra are given by the binomial coefficients.

Simulated spectra for four different sets of coupling constants are shown in Figure 5.1. The magnitudes of the couplings are those measured previously for $Ru(C_5Me_5)(PMe_3)H_3$. The signs were varied to observe the differences between spectra with various combinations of the relative signs of the couplings. All the simulations used J_{MX} = -11.2 Hz, an average of values observed in several metal trimethylphosphine compounds. Gilbert measures a value of $|J_{PH}(P\text{-}CH_3)|$ = 11.8 Hz for $Ir(C_5Me_5)(PMe_3)H_3$.[14] The line broadening used in all simulations was 1 Hz. The sets of couplings which result in the spectra in Figure 5.1 are presented in Tables 5.1 and 5.2.

Figure 5.1 demonstrates that the asymmetry observed in the AB_2X spectrum is still observable in the AB_2M_9X system. All four sets were simulated in order to consider all

Table 5.1. The sets of couplings which result in the spectrum given in Figure 1(top spectrum).

	J_{AX}	J_{BX}	J_{AB}
Set 1	-6.25	20.0	-180.0
Set 2	6.25	-20.0	180.0

Table 5.2. The sets of couplings which result in the spectrum given in Figure 1(bottom spectrum).

	J_{AX}	J_{BX}	J_{AB}
Set 3	-6.25	20.0	180.0
Set 4	6.25	-20.0	-180.0

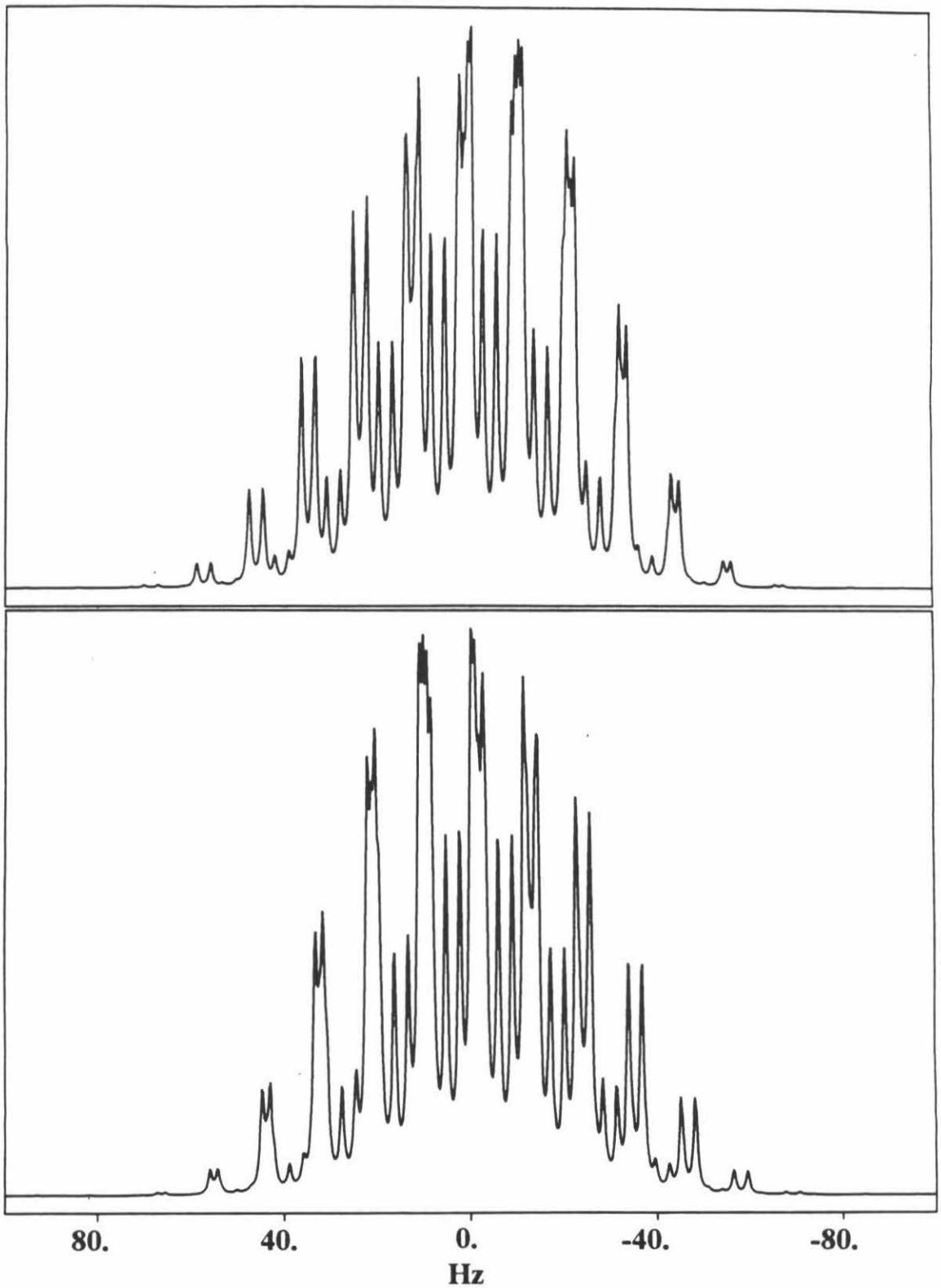

Figure 5.1. The simulated phosphorous NMR spectra in the AB_2M_9X spin system of $Cp^*RuH_3(PMe_3)$. Couplings of Sets 1 and 2 yield top spectrum. Sets 3 and 4 yield the bottom spectrum.

reasonable combinations of signs; however, Sets 1 and 3, which clearly result in different spectra, are the only likely sets of true couplings. While Sets 2 and 4 are significant in that they yield the same result as Sets 1 and 3, respectively, the previously cited investigations of phosphorous-hydride couplings suggest that the values of *cis* and *trans* couplings used in Sets 2 and 4 are incorrect. The results of the simulation of the spin system for Sets 1 and 3 demonstrate that the sign of J_{AB} can be determined from a simple phosphorous spectrum of a tunnelling hydride.

Although they provided the impetus for questioning the methods of calculating stochastic averages of spin parameters, the tunnelling trihydrides have properties that make them less than ideal systems for validating one or the other of the averaging methods. Depending on the spatial model used for the tunnelling, the different averaging methods yield very different averaged values for the scalar couplings. While the spatial model used also yields values for the scalar coupling (tunnel splitting) in each spatial state that is averaged over, there is no experimental evidence available that confirms these individual spatial level values. Such experiments would involve obtaining separate NMR spectra for spatial levels that are separated by energies on the order of hundreds of wavenumbers. At temperatures where no vibrational averaging occurred, the resulting spectrum would only yield the scalar coupling in the lowest spatial level. While this number is the asymptotic value of the scalar coupling at low temperature, no additional information about the scalar couplings in other spatial levels is provided. The issue of averaging a spin parameter over vibrational levels appears also in investigations of temperature-dependent spin parameters in gas-phase diatomics, as will be discussed in Section 5.6 of this chapter.

5.4 Rotational Isomers of Substituted Ethanes

Since the physical properties of the trihydride system render it ineffective in resolving the stochastic averaging issue, experimental investigations centered on substituted ethanes, one of the earliest classes of compounds known to display chemical exchange and averaging in NMR. Substituted ethanes in solution[15-27] are the most studied systems and include cases which nearly meet the requirements of Section 5.2. The averaging in these systems occurs over the rotational isomers of the substituted ethane such as 1-fluoro-1,1,2,2-tetrachloroethane, shown in Figure 5.2. The molecule has two degenerate *gauche* isomers and one *trans* isomer. The barrier to rotation is such that both the fast- and slow-exchange regimes are observable by variable temperature NMR. The low-temperature spectra yield the spin parameters for the separate rotamers and provide a measure of the free-energy difference between rotamers through the relative intensities of the spectra. Many substituted ethanes have been studied using variable temperature NMR. Table 5.3 is a partial listing of the ethanes that have been investigated.

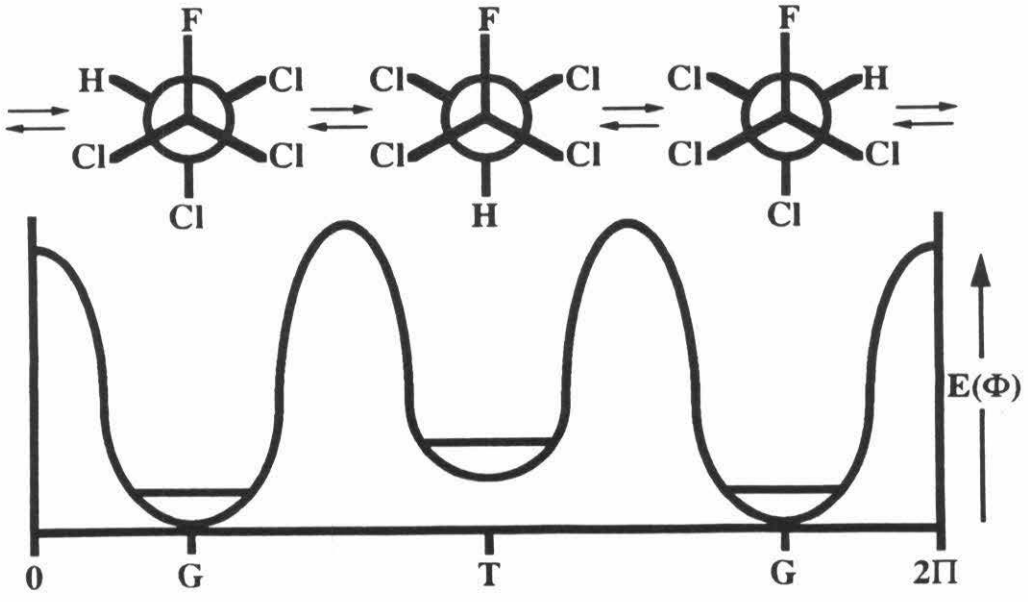

Figure 5.2. Potential energy versus dihedral angle (Φ) for the conformers of 1-fluoro-1,1,2,2-tetrachloroethane.

The two spin parameters that will be examined in the liquid-state rotational averaging of the substituted ethanes are the chemical shift and scalar coupling. Unlike chemical shifts, scalar couplings do not require a nominally temperature-independent reference resonance to compensate for the usual uncontrolled shifts of internal field with temperature. Also, scalar couplings are generally believed to be less sensitive to intermolecular interactions which could provide a confounding mechanism of temperature dependence. The issue of solvent-solute interactions and solute concentration effects will be discussed in Section 5.7.

1-fluoro-1,1,2,2-tetrachloroethane (FTCE) and **1-fluoro-1,1,2,2-tetrabromo-ethane (FTBE).** The temperature dependence of the three-bond vicinal coupling $\langle J_{HF} \rangle$ in the fast-exchange regime has been attributed to the averaging of the distinct values of J_t and J_g for the *trans* and *gauche* conformers, respectively. The temperature dependence of this three-bond $\langle J_{HF} \rangle$ is shown in Figure 5.3. Although this molecule has been studied previously,[16,17] the actual measurement of the relevant parameters (J_g, J_t, ΔH, and ΔS) had not been accomplished. The initial NMR study[16] of this molecule had used a ΔH measured via variable temperature infrared spectroscopy[27] and assumed $\Delta S = 0$. The couplings were determined only by best-fit results to the fast-exchange data. The values that yielded satisfactory fits to the data were: $J_g = 1.03$ Hz, $J_t = 18.08$ Hz, $\Delta S = 0$

Table 5.3. Substituted ethanes displaying dynamic NMR behavior and stochastic averaging of spin parameters.

Compound	Reference
$CFCl_2CHCl_2$	16,17
$CF_2BrCFBrCl$	18-23
$CF_2BrCHBrCl$	19
CF_2ICFCl_2	22
$CFBr_2CHBr_2$	24-26

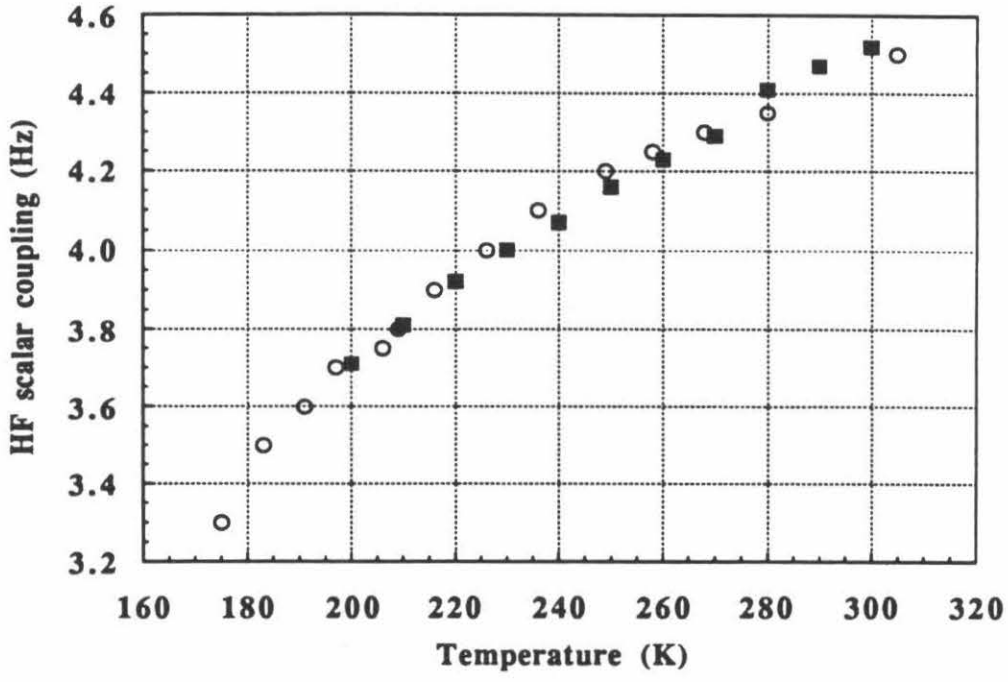

Figure 5.3. The fast-exchange scalar coupling $\langle J_{HF} \rangle$ in Hz in 1-fluoro-1,1,2,2-tetrachloroethane. O represents data from reference 17. ■ represents data of Jones, Kurur, and Weitekamp..

cal deg^{-1} mol^{-1}, and ΔH = 400 cal mol^{-1}. A subsequent study[17] of the same molecule in the slow-exchange regime found: $J_g < 2$ Hz, $J_t = 17.9 \pm 0.5$ Hz, ΔH = 400 cal mol^{-1}. Here, all parameters were assumed to be constant over the temperature range of the experiments. This assumption was based on the similar behavior of the scalar coupling in a 50/50 CS_2/FTCE sample and a neat FTCE sample. While this may address solvent-solute interaction effects, such a test does not address the intrinsic temperature-dependence of any of the quantities. No attempts to measure the intrinsic temperature dependence of these quantities was made.

Simulations showed that an unresolved J_g coupling in the 1-2 Hz range with a very modest temperature dependence could fit either the traditional or alternative forms of the stochastic average. Since both these quantities have been unmeasured, slow-exchange fluorine spectra were obtained for 50/50 CS_2/FTCE at 470 MHz at temperatures between

148 and 164 K in a sealed tube. The assignment is that the *gauche* is the more stable conformer found 18.7 ppm downfield of the smaller *trans* doublet. The areas under the gauche and trans doublets were fit by $\Delta H_{tg} = 540^{+470}_{-530}$ cal mol^{-1} and $\Delta S_{tg} = 1.2^{+3.0}_{-3.6}$ cal deg^{-1} mol^{-1}. The gauche entropy refers to either of the two gauche conformers separately. These current measurements are consistent within reported error ranges to an earlier observation[17] at 156 K. The error ranges on ΔH_{tg} and ΔS_{tg} are correlated, having been obtained by drawing the lines of greatest and least slope which pass within 8% error bars ($\cong$ 5% errors in the line areas) on all experimental ΔG_{tg} points.

These experiments did not resolve all parameters, however, since the slow-exchange fluorine spectra are complicated by chemical shift isotope effects due to the neighboring ^{37}Cl and ^{35}Cl nuclei. These isotope effects result in a three-line gauche fluorine resonance with a line separation of $\approx$ 4.5 Hz. While the proton spectrum would allow one to observe the J_g without these effects, the slow-exchange regime of the protons at 150 K still shows significant exchange between the *gauche* and *trans* proton resonances which are only separated by $\approx$ 0.07 ppm. The resulting proton lines are too broadened to resolve the *gauche* coupling.

Simulations of the fast-exchange values of the average scalar coupling can still be carried out. If the upper bound of the unresolved J_g is taken as 2 Hz, then the data are consistent with the traditional average. However, a temperature dependence of 0.005-0.01 Hz K^{-1} between 150 K, where the slow-exchange observations have been made on the ^{19}F resonances, and 300 K, where the ^{1}H spectrum is motionally averaged, would allow the alternative stochastic average to fit the data as well or better.

Reason to suspect such a temperature dependence can be found from a close reading of the literature on the related system 1-fluoro-1,1,2,2-tetrabromoethane.[24-26] A value of $J_g = 2.4 \pm 0.3$ Hz in dimethylether at 188 K can be measured from published data,[26] but has been reported as 1.7 Hz at 180 K in the same solvent.[25] In $CFCl_3$ this

coupling has been tabulated as 1.15 Hz from 171 to 178 K,[20] but recent fits of the spectrum (at 171 K only) in reference 20 indicate $J_g = 1.5 \pm 0.3$ Hz. Thus the reported absence of temperature dependence to three significant figures is dubious and further experimental work is needed. Specifically, 2D spin echo measurements on the ^{19}F slow-exchange spectrum might provide the resolution needed to experimentally determine the temperature dependence of J_g and J_t.

1,1,2-trifluoro-1,2-dibromo-2-chloroethane ($CF_2BrCFBrCl$). The rotational averaging of spin parameters in $CF_2BrCFBrCl$ has been studied extensively.[19-21,23,28] The experimental situation in this molecule is complicated by the fact that all three conformers yield different NMR spectra at low temperature. The free-energy differences between conformers had previously been measured[28] as $\Delta G_{12} = 305$ cal mol^{-1} and $\Delta G_{13} = 780$ cal mol^{-1}. These differences would cause the difference between the old and new forms of the stochastic average to be large, providing a good test system provided all the slow-exchange spin parameters could be measured.

The low temperature ^{19}F spectrum of $CF_2BrCFBrCl$ consists of three ABX spectra. The averaging of the spectrum results in a single ABX system with temperature-dependent $\langle J_{AX} \rangle$, $\langle J_{BX} \rangle$ and $\langle \nu_A - \nu_B \rangle$. The fast-exchange $\langle J_{AX} \rangle$ and $\langle J_{BX} \rangle$ are shown in Table 5.4. The temperature dependence of these couplings is relatively small. This results from the two most-populated conformers having couplings which are similar in value. The total change in the couplings in Table 5.4 is only 0.15 Hz for $\langle J_{AX} \rangle$ and 0.17 Hz for $\langle J_{BX} \rangle$ over the sixty degree temperature change, corresponding to a 0.0025 and 0.0028 Hz/K temperature dependence, respectively.

Table 5.4. The fast-exchange temperature-dependent scalar couplings $\langle J_{AX} \rangle$ and $\langle J_{BX} \rangle$ in $CF_2BrCFBrCl$.

T (K)	$\langle J_{AX} \rangle$	$\langle J_{BX} \rangle$
310	13.84	14.15
320	13.78	14.07
330	13.77	14.08
340	13.80	14.07
350	13.76	14.04
360	13.68	13.99
370	13.70	13.98

The data in Table 5.4 is accurate to ± 0.05 Hz. Efforts were made to obtain spectra fairly quickly to avoid temperature fluctuations from occurring during the experiment. Fluctuations of no more than 0.5 K occurred during experiments. The observed deviations in the $\langle J_{AX} \rangle$ from a smooth curve are to be expected with errors on the order of 0.05 Hz and the small changes in the coupling due to averaging. Similar deviations were observed in measurements of $\langle J_{AX} \rangle$ and $\langle J_{BX} \rangle$ reported previously.[18] The magnitudes of the $\langle J_{AX} \rangle$ and $\langle J_{BX} \rangle$ changed 0.52 and 0.98 Hz, respectively, with a temperature change from 224 K to 466 K. These changes correspond to a 0.0021 and 0.0040 Hz/K temperature dependence. Considering the errors of ± 0.10 to ± 0.25 Hz cited in the previous study,[14] the agreement between the measured temperature dependence of the fast-exchange averages from these two studies is good.

All previous studies of this molecule have failed to cite any temperature dependence of the couplings in each conformer. In order to model fast-exchange spin parameters that have such small temperature dependence, measuring slow-exchange behavior is crucial. The 470 MHz ^{19}F data of Figure 5.4 shows that in fact there is a large

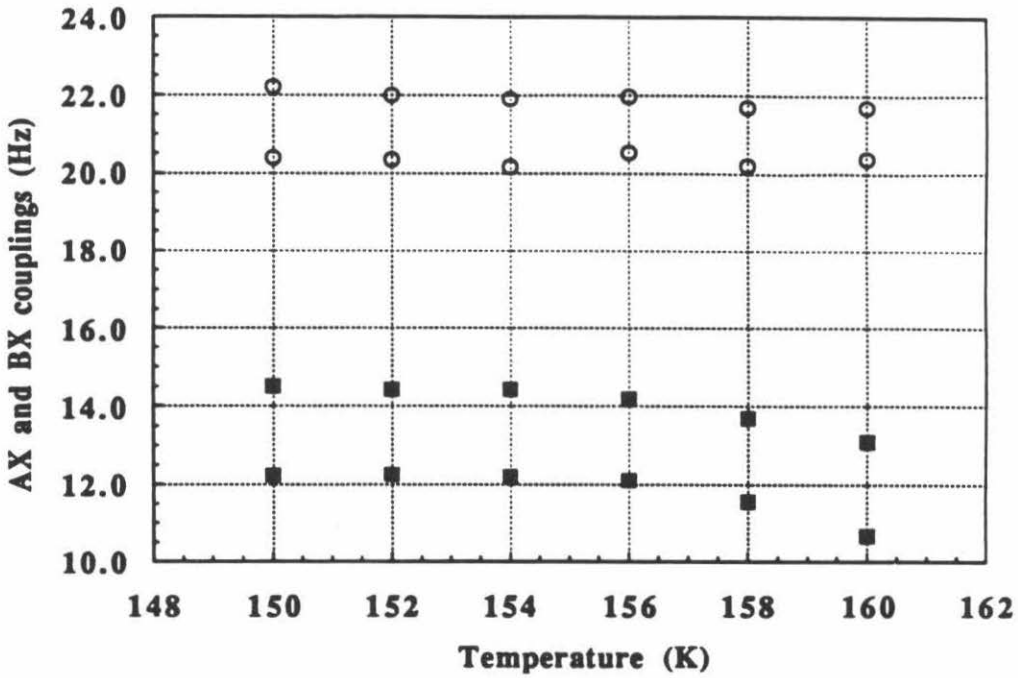

Figure 5.4. The slow-exchange J_{AX} and J_{BX} scalar couplings for conformers 1 (■) and 3 (O) in $CF_2BrCFBrCl$.

temperature dependence of the slow-exchange J_{AX} and J_{BX} couplings for conformers 1 and 3.

The best fit lines for both the conformer-1 J_{AX} and J_{BX} have a slope of -0.14 Hz/K. The conformer-3 J_{AX} best-fit slope is -0.05 Hz/K, while the conformer-3 J_{BX} best-fit slope is -0.002 Hz/K. The couplings at each temperature were taken from the same spectrum and provide a check that drifts in temperature are not dominating the observed temperature dependence. The steady decrease in the conformer-3 J_{AX}, which does not parallel the changes in the conformer-1 couplings' behavior indicates that the observed behavior results from the actual and distinctive temperature dependence of each coupling.

The large temperature dependence of the couplings makes fitting the extremely small temperature dependence of the fast-exchange averages very difficult and probably

unreliable. To make the task even more difficult, the conformer-2 couplings in the molecule are also very close in value. When calculating the average quantities, one would need no prior knowledge of which coupling in one conformer to average with which coupling in another, since the fast-exchange average would hopefully make the choice of corresponding resonances clear. In the present case, however, the closeness in value of the conformer-2 couplings and the conformer-3 couplings results in the various permutations yielding good fits for either form of the stochastic average. Although this situation might be resolved by carrying out a spin tickling experiment at a temperature displaying significant amounts of chemical exchange, this would be difficult in the present case where $\delta = \nu_A - \nu_B = 0.34$ ppm for conformer 2 at 150 K. The effort to resolve the issue would still be plagued by temperature-dependent behavior of the slow- and fast-exchange parameters.

For the reasons cited, the averaging of the scalar couplings in $CF_2BrCFBrCl$ does not provide the information needed to resolve the issue of stochastic averaging. It seems worthwhile, however, to address the question of whether the averaging of chemical shifts in this molecule might prove enlightening. The temperature dependence of the fast-exchange $\delta = \langle \nu_A - \nu_B \rangle$ is shown in Figure 5.5.

The total changes for the data sets that have measurements at more than one temperature correspond to -3.67×10^{-3} ppm/K for the present work (labeled JK+W), while the data from reference 18 and reference 20 have temperature dependences of -3.97×10^{-3} ppm/K and -4.42×10^{-3} ppm/K, respectively. All previous studies of this molecule fail to report the slow-exchange values of $(\nu_A - \nu_B)$ for each conformer at various temperatures. The slow-exchange values obtained in these investigations are presented in Table 5.5.

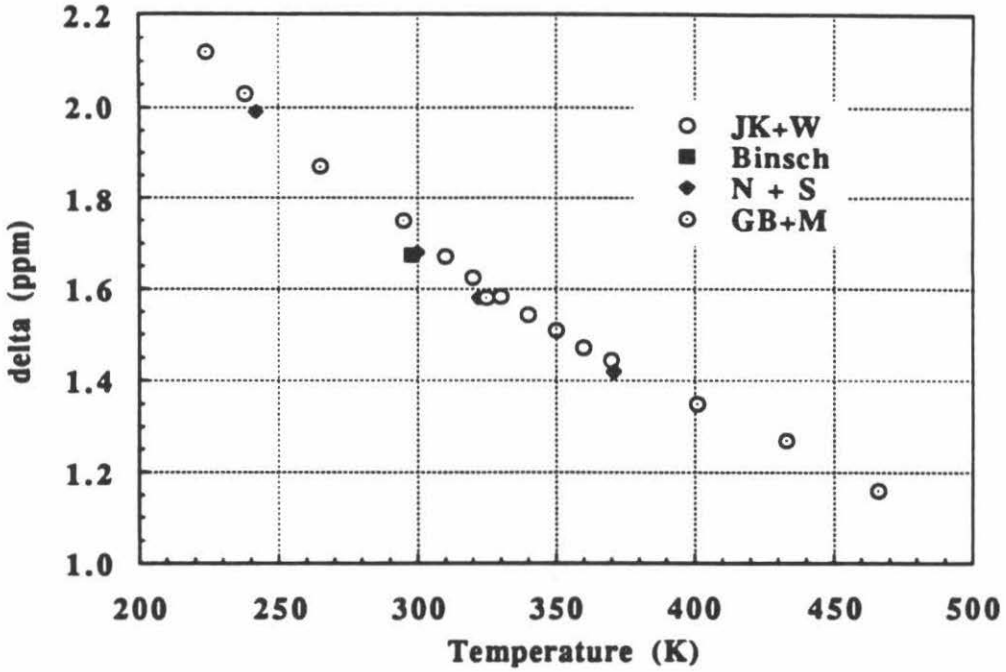

Figure 5.5. The fast-exchange measurements of $\delta = \langle \nu_A - \nu_B \rangle$ in the molecule $CF_2BrCFBrCl$.

The same complication occurs here as in the averaging of the spin couplings. The temperature dependence of the slow-exchange parameters is large enough to dominate the fast-exchange behavior of the average parameter. The calculated fast-exchange average would be more sensitive to errors in the measurement of the slow-exchange values and their temperature dependences than to which formulation one used to calculate the average.

The trends observed in the slow-exchange data are important for another reason which is not recognized in the absence of such information. The changes in the chemical shift differences of each conformer lead to the question of whether one (or both) of the ν_A and ν_B resonances is temperature-dependent. Measuring the frequencies ν_A and ν_B relative to a chemical shift reference such as $CFCl_3$ would not prove sufficient, since the temperature dependence of the reference chemical shift would have to be known

Table 5.5. The slow-exchange $\delta = (\nu_A - \nu_B)$ in ppm for each of the conformers in $CF_2BrCFBrCl$.

Temperature (K)	conformer 1	conformer 2	conformer 3
150	4.532	0.337	3.603
152	4.529	0.331	3.604
154	4.526	0.325	3.605
156	4.521	NA	3.608
158	4.515	NA	3.610
160	4.511	NA	3.612

NA (not available): At 156 K, the small chemical shift difference becomes obscured by the onset of chemical exchange.

independently. $CFCl_3$ has been used as a ^{19}F chemical shift reference in many investigations, including studies[20,23,28] of $CF_2BrCFBrCl$. The observation[29-30] of chemical shift isotope effects from neighboring chlorine nuclei and the temperature dependence of such effects suggests that $CFCl_3$ is not an ideal reference compound. External frequency references may be preferable for variable-temperature ^{19}F NMR experiments. Another alternative is to consider the fundamental observable to be frequency differences between nuclear sites in the same molecule. This guarantees the same local field and the same conformer probabilities, but does not eliminate the need to separately measure the temperature dependence of the shift difference in each conformer and extrapolate to the fast-exchange temperature.

Fourteen asymmetric fluoroethanes. Binsch has investigated the chemical shift averaging in fourteen asymmetric fluoroethanes.[28,31,32] The compounds studied include ten compounds with the formula $CF_2BrCXYZ$, where the substituents X, Y, and Z correspond to all possible combinations of the five ligands hydrogen, fluorine, chlorine, bromine, and phenyl. The other four compounds are $CF_2ClCHClPh$, $CF_2ClCHBrPh$, $CF_2ClCFClPh$, and $CF_2ClCHFI$. The data[28] consists of single slow-exchange values of

the chemical shift difference in each conformer and one fast-exchange value of the averaged chemical shift difference. Investigating the predictions of the fast-exchange parameter using the two forms of the stochastic average underscores the need for a more complete data set that includes data at several slow-exchange temperatures and some absolute reference of the observed frequencies. Table 5.6 shows the deviation of the predicted values from the measured average for both the traditional and alternative stochastic average.

Table 5.6. The difference for the calculated and experimental values of the average chemical shift difference (in ppm) between the AB fluorines in fourteen asymmetric fluoroethanes.

Compound	Formula	$\lvert(x_{old} - x_{ex})\rvert$	$\lvert(x_{new} - x_{ex})\rvert$	better fit
1	$CF_2BrCHFCl$	.31	.63	old
2	$CF_2BrCHFBr$	.80	.61	new
3	$CF_2BrCHClBr$	.10	2.30	old
4	$CF_2BrCHBrPh$	3.50	5.71	old
5	$CF_2BrCHClPh$	.07	4.27	old
6	$CF_2ClCHBrPh$	.26	4.44	old
7	$CF_2ClCHClPh$	.03	2.99	old
8	$CF_2ClCHFI$	.22	.10	new
9	$CF_2BrCHFPh$	.11	.36	old
10	$CF_2BrCClBrPh$	.41	.82	old
11	$CF_2BrCFBrPh$	.87	1.93	old
12	$CF_2ClCFClPh$	.06	.13	old
13	$CF_2BrCFClPh$	.21	.44	old
14	$CF_2BrCFClBr$	.16	1.02	old

While Table 5.6 clearly demonstrates a tendency for the traditional formulation to fit the single-point data sets better than the new formulation, the general quality of the fits is not compelling. Only five of the fits predict the fast-exchange average to 0.10 ppm or better (9.4 Hz for the 94 MHz fluorine NMR data). One of these best five fits results from the new formulation of the stochastic average. Perhaps if there were a larger number of good fits, some conclusions could be made regarding the validity of one or the other theory. With only five good fits, however, the four-to-one advantage of the old theory is not definitive evidence for its correctness. A more important consideration is that only five of the fourteen compounds are fit to an accuracy of 0.10 ppm or better. These poor fits possibly result from the lack of slow-exchange values of both the A and B resonances and the temperature dependence of the free-energy differences between conformers. Compound 14 in Table 5.6 is the same compound discussed previously. The dramatic temperature dependence of the slow-exchange chemical shifts observed for $CF_2BrCFClBr$ again points to the need for measuring the slow-exchange spin parameters and including the temperature dependence in the calculation of the averages. For $CF_2BrCFClBr$, the old average also fits the fast-exchange data from 310-370 K, presented in Figure 5.5, better than the new formulation. The old average yields a fit with a root-mean-squared deviation of 0.0035 ppm compared to 0.2178 ppm for the new average. These calculations were performed over a grid of points allowing the ΔH and ΔS to vary as long as they agreed with the measured free-energy differences at slow-exchange to within $\pm$ 8%. This error is estimated from slow-exchange spectra where variations in integrated peak areas of $\pm$ 4% can lead to 8% errors in the calculated free energies. The range of free-energy differences searched was ΔH_{12} = 0.0-600 cal mol^{-1}, and ΔH_{13} = 300.0-1200 cal mol^{-1}. The entropy difference range for both conformers was searched from -5.0-5.0 cal deg^{-1} mol^{-1}. The temperature dependences of the slow-exchange chemical shifts presented in Table 5.5 were linearly extrapolated and included in the fast-exchange calculations.

Although the traditional average fits the data better again, this may only prove the ability of the traditional form to fit any fast-exchange value when allowed to vary in such a large parameter space as the grid searched here. The dependence of the two forms on ΔG is obviously different. The free energy enters in both forms through the exponential term but also enters into the new average in the offset term, which changes linearly with ΔG. This difference could allow the traditional average to take on a wider range of values in a particular parameter space, but such behavior would not necessarily reflect the correctness of the traditional form.

The temperature-dependent spin parameters observed in $CF_2BrCFClBr$, which were not included in the calculations presented in Table 5.6, support the argument that the success of the traditional formulation for these data sets may be merely coincidental. The need for conclusive data sets in verifying either stochastic average certainly still exists.

5.5 Isomers of Cyclic Compounds

The averaging of spin parameters occurs in many larger cyclic compounds. The free-energy differences and barriers affecting the thermal averaging between axial and equatorial conformers are often of a magnitude allowing both slow- and fast-exchange spectra to be obtained. The energy barriers regulating conformational averaging in most four- and five-membered rings are too small to investigate with variable-temperature NMR at experimentally feasible temperatures, so larger cycloalkanes and their heterocycles prove to be the most-studied ring compounds. In this section, the emphasis of the discussion will be on derivatives of cyclohexane. As mentioned previously for the motional averaging of NMR spectra in acetaldehyde, the conformational averaging in cyclohexane will not lead to temperature-dependent fast-exchange spin parameters because the conformers are degenerate in energy. This degeneracy also causes the difference between the two stochastic averages to vanish. For this reason, only substituted

cyclohexanes are possibly useful test systems. A few examples of cyclohexane derivatives that have been studied are presented in Table 5.7.

Table 5.7. Ring compounds displaying dynamic NMR behavior and stochastic averaging of spin parameters.

Compound	Reference
$C_6H_{11}D$	33-35
$C_6H_{11}T$	36
$C_6H_{11}F$	37,38
$C_6H_{11}CH_3$	39,40

The hydrogen isotopes in monodeuterio- and monotritiocyclohexane break the degeneracy of the axial and equatorial conformers. The reported free-energy differences in these molecules have been measured as 6.3 ± 1.5 cal mol^{-1} for $C_6H_{11}D$[33] and 11.2 ± 0.5 cal mol^{-1} for $C_6H_{11}T$.[36] These differences are much smaller than those observed in many substituted ethanes, which are often on the order of hundreds of cal mol^{-1}. Such molecules prove to be inadequate for testing the stochastic averages, since the difference term between the two theories will be almost negligible.

The halocyclohexanes prove to have much larger free-energy differences between conformers. Reported[37,38] ΔG_{298}(axial-equatorial) values are 180 cal mol^{-1} for $C_6H_{11}F$, 340 cal mol^{-1} for $C_6H_{11}Cl$, and 270 cal mol^{-1} for $C_6H_{11}Br$ (all neat samples). The free-energy difference for $C_6H_{11}F$ displays a large solvent dependence, ranging from 90 cal mol^{-1} in nitrobenzene to 200 cal mol^{-1} in acetic acid.[37,38] The relatively large, solvent-dependent free-energy differences are expected between conformers that differ in polarity as much as the axial and equatorial forms of halocyclohexanes. Such interactions also prove to be temperature dependent, making it difficult to account for such effects in a quantitative manner. These effects will be discussed in Section 5.7.

While the free-energy difference observed in $C_6H_{11}CH_3$[39,40] is 1600-1800 cal mol^{-1}, making the difference term between the traditional and alternative stochastic averages significant, a ΔG(axial-equatorial) of this size presents other experimental difficulties. Unlike the determination of ΔG(axial-equatorial) for $C_6H_{11}D$ and $C_6H_{11}T$, which depends on measuring very small differences between two comparable numbers, determining the ΔG of $C_6H_{11}CH_3$ involves the integration of very small resonances for the unfavored conformer. The situation results in very large experimental errors and can preclude the measurement of accurate ΔG values over a range of slow-exchange temperatures. Nevertheless, Anet and Freedberg[41] have recently reanalyzed using both stochastic theories the unpublished observations of Basus[42] on ^{13}C chemical shifts in methylcyclohexane and argue that it provides a strong counterexample to the JKW hypothesis.

5.6 Isotopomers of Hydrogen, Methane, HF, and CH_3F

The HD molecule was one of the first systems used to demonstrate the mechanism of spin coupling.[43] The subsequent measurement[44] of J_{HD} equal to 43.5 ± 1 Hz contrasted with an initial calculation of 70 Hz.[43] With improvements in experimental procedures, the temperature dependence of the spin coupling was observed, the value changing -0.20 Hz over the temperature range 20-300 K.[45] A molecular beam magnetic resonance method proved to be less accurate than other techniques, but measured a value of $J_{HD} = +(36 \pm 16)$ Hz, revealing the sign of the HD coupling to be positive.[46]

The HD molecule proves to be the simplest example of a molecule with which to test theoretical treatments of the temperature dependence of spin parameters. Other isotopomers of molecular hydrogen, such as HT and DT, and other simple molecules such as $^{13}CH_4$, $CH_{4-n}D_n$, HF, DF, and CH_3F have been the subject of extensive experimental and theoretical efforts.[47-55] Theoretical and experimental values of the temperature dependence of the spin couplings in some of these molecules are presented in Table 5.8.

Table 5.8. The calculated changes in the spin couplings observed in some simple molecules which undergo averaging over eigenstates. Results are theoretical (ref. 47) and experimental (refs. 48, 53).

Molecule, J	Temp. Range (K)	ΔJ(hi-T - low-T) (Hz)	Reference
HD, $^1J_{HD}$	0 - 600	0.38	47
HT, $^1J_{HT}$	0 - 600	2.60	47
DT, $^1J_{DT}$	0 - 600	0.41	47
$^{13}CH_4$, $^1J_{CH}$	200 - 370	0.08	48
CH_3D, $^2J_{HD}$	223 - 295	0.005	53

These systems, although relatively simple to treat theoretically, do not meet the experimental criteria outlined in Section 5.2. At the present time, measurement of the spin parameters in each individual molecular eigenstate is not experimentally possible. Current theoretical treatments attempt to account for the temperature dependent behavior of these systems by calculating the spin parameters as functions of average bond length and electronic properties which are affected by changes in temperature. If indeed the individual spin parameters could be measured, these systems, in addition to validating procedures of stochastic averaging, might provide verification of various theoretical treatments of spin parameters.

5.7 Solvent and Concentration Effects

The incorrect assumption that conformer free energies and spin parameters were temperature-independent led to difficulties in early attempts to calculate averaged NMR

spectra. Discussing the temperature dependence of these quantities in an early review of solvent effects in NMR, Laszlo[56] wrote, "The same is also true for chemical shifts, which like coupling constants, are affected by association effects with the solvent, which are themselves temperature dependent." Barfield and Johnston[57] also review medium effects on spin couplings arising from solvent-solute interactions but note that, from the fast-exchange data alone, it is "not generally possible to infer the importance" of these effects in studies of conformational averaging.

In both the substituted ethanes and cyclohexane derivatives, solvent-dependent spin parameters and ΔG's have been observed.[24-26,38] While these effects can be measured, albeit over a usually narrow range of slow-exchange temperatures, and included in the calculation of fast-exchange averages, such efforts assume that the observed slow-exchange behavior is followed for all temperatures through the fast-exchange regime. For those systems discussed in this chapter in which averaging over molecular conformers occurs, there is some range of temperatures between the slow- and fast-exchange regimes. This intermediate-exchange regime increases the range of temperatures over which these assumptions must be used and cannot be verified.

While ideal systems would have little or no temperature or solvent dependence, these properties may be inherently connected to the existence of nondegenerate conformers, a condition necessary for fast-exchange conformational averaging. Two interactions can be identified as major contributors to the free-energy difference between the axial and equatorial forms of the cyclohexane derivatives discussed: the unfavored 1,3-interactions between the substituent and protons on C-3, and the solvent-solute interactions arising from the polarity difference between the axial and equatorial conformers. The latter contribution is probably responsible for most of the solvent dependence of ΔG_{ae} for fluorocyclohexane. As pointed out by Laszlo, these interactions can be expected to be quite temperature-dependent.

The solvent dependence of the cyclohexanes can be contrasted with that of the substituted ethanes. The ΔG_{tg} of FTBE shows a solvent dependence, changing from 422 cal mol^{-1} in $CFCl_3$ (ε = 2.88) to 382 cal mol^{-1} in acetone (ε = 32.5). The change is certainly not as dramatic as the more than twofold change observed for fluorocyclohexane in different solvents. It is difficult to assign solvent and temperature dependence to certain interactions and more data is needed to compare rigorously these effects in the ethanes and cyclohexanes. However, as a general guideline, good test systems would be those in which the free-energy differences between conformers are determined by intramolecular as opposed to intermolecular (solvent-solute) interactions.

Solvent-solute interactions are crucial in determining stochastically averaged NMR spectra. However solute concentration could prove to be even more important. The importance of resonant molecular collisions in bringing about the conformational averaging that occurs on the timescale of the NMR experiment could invalidate the entire notion of single-molecule statistical mechanics as being adequate to the problem. The rate of solute-solute collisions in a typical NMR sample is orders of magnitude higher than that of chemical exchange. Thus, the states which are coming to spatial equilibrium at a rate determined by chemical exchange may in effect be delocalized over many molecules in different spin states. Calculations with such delocalized states are needed to ascertain whether in fact the theories differ in this regime. If they do not, then experiments to test this hypothesis may require solute concentrations which are at or beyond the limit of NMR detectability or confinement methods to prevent delocalization. Investigations of the effects of solute concentration on the averaging process are currently being considered.

5.8 Improved Accuracy by Field Cycling

In comparing either stochastic average with experiment the most striking observation is how rarely possible it is to predict fast-exchange data from slow-exchange data within the experimental accuracy of the latter. This is so despite there being large

parameter spaces available to search due to errors inherent in extrapolating over temperature. One promising approach to improving the accuracy with which stochastic averaging could be tested is to eliminate the need for varying temperatures in passing from slow to fast exchange. Since magnetic field can readily be varied by a factor of $\sim 10^4$, without changing the spin eigenstates of an AX system, for example, the same sample would satisfy the slow-exchange condition $\nu_A - \nu_X \gg k$ at high field and the fast-exchange condition $\nu_A - \nu_X \ll k$ at low field with the same k. Field cycling could be used to retain the sensitivity of high-field polarization and detection. Measurement of J_{AX} of such a system in this way should improve the accuracy available for testing statistical theories by more than an order of magnitude.

There are in fact two very different problems involved in the usual experimental paradigm of varying temperature. The first is the possible complexities of describing the change in thermodynamic state of a liquid with temperature and its NMR consequences. The second is the present uncertainty in the very definition of what quantities are measured by a fast-exchange spin Hamiltonian. Field cycling experiments would allow the latter question to be examined independently of the former.

5.9 Conclusions

The importance of stochastic averaging in magnetic resonance cannot be overstated. The correct interpretation of thousands of variable-temperature NMR investigations depends on the proper calculation of averaged spin parameters. The subject systems of these investigations range from small molecules, such as those discussed here, to large polymers and biomolecules, such as proteins.

The question of how to calculate a stochastically averaged NMR spectrum remains unanswered. While important physical objections to the traditional form can be made, experimental evidence in support of the new formulation is still lacking. That recent efforts have not uncovered test systems suited to resolving the averaging issue is both

somewhat surprising and somewhat expected. A large number of NMR studies have been carried out for the purpose of investigating temperature-dependent motional averaging of molecules and yet in the absence of any alternative theoretical formulation there was little motivation to view the results critically or improve their accuracy. Only with the formulation of the alternative theory did the experimental criteria of Section 5.2 become important. Although the poor predictive ability of the traditional theory has often been noted, it has never been considered conceptually suspect. Rather the difficulty has always been attributed to inadequacies of the slow-exchange data or their extrapolation to higher temperature.

The validation of one or the other form of the stochastic average will require a good test system or a new experimental approach, such as field cycling, to obtain the needed data, or both. Other experimental conditions which affect stochastic averaging, such as solute concentration, must also be addressed. Establishing the connection between NMR and vibrational, rotational, or other degrees of freedom is the goal of the stochastic averaging procedures discussed. As the work presented here shows, investigations of stochastic averaging in NMR remain theoretically and experimentally challenging.

References

1. C.R. Bowers, D.H. Jones, N.D. Kurur, J.A. Labinger, M.G. Pravica, and D.P. Weitekamp, *Adv. Magn. Reson.* **14**, 269 (1990).
2. K.W. Zilm, D.M. Heinekey, J.M. Millar, N.G. Payne, S.P. Neshyba, J.C. Duchamp, and J. Szczyrba, *J. Amer. Chem. Soc.* **112**, 920 (1990).
3. H.-H. Limbach, G. Scherer, M. Maurer, and B. Chaudret, *Angew. Chem. Int. Ed. Engl.* **31**, 1369 (1992).
4. E.M. Hiller and R.A. Harris, *J. Chem. Phys.* **98**, 2077 (1993).
5. T.M. Gilbert and R.G. Bergman, *J. Amer. Chem. Soc.* **107**, 3502 (1985).
6. R.A. Paciello, Ph.D. Dissertation, California Institute of Technology, 1987.
7. W. McFarlane, *Chem. Comm.*, 772 (1967).
8. P.C. Lauterbur and R.J. Kurland, *J. Amer. Chem. Soc.* **84**, 3405 (1962).
9. B.E. Mann, C. Masters, and B.L. Shaw, *Chem. Comm.*, 846 (1970).
10. J.P. Jesson, in "Transition Metal Hydrides," E.L. Muetterties, ed.; Marcel Dekker, Inc., New York, 1971.
11. P. Diehl and J.A. Pople, *Mol. Phys.* **3**, 545, 557 (1960).
12. R.J. Abraham, E.O. Bishop, and R.E. Richards, *Mol. Phys.* **3**, 485 (1960).
13. T.W. Dingle and K.R. Dixon, *Inor. Chem.* **13**, 846 (1974).
14. T.M. Gilbert, Ph.D. Dissertation, University of California, Berkeley, 1985.
15. J.C. Schug, P.E. McMahon, and H.S. Gutowsky, *J. Chem. Phys.* **33**, 843 (1960).
16. R.J. Abraham and H.J. Bernstein, *Can. J. Chem.* **39**, 39 (1961).
17. T.D. Alger, H.S. Gutowsky, and R.L. Vold, *J. Chem. Phys.* **47**, 2818 (1967).
18. H.S. Gutowsky, G.G. Belford, and P.E. McMahon, *J. Chem. Phys.* **36**, 3353 (1962).
19. R.A. Newmark and C.H. Sederholm, *J. Chem. Phys.* **43**, 602 (1965).
20. R.A. Newmark and C.H. Sederholm, *J. Chem. Phys.* **39**, 3131 (1963).
21. S. Ng, J. Tang, and C.H. Sederholm, *J. Chem. Phys.* **42**, 79 (1965).
22. R.R. Dean and J. Lee, *Trans. Faraday Soc.* **65**, 1 (1969).

23. W.S. Brey, Jr., and K.C. Ramey, *J. Chem. Phys.* **39**, 844 (1963).

24. G. Govil and H.J. Bernstein, *J. Chem. Phys.* **47**, 2818 (1967).

25. G. Govil and H.J. Bernstein, *J. Chem. Phys.* **48**, 285 (1968).

26. G. Govil and H.J. Bernstein, *Mol. Phys.* **14**, 197 (1968).

27. R.E. Kagarise, *J. Chem. Phys.* **29**, 680 (1967).

28. R.D. Norris and G. Binsch, *J. Amer. Chem. Soc.* **95**, 182 (1973).

29. P.R. Carey, H.W. Kroto, and M.A. Turpin, *Chem. Commun.*, 188 (1969).

30. S.L. Manatt and J.R. Young, *J. Magn. Reson.* **40**, 347 (1980).

31. G.R. Franzen and G. Binsch, *J. Amer. Chem. Soc.* **95**, 175 (1973).

32. G. Binsch, *J. Amer. Chem. Soc.* **95**, 190 (1973).

33. F.A.L. Anet and D.J. O'Leary, *Tetr. Lett.* **30**, 1059 (1989).

34. R. Aydin and H. Günther, *Angew. Chem. Int. Ed. Engl.* **20**, 985 (1981).

35. R. Aydin, J.R. Wesener, H. Günther, R.L. Santillan, M.-E. Garibay, and P. Joseph-Nathan, *J. Org. Chem.* **49**, 3845 (1984).

36. F.A.L. Anet, D.J. O'Leary, and P.G. Williams, *J. Chem. Soc., Chem. Comm.* **20**, 1427 (1990).

37. E.L. Eliel and R.J.L. Martin, *J. Amer. Chem. Soc.* **90**, 689 (1968).

38. P.-S. Chu and N.S. True, *J. Phys. Chem.* **89**, 5613 (1985).

39. D.K. Dalling and D.M. Grant, *J. Amer. Chem. Soc.* **89**, 6612 (1967).

40. F.A.L. Anet, C.H. Bradley, and G.W. Buchanan, *J. Amer. Chem. Soc.* **93**, 258 (1971).

41. F.A.L. Anet and D. Freedberg, 34th Experimental NMR Conference, March 15, 1993.

42. V.J. Basus, Ph.D. Dissertation, University of California, Los Angeles, 1975.

43. N.F. Ramsey and E.M. Purcell, *Phys. Rev.* **85**, 143 (1952).

44. H.Y Carr and E.M. Purcell, *Phys. Rev.* **88**, 415 (1952).

45. D.K. Green, A. Hartland, and H.Y. Carr, *Bull. Am. Phys. Soc.* **11**, 311 (1966).

46. I. Ozier, P.-N. Yi, A. Khosla, and N.F. Ramsey, *Bull. Am. Phys. Soc.* **12**, 132 (1967).

47. W.T. Raynes and J.P. Riley, *Mol. Phys.* **27**, 337 (1974).

48. B. Bennett, W.T. Raynes, and C.W. Anderson, *Spectrochim. Acta* **45A**, 821 (1989).

49. W.T. Raynes and N. Pantelli, *Chem. Phys. Lett.* **94**, 558 (1983).

50. J. Oddershede, J. Geersten, and G.E. Scuseria, *J. Phys. Chem.* **92**, 3056 (1988).

51. I. Solomon and N. Bloembergen, *J. Chem. Phys.* **25**, 261 (1956).

52. J.S. Muenter and W. Klemperer, *J. Chem. Phys.* **52**, 6033 (1970).

53. F.A.L. Anet and D.J. O'Leary, *Tetr. Lett.* **30**, 2755 (1989).

54. M.J. Packer and W.T. Raynes, *Mol. Phys.* **69**, 391 (1990).

55. J. Geersten, J. Oddershede, W.T. Raynes, and G.E. Scuseria, *J. Magn. Reson.* **93**, 458 (1991).

56. P. Laszlo, in "Progress in Nuclear Magnetic Resonance Spectroscopy," J.W. Emsley, J. Feeney, and L.H. Sutcliffe, eds.; Pergamon Press, New York, 1967.

57. M. Barfield and M.D. Johnston, Jr., *Chem. Rev.* **73**, 53 (1973).

Appendix 1

The following is the full treatment of the AB spin system using Redfield relaxation theory as discussed in Chapter 3. The relaxation terms come from the large, oscillating J-couplings which operate between spin states of the AB spin system as occurs in the transition metal hydrides. The Liouvillian superoperator formalism is used throughout.

The level-shift operator basis is formed by the bras and kets of the singlet/triplet spin-state basis. The level-shift operators must be defined such that they operate in the same direction, i.e., "raising" or "lowering" level-shift operators. The following notation, based upon the diagram below, will be used throughout the treatment.

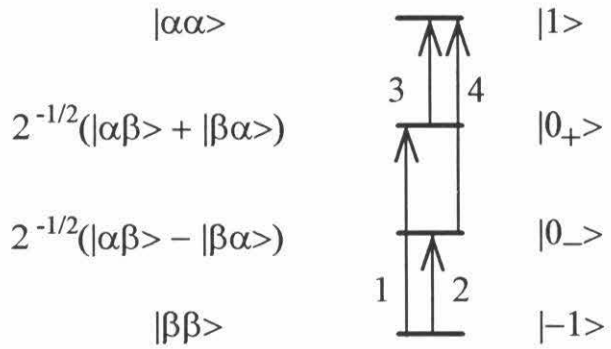

$1 = |0_+\rangle\langle -1| = 2^{-1/2}(|\alpha\beta\rangle + |\beta\alpha\rangle)\langle\beta\beta|$

$2 = |0_-\rangle\langle -1| = 2^{-1/2}(|\alpha\beta\rangle - |\beta\alpha\rangle)\langle\beta\beta|$

$3 = |1\rangle\langle 0_+| = 2^{-1/2}|\alpha\alpha\rangle(\langle\alpha\beta| + \langle\beta\alpha|)$

$4 = |1\rangle\langle 0_-| = 2^{-1/2}|\alpha\alpha\rangle(\langle\alpha\beta| - \langle\beta\alpha|)$

The elements of the matrix Λ are:

$$[|0_+\rangle\langle -1|,|-1\rangle\langle 0_+|] = |0_+\rangle\langle -1|-1\rangle\langle 0_+| - |-1\rangle\langle 0_+|0_+\rangle\langle -1| = |0_+\rangle\langle 0_+| - |-1\rangle\langle -1|,$$

$[|0_+\rangle\langle -1|,|-1\rangle\langle 0_-|] = |0_+\rangle\langle -1|-1\rangle\langle 0_-| - |-1\rangle\langle 0_-|0_+\rangle\langle -1| = |0_+\rangle\langle 0_-|$,

$[|0_-\rangle\langle -1|,|-1\rangle\langle 0_+|] = |0_-\rangle\langle -1|-1\rangle\langle 0_+| - |-1\rangle\langle 0_+|0_-\rangle\langle -1| = |0_-\rangle\langle 0_+|$, and

$[|0_-\rangle\langle -1|,|-1\rangle\langle 0_-|] = |0_-\rangle\langle -1|-1\rangle\langle 0_-| - |-1\rangle\langle 0_-|0_-\rangle\langle -1| = |0_-\rangle\langle 0_-| - |-1\rangle\langle -1|$.

This completes the terms in the upper 2X2 matrix. Other terms may give a level-shift operator, but these will have zero trace and can be ignored. They are terms such as $|1\rangle\langle -1|$ terms and $\mathcal{H}$ won't yield a $|j\rangle\langle k|$ with $j = k$. The lower Λ 2X2 matrix has the terms:

$[|1\rangle\langle 0_+|,|0_+\rangle\langle 1|] = |1\rangle\langle 0_+|0_+\rangle\langle 1| - |0_+\rangle\langle 1|1\rangle\langle 0_+| = |1\rangle\langle 1| - |0_+\rangle\langle 0_+|$,

$[|1\rangle\langle 0_+|,|0_-\rangle\langle 1|] = |1\rangle\langle 0_+|0_-\rangle\langle 1| - |0_-\rangle\langle 1|1\rangle\langle 0_+| = -|0_-\rangle\langle 0_+|$,

$[|1\rangle\langle 0_-|,|0_+\rangle\langle 1|] = |1\rangle\langle 0_-|0_+\rangle\langle 1| - |0_+\rangle\langle 1|1\rangle\langle 0_-| = -|0_+\rangle\langle 0_-|$,

and $[|1\rangle\langle 0_-|,|0_-\rangle\langle 1|] = |1\rangle\langle 0_-|0_-\rangle\langle 1| - |0_-\rangle\langle 1|1\rangle\langle 0_-| = |1\rangle\langle 1| - |0_-\rangle\langle 0_-|$.

$\mathcal{H} = -\nu_A I_{ZA} - \nu_B I_{ZB} + J_{AB} I_A \cdot I_B$

$= -\nu_A I_{ZA} - \nu_B I_{ZB} + J_{AB} I_{ZA} I_{ZB} + (J_{AB}/2)(I_{+A} I_{-B} + I_{-A} I_{+B})$

$\langle 1|\mathcal{H} = \langle \alpha\alpha|\mathcal{H} = \langle 1|[(-1/2)(\nu_A + \nu_B) + J/4]$

$\langle -1|\mathcal{H} = \langle \beta\beta|\mathcal{H} = \langle -1|[(1/2)(\nu_A + \nu_B) + J/4]$

$\langle 0_-|\mathcal{H} = 2^{-1/2}(\langle \alpha\beta| - \langle \beta\alpha|)\mathcal{H} = 2^{-1/2}\{\langle \alpha\beta|[(-1/2)(\nu_A - \nu_B)-J/4] + \langle \beta\alpha|(J/2)$

$- \langle \beta\alpha|[(1/2)(\nu_A - \nu_B)-J/4] - \langle \alpha\beta|(J/2)\} = (-3J/4)\langle 0_-| - (1/2)(\nu_A - \nu_B)\langle 0_+|$

$\langle 0_+|\mathcal{H} = 2^{-1/2}(\langle \alpha\beta| + \langle \beta\alpha|)\mathcal{H} = 2^{-1/2}\{\langle \alpha\beta|[(-1/2)(\nu_A - \nu_B)-J/4] + \langle \beta\alpha|(J/2)$

$+ \langle \beta\alpha|[(1/2)(\nu_A - \nu_B)-J/4] + \langle \alpha\beta|(J/2)\} = (J/4)\langle 0_+| - (1/2)(\nu_A - \nu_B)\langle 0_-|$

Now the actual terms of the Λ can be found. Only the terms with $|j\rangle\langle j|$ that yield non-zero trace elements will be written.

$-\mathrm{Tr}\{(|0_+\rangle\langle 0_+| - |-1\rangle\langle -1|)\mathcal{H}\} = -\mathrm{Tr}\{|0_+\rangle\langle 0_+|(J/4) - |-1\rangle\langle -1|[(1/2)(\nu_A + \nu_B) + (J/4)]\}$

$= (1/2)(\nu_A + \nu_B)$

$-\mathrm{Tr}\{|0_+\rangle\langle 0_-|\mathcal{H}\} = (1/2)(\nu_A - \nu_B)$

$-\mathrm{Tr}\{|0_-\rangle\langle 0_+|\mathcal{H}\} = (1/2)(\nu_A - \nu_B)$

$-\mathrm{Tr}\{(|0_-\rangle\langle 0_-| - |-1\rangle\langle -1|)\mathcal{H}\} = -\mathrm{Tr}\{|0_-\rangle\langle 0_-|(-3J/4) - |-1\rangle\langle -1|[(1/2)(\nu_A + \nu_B) + (J/4)]\}$

$= (1/2)(\nu_A + \nu_B) + J$

The terms in the other 2X2 are written:

$$-\mathrm{Tr}\{(|1\rangle\langle 1| - |0_+\rangle\langle 0_+|)\mathcal{H}\} = -\mathrm{Tr}\{|1\rangle\langle 1|[(-1/2)(\nu_A + \nu_B) + (J/4)] - |0_+\rangle\langle 0_+|(J/4)\}$$

$$= (1/2)(\nu_A + \nu_B)$$

$$-\mathrm{Tr}\{-|0_-\rangle\langle 0_+|\mathcal{H}\} = (-1/2)(\nu_A - \nu_B)$$

$$-\mathrm{Tr}\{-|0_+\rangle\langle 0_-|\mathcal{H}\} = (-1/2)(\nu_A - \nu_B)$$

$$-\mathrm{Tr}\{(|1\rangle\langle 1| - |0_-\rangle\langle 0_-|)\mathcal{H}\} = -\mathrm{Tr}\{|1\rangle\langle 1|[(-1/2)(\nu_A + \nu_B) + (J/4)] - |0_-\rangle\langle 0_-|(-3J/4)\}$$

$$= (1/2)(\nu_A + \nu_B) - J$$

Now the terms of Γ can be calculated. By inspecting the form of Γ_{jk}, it can be seen that Γ_{jk} will be diagonal in the level-shift operator basis since all off-diagonal terms will include inner-products of orthogonal states and will equal zero.

$$(k_J/2)\mathrm{Tr}\{[|0_+\rangle\langle -1|, I_A \cdot I_B][|-1\rangle\langle 0_+|, I_A \cdot I_B]\} = 0$$

$$(k_J/2)\mathrm{Tr}\{[|0_-\rangle\langle -1|, I_A \cdot I_B][|-1\rangle\langle 0_-|, I_A \cdot I_B]\} = (k_J/2)\mathrm{Tr}\{[(1)(-1)|0_-\rangle\langle 0_-|\} = -(k_J/2)$$

$$(k_J/2)\mathrm{Tr}\{[|1\rangle\langle 0_+|, I_A \cdot I_B][|0_+\rangle\langle 1|, I_A \cdot I_B]\} = 0$$

$$(k_J/2)\mathrm{Tr}\{[|1\rangle\langle 0_-|, I_A \cdot I_B][|0_-\rangle\langle 1|, I_A \cdot I_B]\} = (k_J/2)\mathrm{Tr}\{[(-1)(1)|1\rangle\langle 1|\} = -(k_J/2)$$

With the following substitutions, we can simplify the resulting $(\Gamma - i\Lambda)$ matrix.

$$(1/2)(\nu_A + \nu_B) = a$$

$$(1/2)(\nu_A - \nu_B) = d$$

$(k_J/2) + iJ = c$, with c^* being the complex conjugate of c.

$$\Gamma - i\Lambda = \begin{bmatrix} -ia & -id & 0 & 0 \\ -id & -c - ia & 0 & 0 \\ 0 & 0 & -ia & id \\ 0 & 0 & id & -c^* - ia \end{bmatrix}$$

The eigenvalues and eigenvectors of this matrix are found by solving each 2X2 matrix. The eigenvalues λ for the first 2X2 are given by:

$$\lambda_{\pm} = (-1/2)(c + 2ia) \pm [(c/2)^2 - d^2]^{1/2}.$$

The corresponding eigenvectors for the two eigenvalues are:

$$\begin{pmatrix} x \\ y \end{pmatrix} = \begin{pmatrix} id \\ (c/2) - [(c/2)^2 - d^2]^{1/2} \end{pmatrix}, \text{ and}$$

$$\begin{pmatrix} x \\ y \end{pmatrix} = \begin{pmatrix} id \\ (c/2) + [(c/2)^2 - d^2]^{1/2} \end{pmatrix}.$$

The general form of the solution is given by:

$$\sigma(t) = c_+ e^{\lambda_+ t} v_+ + c_- e^{\lambda_- t} v_-.$$

Here, the $c_\pm$ are the normalization constants and the $v_\pm$ are the corresponding eigenvectors given above. At time zero, the initial condition will be:

$$\sigma(0) = c_+ v_+ + c_- v_-.$$

$\sigma(0)$ is the state of the system after an initial 90° y pulse, it is proportional to I_X. I_X in the level-shift operator basis is a vector which we can find by expressing I_X in the singlet/triplet basis.

$$-\mathrm{Tr}\{(|1\rangle\langle 1| - |0_+\rangle\langle 0_+|)\mathcal{H}\} = -\mathrm{Tr}\{|1\rangle\langle 1|[(1/2)(\nu_A + \nu_B) + (J/4)] - |0_+\rangle\langle 0_+|(J/4)\}$$

$$I_X = (1/2)(I_{+A} + I_{-A} + I_{+B} + I_{-B})$$

$$\langle 1|I_X|0_+\rangle = \langle\alpha\alpha|(1/2)(I_{+A} + I_{-A} + I_{+B} + I_{-B})(2^{-1/2})(\langle\alpha\beta| + \langle\beta\alpha|)$$

$$= (2^{-1/2}/2)\langle\alpha\alpha|\alpha\alpha + \beta\beta + \alpha\alpha + \beta\beta\rangle = (2^{-1/2})\langle\alpha\alpha|\alpha\alpha\rangle = (2^{-1/2})$$

The matrix elements have values of either $(2^{-1/2})$ or zero. Solving the above equations at $t = 0$, the resulting normalization constants are written:

$$c_+ = \frac{-i}{2\sqrt{2}d}\left[\frac{(c/2) + [(c/2)^2 - d^2]^{1/2}}{[(c/2)^2 - d^2]^{1/2}}\right], \text{ and}$$

$$c_- = \frac{i}{2\sqrt{2}d}\left[\frac{(c/2) - [(c/2)^2 - d^2]^{1/2}}{[(c/2)^2 - d^2]^{1/2}}\right].$$

The other 2X2 of the $(\Gamma - i\Lambda)$ matrix yields similar solutions. The signal can now be calculated from the expressions that have been obtained. The signal is

$$S(t) = \mathrm{Tr}(\sigma(t)I_+).$$

Since

$\sigma_{11}(0) = \sigma_{33}(0) = (2^{-1/2})$, and

$\sigma_{22}(0) = \sigma_{44}(0) = 0$,

and considering only the non-zero terms, the signal becomes:

$$S(t) = \sigma_{11}(t)\sigma_{11}(0) + \sigma_{33}(t)\sigma_{33}(0) = (2^{-1/2})\sigma_{11}(t) + (2^{-1/2})\sigma_{33}(t).$$

Using the additional substitutions:

$sq = [(c/2)^2 + d^2]^{1/2}$, and

$sq^* = [(c^*/2)^2 + d^2]^{1/2}$,

$$S(t) = \frac{1}{4}\left\{\frac{\frac{c}{2}+sq}{sq}\exp\left[\left(-\frac{(c+2ia)}{2}+sq\right)t\right]\right\}$$

$$-\frac{1}{4}\left\{\frac{\frac{c}{2}-sq}{sq}\exp\left[\left(-\frac{(c+2ia)}{2}-sq\right)t\right]\right\}$$

$$+\frac{1}{4}\left\{\frac{\frac{c^*}{2}+sq^*}{sq^*}\exp\left[\left(-\frac{(c^*+2ia)}{2}+sq^*\right)t\right]\right\}$$

$$-\frac{1}{4}\left\{\frac{\frac{c^*}{2}-sq^*}{sq^*}\exp\left[\left(-\frac{(c^*+2ia)}{2}-sq^*\right)t\right]\right\}$$

Appendix 2

The following is a calculation of the effects of large, fluctuating spin parameters on zero-quantum transitions. This is of interest in relating the results of Appendix 1, as discussed in Chapter 3, to previous studies of tunnelling systems carried out by Wertheimer and Silbey.[1] Using the same notation as in Appendix 1, the level-shift operator basis for the zero-quantum calculation is written:

$$A_1 = (1/2)(|1\rangle\langle 1| - |-1\rangle\langle -1|)$$

$$A_2 = (2^{1/2}/4)(|0_+\rangle\langle 0_+| + |0_-\rangle\langle 0_-| - |1\rangle\langle 1| - |-1\rangle\langle -1|)$$

$$A_X = (1/2)(|0_+\rangle\langle 0_-| + |0_-\rangle\langle 0_+|)$$

$$A_Y = (-i/2)(|0_+\rangle\langle 0_-| - |0_-\rangle\langle 0_+|)$$

$$A_Z = (1/2)(|0_+\rangle\langle 0_+| - |0_-\rangle\langle 0_-|)$$

This level-shift operator basis follows the same commutation relations as the angular momentum operator basis in which

$$[A_X, A_Y] = (-i/4)(-|0_+\rangle\langle 0_+| + |0_-\rangle\langle 0_-| + |0_-\rangle\langle 0_-| - |0_+\rangle\langle 0_+|) = iA_Z$$

and cyclic permutations of X, Y, and Z. The following identities are also useful for expressing the total spin Hamiltonian in terms of this level-shift operator basis.

$$(1/2)(I_{ZA} - I_{ZB}) = A_X$$

$$I_A \cdot I_B = (1/4)(|1\rangle\langle 1| + |0_+\rangle\langle 0_+| + |-1\rangle\langle -1| - 3|0_-\rangle\langle 0_-|)$$

$$= (-2^{-1/2})A_2 + A_Z$$

In a manner analogous to Appendix 1, the matrix Λ_{jk} will be calculated in the A_X, A_Y, A_Z, A_1, and A_2 basis. The commutators of the level-shift operators are:

$$[A_1, A_2] = (2^{1/2}/8)(|1\rangle\langle 1| - |-1\rangle\langle -1|)(|0_+\rangle\langle 0_+| + |0_-\rangle\langle 0_-| - |1\rangle\langle 1| - |-1\rangle\langle -1|)$$

$$- (2^{1/2}/8)(|0_+\rangle\langle 0_+| + |0_-\rangle\langle 0_-| - |1\rangle\langle 1| - |-1\rangle\langle -1|)(|1\rangle\langle 1| - |-1\rangle\langle -1|) = 0,$$

$$[A_1, A_X] = (1/4)(|1\rangle\langle 1| - |-1\rangle\langle -1|)(|0_+\rangle\langle 0_-| + |0_-\rangle\langle 0_+|)$$
$$- (1/4)(|0_+\rangle\langle 0_-| + |0_-\rangle\langle 0_+|)(|1\rangle\langle 1| - |-1\rangle\langle -1|) = 0,$$
$$[A_2, A_X] = (2^{1/2}/8)(|0_+\rangle\langle 0_+| + |0_-\rangle\langle 0_-| - |1\rangle\langle 1| - |-1\rangle\langle -1|)(|0_+\rangle\langle 0_-| + |0_-\rangle\langle 0_+|)$$
$$- (2^{1/2}/8)(|0_+\rangle\langle 0_-| + |0_-\rangle\langle 0_+|)(|0_+\rangle\langle 0_+| + |0_-\rangle\langle 0_-| - |1\rangle\langle 1| - |-1\rangle\langle -1|) = 0, \text{ and}$$
$$[A_1, A_Y] = [A_1, A_Z] = [A_2, A_Y] = [A_2, A_Z] = 0.$$

$$[Q_j, Q_k^+] = \begin{array}{c} \\ A_1 \\ A_2 \\ A_X \\ A_Y \\ A_Z \end{array} \begin{array}{c} \begin{array}{ccccc} \quad & \quad & \quad & \quad & \quad \end{array} \\ \begin{pmatrix} 0 & 0 & 0 & 0 & 0 \\ 0 & 0 & 0 & 0 & 0 \\ 0 & 0 & 0 & iA_Z & -iA_Y \\ 0 & 0 & -iA_Z & 0 & iA_X \\ 0 & 0 & iA_Y & -iA_X & 0 \end{pmatrix} \end{array}$$

The Hamiltonian can be written in terms of the level-shift operator basis as:

$$\mathcal{H} = (1/2)(\nu_A - \nu_B)(I_{ZA} - I_{ZB}) + JI_A \cdot I_B = (\nu_A - \nu_B)A_X + J[(-2^{-1/2})A_2 + A_Z].$$

The terms in Λ_{jk} are written:

$$\mathrm{Tr}\{[iA_X][(\nu_A - \nu_B)A_X + J[(-2^{-1/2})A_2 + A_Z]]\} = \mathrm{Tr}[i(\nu_A - \nu_B)(A_X)^2]$$
$$= \mathrm{Tr}\{(i/4)(\nu_A - \nu_B)(|0_+\rangle\langle 0_-| + |0_-\rangle\langle 0_+|)(|0_+\rangle\langle 0_-| + |0_-\rangle\langle 0_+|)\}$$
$$= (i/2)(\nu_A - \nu_B),$$
$$\mathrm{Tr}\{[iA_Y][(\nu_A - \nu_B)A_X + J[(-2^{-1/2})A_2 + A_Z]]\} = \mathrm{Tr}\{i(\nu_A - \nu_B)(|0_+\rangle\langle 0_+| - |0_-\rangle\langle 0_-|)\}$$
$$= 0, \text{ and}$$
$$\mathrm{Tr}\{[iA_Z][(\nu_A - \nu_B)A_X + J[(-2^{-1/2})A_2 + A_Z]]\} = \mathrm{Tr}\{(iJ/4)(|0_+\rangle\langle 0_+| + |0_-\rangle\langle 0_-|)\}$$
$$= (iJ/2).$$

$$\Lambda_{jk} = \begin{array}{c} \\ A_1 \\ A_2 \\ A_X \\ A_Y \\ A_Z \end{array} \begin{array}{c} \begin{array}{ccccc} \quad & \quad & \quad & \quad & \quad \end{array} \\ \begin{pmatrix} 0 & 0 & 0 & 0 & 0 \\ 0 & 0 & 0 & 0 & 0 \\ 0 & 0 & 0 & -iJ/2 & 0 \\ 0 & 0 & iJ/2 & 0 & -i(\nu_A - \nu_B)/2 \\ 0 & 0 & 0 & i(\nu_A - \nu_B)/2 & 0 \end{pmatrix} \end{array}$$

Now the Γ_{jk} matrix can be calculated. In order to compare the present treatment to that of Wertheimer and Silbey, the effects of oscillating chemical shift differences and scalar couplings will be calculated. The oscillating terms that we wish to consider constitute the whole spin Hamiltonian written earlier. The commutators of the relevant terms are presented in the following table

Q_j	$[Q_j, (\nu_A - \nu_B)A_X + J\{(-2^{-1/2})A_2 + A_Z\}]$
A_1	0
A_2	0
A_X	$-iJA_Y$
A_Y	$-i(\nu_A - \nu_B)A_Z + iJA_X$
A_Z	$i(\nu_A - \nu_B)A_Y$

The $[Q_k^+,(\nu_A - \nu_B)A_X + J\{(-2^{-1/2})A_2 + A_Z\}]$ terms are equal to the corresponding terms above.

Looking at all the trace products that may result in Γ_{jk} and using the substitution $X = (\nu_A - \nu_B)A_X + J\{(-2^{-1/2})A_2 + A_Z\}$, the following terms result.

$$(G/2)Tr\{[A_X, X][A_X^+, X] = (G/2)Tr\{i^2J^2(A_Y)^2\} = -(GJ^2/4)$$

$$(G/2)Tr\{[A_X, X][A_Y^+, X] = (G/2)Tr\{i^2J\delta A_YA_Z - i^2J^2A_YA_X\} = 0$$

$$(G/2)Tr\{[A_X, X][A_Z^+, X] = (G/2)Tr\{-i^2J\delta(A_Y)^2\} = (GJ\delta/4)$$

$$(G/2)Tr\{[A_Y, X][A_Y^+, X] = (G/2)Tr\{i^2\delta^2(A_Z)^2 + i^2J^2(A_X)^2\} = -(GJ^2 + G\delta^2)/4$$

$$(G/2)Tr\{[A_Y, X][A_Z^+, X] = (G/2)Tr\{-i^2\delta^2A_ZA_Y + i^2J\delta A_XA_Y\} = 0$$

$$(G/2)Tr\{[A_Z, X][A_Z^+, X] = (G/2)Tr\{i^2\delta^2(A_Z)^2\} = -(G\delta^2/4)$$

The Γ matrix is

$$\Gamma_{jk} = \begin{matrix} A_X \\ A_Y \\ A_Z \end{matrix} \begin{pmatrix} -(GJ^2/4) & 0 & (GJ\delta/4) \\ 0 & -(GJ^2 + G\delta^2)/4 & 0 \\ (GJ\delta/4) & 0 & -(G\delta^2/4) \end{pmatrix}$$

The level-shift operator basis used here is related to the basis used by Wertheimer and Silbey by the relation:

$$\begin{pmatrix} A_Z \\ A_X \\ A_Y \\ \overline{1}/2 \end{pmatrix} = \begin{pmatrix} (1/2)(|0_+\rangle\langle 0_+| - |0_-\rangle\langle 0_-|) \\ (1/2)(|0_+\rangle\langle 0_-| + |0_-\rangle\langle 0_+|) \\ (-i/2)(|0_+\rangle\langle 0_-| - |0_-\rangle\langle 0_+|) \\ (1/2)(|0_+\rangle\langle 0_+| + |0_-\rangle\langle 0_-|) \end{pmatrix}.$$

This yields the transformation matrices U and U^{-1} to the Wertheimer-Silbey basis.

$$U = \begin{pmatrix} 1 & 0 & 0 & 1 \\ 0 & 1 & i & 0 \\ 0 & 1 & -i & 0 \\ -1 & 0 & 0 & 1 \end{pmatrix} \qquad U^{-1} = \begin{pmatrix} 1/2 & 0 & 0 & -1/2 \\ 0 & 1/2 & 1/2 & 0 \\ 0 & -i/2 & i/2 & 0 \\ 1/2 & 0 & 0 & 1/2 \end{pmatrix}$$

The Γ in the Wertheimer-Silbey basis, Γ_{WS}, can now be calculated from Γ_A, the matrix already found in the A_X, A_Y, A_Z basis.

$$\Gamma_{WS} = U\Gamma_A U^{-1}$$

In order to make the dimensions of the matrices the same, a row and column of zeros are added to the A_X, A_Y, A_Z basis matrix. This row and column comes from the eigenoperator $\overline{1}/2 = (1/2)(|0_+\rangle\langle 0_+| + |0_-\rangle\langle 0_-|)$, which has no time dependence and gives rise to zeros in Γ.

$$\Gamma_{ws} = \begin{array}{c} \\ |0_+\rangle\langle 0_+| \\ |0_-\rangle\langle 0_-| \\ |0_+\rangle\langle 0_-| \\ |0_-\rangle\langle 0_+| \end{array} \begin{pmatrix} -(G\delta^2/8) & (G\delta^2/8) & (GJ\delta/8) & (GJ\delta/8) \\ (G\delta^2/8) & -(G\delta^2/8) & -(GJ\delta/8) & -(GJ\delta/8) \\ (GJ\delta/8) & -(GJ\delta/8) & -(GJ^2+G\delta^2/2)/4 & (G\delta^2/8) \\ (GJ\delta/8) & -(GJ\delta/8) & (G\delta^2/8) & -(GJ^2+G\delta^2/2)/4 \end{pmatrix}$$

This relaxation matrix is analogous to that obtained by Wertheimer and Silbey. The various terms are defined as following:

$GJ\delta \equiv$ cross correlation terms,

$GJ^2 \equiv$ the pure dephasing rate, and

$G\delta^2 \equiv$ the population relaxation rate.

An alternative treatment of the NMR spin system is provided by the Haken-Strobl model.[2] This model was developed assuming high-temperature conditions. Particularly important is that $|\hbar\omega_{-+}| \ll k_B T$, as is the case in NMR experiments except at very low temperatures. This condition may not be fulfilled by systems of dimers in condensed phases where energy differences between states can be on the order of several wavenumbers and experiments are carried out in the range of 1-4 K. However, the present treatment is more general and could be applied to various molecular systems coupled to bath degrees of freedom.

References

1. R. Wertheimer and R. Silbey, *Chem. Phys. Lett.* **75**, 243 (1980).

2. H. Haken and G. Strobl, *Z. Physik* **262**, 135 (1973).